



## **Stave Falls Project Water Use Plan**

### **Littoral Productivity Assessment**

### **Implementation Year 10 (Meta-Analysis)**

**Reference: SFLMON-02**

### ***A Meta-Analysis of Littoral Zone Related Data***

**Study Period: 2000-2009**

**Final Report**

**James Bruce, MSc**  
Creekside Aquatic Sciences  
2754 Hwy 101  
Roberts Creek, BC,  
V0N 2W3

**Julie Beer, MSc, P.Geo.**  
Ness Environmental Sciences  
2774 William Street  
Vancouver, BC,  
V5K 2Y8

**July 30, 2016**

# Stave Falls Water Use Plan: Littoral Productivity Assessment (SFLMON #2)

A Meta-Analysis of Littoral Zone Related Data Collected  
Between 2000-2009 Testing Impact Hypotheses and  
Addressing Management Questions

Technical Report: CAQ-004

July 30, 2016

Prepared for

**BC Hydro**  
**Environmental Risk Management**  
6911 Southpoint Drive  
Burnaby, BC  
V3N 4X8

by

**James Bruce, MSc**  
Creekside Aquatic Sciences  
2754 Hwy 101  
Roberts Creek, BC, V0N 2W3  
james@creeksideaq.com  
(604) 788-4670 or (604) 886-9030

and

**Julie Beer, MSc., P. Geo.**  
Ness Environmental Sciences.  
2774 William Street  
Vancouver, British Columbia, V5K 2Y8  
nessenvironmental@shaw.ca  
(604) 874-8095 or (604) 729-0925

Suggested Citation:

Bruce, J.A. and J. Beer. 2016. Stave Falls Water Use Plan: Littoral Productivity Assessment (SFNMON #2). A Meta-Analysis of Littoral Zone Related Data Collected Between 2000 -2009 Testing Impact Hypotheses and Addressing Management Questions. Report Prepared for BC Hydro, Burnaby BC. Creekside Aquatic Sciences Report No. CAQ-004: 76 p + App

## Acknowledgments

The following people are gratefully acknowledged for their contribution and assistance during this study:

**John Stockner**, EcoLogic Ltd., for assisting in preparing study design and providing invaluable knowledge on the ecology of primary producers and zooplankton in west coast waters.

**Jeff Greenbank**, Greenbank Environmental Ltd., for assisting in collecting the water quality samples, including the effort required to manage and operate the sampling boat.

**Brent Wilson**, BC Hydro, for giving our field crew access to their jet boat for travel to and from the study site.

**Darin Nishi**, BC Hydro, for providing funding support to the project.

## Executive Summary

Over a 2-year period ending in 1999, BC Hydro carried out a Water Use Planning (WUP) process for the Stave Falls Project with the objective of better balancing facility operations driven by hydro-electric power generation with other social and environmental values of water use (Failing 1999). A broad range of interests were considered during the WUP process, one of which was reservoir productivity and more specifically, the effect of water level fluctuation on the productivity of the littoral zone in each of the Hayward and Stave Lake reservoirs. It was generally believed by those with fisheries interests that the littoral zone in Stave Lake Reservoir had been (and continues to be) seriously impacted by water level fluctuations, which historically approached or exceeded 10 m in amplitude, and was no longer functioning. To carry out the trade-off processes of the various interest groups involved in the WUP, an Effective Littoral Zone (ELZ) performance measure was developed to track relative differences in littoral productivity as operating constraints were varied at both the Stave Falls and Ruskin dams. The adopted metric was derived based on a simple conceptual model of periphyton growth on fixed (epilithic) substrate, quantifying the area of aquatic shoreline habitat that received adequate photosynthetically active radiation (PAR) to promote photosynthesis for periphyton growth and at the same time, remained continuously wetted to prevent mortality from desiccation.

Although the ELZ performance measure was used throughout the development of the WUP, its accuracy as a measure of productive littoral habitat was untested. This proved to be a particular concern when simulation modeling found that even small increases in littoral habitat area, as defined by the ELZ measure, could only occur with significant losses in power generation. Because of this uncertainty, the Consultative Committee (CC) found it difficult to justify any operational change that would intentionally increase littoral habitat, despite general consensus that such changes were likely to be beneficial. As a result, a 10-year monitoring program was initiated to address this uncertainty. Associated with this monitoring program were eleven impact hypotheses that captured the range on uncertainties linked to the use of the conceptual ELZ model and its possible outcomes. To help guide the monitoring program, five management questions were also identified.

The monitoring program was started in year 2000 and completed at the end of 2009. Technical data Reports were produced for each monitoring year. The present report summarizes the outcome of a meta-analysis of all years of data, as well as an evaluation of the ELZ metric used in the WUP. Out of these analyses, a new, more robust ELZ metric was developed, one based more on empirical data rather than an untested conceptualization of epilithic periphyton ecology. More importantly, the meta-analysis and WUP ELZ model development exercises allowed all impact hypotheses to be addressed. The outcomes are summarised in Table A.

Overall, the WUP ELZ modelling exercise, which was empirically based, was able to show that implementation of the 'Combo 6' operative strategy likely had a negative impact on littoral development compared to pre-WUP operations. This is opposite to what was expected based on the results of the conceptually based ELZ modelling during the pre-WUP (i.e., pre-Combo 6). The WUP ELZ modelling was able to show that, while littoral development was high during the summer months in most years due to relatively high and stable water levels, the need to draft the reservoir in early September to accommodate increased winter inflows resulted in significant losses to this production. This was because most of the summer time gains in littoral production occurred at the highest reservoir elevations, thus ensuring largescale dewatering and ultimate desiccation of this production when the draw down occurred. There was also more shoreline area with slopes < 15% (where sloughing is less likely to occur) at lower reservoir

elevations than at the higher elevations. With the pre-WUP operating strategy, there were many years when reservoir elevation did not reach the targeted summer time levels of 'Combo 6', thus the magnitude of the September reservoir draft was not as great, which left a greater proportion of the year's production under water. Also, there was larger areal extent of shoreline habitat with more gradual gradients (i.e. <15%).

Given this outcome, some changes to the 'Combo 6' operating strategy are proposed that could help increase littoral production. The first would be to delay the September drawdown for several weeks, allowing the littoral zone to continue functioning until the end of the growing season in mid to late October. The longer the delay, more of the summer production remains accessible to littoral organisms. The benefit of this to fish production however is unknown and cannot be determined with the present data. The other operating strategy would be to consider lowering the summer time targeted reservoir elevation, thus reducing the magnitude of reservoir drawdown in the fall. This would also marginally increase the shoreline area with slopes < 15%. Both of the changes however, would have significant impacts to other values in the reservoir. There is no optimal solution to maximizing littoral production in Stave Falls Reservoir except to reduce reservoir fluctuations completely. No particular reservoir threshold or fall drawdown date can be recommended without assessing trade-offs to other values in a full water use planning exercise.

The empirical ELZ model can be used in future trade-off analyses to assess the littoral zone consequences of operating alternative, but requires an operations model to predict likely Stave Lake Reservoir elevation. A much simpler approach may be to consider the range of reservoir elevations from Mar 1 to Oct 31 each year as a littoral zone performance measure. It was found to be linearly related to the empirical ELZ model predations (Figure 29). However, it would still require an operations model to predict likely Stave Lake Reservoir elevation for each operating alternative.

Table A. Summary of impact hypothesis outcomes arising from analysis of the 2000-2009 littoral productivity monitoring study.

Impact Hypothesis	Description	Status	Rationale
H <sub>01</sub>	Average reservoir concentration of Total Phosphorus (TP), an indicator of general availability of phosphorus is not limiting to littoral primary productivity.	Rejected	TP < 3 µg/L; Ultra-oligotrophic
H <sub>02</sub>	Relative to the availability of phosphorus as indicated by level of total dissolved phosphorus (PO <sub>4</sub> ), the average reservoir concentration of nitrate (NO <sub>3</sub> ) is not limiting to littoral primary productivity.	Not Rejected	NO <sub>3</sub> < 200 µg/L; Ultra-oligotrophic, but not as limiting as TP
H <sub>03</sub>	Water retention time (τ <sub>w</sub> ) is not altered by reservoir operations that vary from year to year such that it significantly affects the level of TP as described by Vollenweider's (1975) phosphorus loading equations (referred to here as TP(τ <sub>w</sub> ))	Not Rejected	TP independent of reservoir operations in Stave Lake Reservoir, inconclusive in Hayward Reservoir (confirmed by Bruce and Beer 2016)
H <sub>04</sub>	Water temperature, and hence the thermal profile of the reservoir, is not significantly altered by reservoir operations that vary from year to year.	Inconclusive	Majority of variance in water temperature accounted for by solar input, but thermal profile breaks down from September drawdown.
H <sub>05</sub>	Changes in TP as a result of reservoir operations (through changes in τ <sub>w</sub> ) are not sufficient to create a detectable change in littoral algae biomass as measured by littoral levels of chlorophyll a (Chl a) and/or ash free dry weight (AFDW).	Not Rejected	No statistically significant relationships were detected in the data
H <sub>06</sub>	Overall primary production (as measured by <sup>14</sup> C inoculation and/or as inferred from ash free dry weight data) of Stave Lake Reservoir is not different than that of Hayward Lake	Rejected	Significant differences were found in the coefficients that describe periphyton growth
H <sub>07</sub>	Pelagic primary production dominates in Stave Lake Reservoir while littoral production dominates in Hayward Reservoir.	Inconclusive	Could not be addressed with available data, though literature suggests that littoral production does play a significant role, especially in oligotrophic systems
H <sub>08</sub>	Stable reservoir levels do not lead to maximum littoral development as measured by <sup>14</sup> C inoculation and/or inferred from ash free dry weight data.	Rejected	Clear relationship was found between reservoir stability and maximum periphyton biomass
H <sub>09</sub>	Water level fluctuations that raise the euphotic zone (defined here as the depth at which photosynthetically active radiation (PAR) is 1% that of the water surface) from lower elevations does not lead to a collapse of littoral primary production (as measured by <sup>14</sup> C inoculation and/or inferred from ash free dry weight data) that occurred near the prior 1% PAR depth.	Not Rejected	Light acclimation and potential mixotrophy appears to delay mortality due to low light conditions (Bruce and Beer 2014)
H <sub>010</sub>	Littoral zone productivity, as measured by <sup>14</sup> C inoculation and/or inferred from ash free dry weight data, remains unchanged as reservoir water level stability increases.	Rejected	Revised ELZ model shows that littoral production is strongly impacted by reservoir fluctuations
H <sub>011</sub>	Changes in littoral productivity (as measured by <sup>14</sup> C inoculation and/or inferred from ash free dry weight data) can be expressed primarily in terms of changes in areal extent as defined by upper and lower boundary elevations. Within these boundaries, primary production does not vary in proportion to accumulated PAR exposure under wetted conditions.	Rejected	The revised ELZ model shows that littoral production is strongly impacted by available light and appears to follow a saturation function.

## Table of Contents

Acknowledgments.....	iii
Executive Summary .....	iv
List of Tables.....	ix
List of Figures.....	xi
Introduction .....	1
Background .....	1
Management Questions.....	3
Impact Hypotheses.....	3
Objective and Scope .....	4
Methods.....	5
Study Area .....	5
General Study Design .....	7
Water Chemistry .....	8
Physical Characteristics .....	9
Light .....	9
Water Temperature .....	10
Hydrology.....	11
Periphyton .....	11
ELZ Modelling.....	15
Results.....	17
Water Chemistry .....	17
Total Phosphate (TP) .....	17
Total Dissolved Phosphate .....	18
Nitrate.....	20
Physical Characteristics .....	22
Light .....	22
Water Temperature .....	27
Hydrology.....	29
Periphyton Growth.....	33
Effective Littoral Zone Modelling.....	52
Post WUP Expectations .....	52
Relationship to Periphyton Biomass Growth.....	52
Relationship to Fish Abundance .....	59
Discussion.....	60
General Observations.....	60
Impact Hypotheses.....	65
Management Questions.....	69
Conclusions .....	71
References.....	74



[Appendix A Relationship between Ash Free Dry Weight and Chlorophyll a](#)

Introduction .....	A1
Laboratory Methods .....	A1
Data Analysis.....	A1
Results.....	A2
Discussion.....	A3

[Appendix B Relationship between Ash Free Dry Weight and Primary Productivity measured by the 14C Method](#)

Introduction .....	B1
Methods.....	B1
Field methods .....	B1
Laboratory Methods .....	B2
Data Analysis.....	B2
Results.....	B3
Discussion.....	B4

## List of Tables

Table 1. Summary of operational constraints that form the Combo 6 operating alternative recommended by the WUP CC (BC Hydro 2003). .....	2
Table 2. Results of a two way, unbalanced factorial ANOVA on the Total Phosphate data ( $\mu\text{g/L}$ ) collected at two sites (Stave Lake and Hayward Reservoirs) over a 10 year period (2000 – 2009).....	18
Table 3. Results of a two way, unbalanced factorial ANOVA on the Total Dissolved Phosphate data ( $\mu\text{g/L}$ ) collected at two sites (Stave Lake and Hayward Reservoirs) over a 10 year period (2000 – 2009).....	19
Table 4. Results of a two way, unbalanced factorial ANOVA on the nitrate levels ( $\mu\text{g/L}$ ) collected at two sites (Stave Lake and Hayward Reservoirs) over a 10year period (2000 – 2009).....	21
Table 5. Results of a single factor ANOVA of the 1% Photosynthetically Active Radiation (PAR) compensation depth data collected at four sites in Stave Lake and a single site at Hayward reservoir (H) testing for significant between year differences (2000 – 2009).....	23
Table 6. Results of a single factor ANOVA of the 1% Photosynthetically Active Radiation (PAR) compensation depth data collected at four sites in Stave Lake (Stave North, SN; Stave opposite the Alouette Powerhouse, SP; Stave South, SS; and Stave West, SW) and a single site at Hayward reservoir (H) over a 10-year period (2000 – 2009). .....	23
Table 7. Yearly summary statistics of reservoir elevation for Stave Lake and Hayward reservoirs during the 10-year littoral periphyton growth monitoring program. Data were provided by BC Hydro .....	33
Table 8. Results of a two-way unbalanced factorial ANOVA on depth integrated periphyton growth rate collected at four sites (Stave North, Stave South, and Hayward) and over a 10-year period (2000 to 2009). In Table A., year 2000 was dropped from the analysis so that all sites could be compared for differences as no data was collected at the Stave West Site. In Table B., the Stave West site was excluded from the analysis so that year 2000 data could be incorporated into the analysis. ....	34
Table 9. Results of correlation analyses of various water chemistry and physical attributes on depth integrated periphyton growth data collected at four sites over a 10 year period (2000 - 2009). Shaded areas highlight correlation coefficients that were found to be statistically significant at $\alpha = 0.05$ given the sample size of paired values (n).....	36
Table 10. Results of a two-way unbalanced ANOVA on maximum growth rate coefficients “A” derived by fitting a hyperbolic saturation equation [of the form $Ax/(x + B)$ ] to growth data calculated at various sampling depths plotted against corresponding PAR intensity data (x). Year and site are the two factors of interest and are based on data collected from years 2000 to 2009. The Student Newman-Kuels procedure was used to compare site means and determine which were significantly different .....	40

Table 11. Results of correlation analyses of various water chemistry and physical attributes on maximum periphyton growth rates derived from Eq. 6 collected at four sites over a 10 year period (2000 - 2009). Shaded areas highlight correlation coefficients that were found to be statistically significant at  $\alpha = 0.05$  given the sample size of paired values (n). ..... 42

Table 12. Results of correlation analyses of various water chemistry and physical attributes on PAR<sub>A50</sub>, the light intensity at which periphyton growth is 50% of maximum, collected at four sites over a 10-year period (2000 - 2009). Shaded areas highlight correlation coefficients that were found to be statistically significant at  $\alpha = 0.05$  given the sample size of paired values (n)...43

Table 13. Yearly values and summary statistics of the ELZ metric and corresponding predicated biomass values indicating periphyton growth potential in Stave Lake reservoir for simulation periods ending Oct 31 each year. Predicted biomass data are also provided for simulation periods ending Aug 30 to illustrate the differences in growth potential before the reservoir is typically drawn down in September. .... 54

Table 14. Yearly estimates of fish abundance and biomass in Stave Lake Reservoir from Stables and Perrin (2015) and corresponding littoral productivity indicators that include the ELZ and periphyton biomass metric developed in the present study. Included in the table are separate abundance estimates for cutthroat and rainbow trout, salmonids that have been shown to feed occasionally on benthic organisms..... 59

Table 15. Correlation matrix between littoral productivity indicators and fish abundance estimates based on the data of Table 13. The critical correlation coefficient for  $n = 10$  and  $\alpha = 0.05$  is 0.632..... 60

Table 16. Summary of impact hypothesis outcomes arising from analysis of the 2000-2009 littoral productivity monitoring study .....73

## List of Figures

Figure 1. Map of Stave Lake and Hayward Lake Reservoirs showing monitor sampling locations. Red circles identify the location of water quality sampling sites while the dashed red line denotes the location of periphyton sampling transects. ....	6
Figure 2. Schematic diagram of periphyton growth plate set up consisting of a scuffed Plexiglas plate as the artificial growth substrate, floating tray holding the plate well above bottom sediments, and a large concrete anchor block. ....	12
Figure 3. Plot of yearly average total phosphorus levels ( $\mu\text{g/L}$ ) in Stave Lake and Hayward Reservoirs for each year of the monitor (2000 – 2009). The error bars mark the 95% confidence limits about the computed yearly means. ....	17
Figure 4. Total phosphorus ( $\mu\text{g/L}$ ) plotted as a function of ordinal date showing lack of a persistent seasonal trend in observations over the 10-year period of data collection (2000 – 2009). This was apparent at both monitoring sites (Stave Lake and Hayward Reservoirs), though there was a tendency for Hayward levels to be higher than those at Stave Lake. ....	18
Figure 5. Plot of yearly average total dissolved phosphorus levels ( $\mu\text{g/L}$ ) in Stave Lake and Hayward Reservoirs for each year of the monitor (2000 – 2009). The error bars mark the 95% confidence limits about the computed yearly means. ....	19
Figure 6. Total dissolved phosphorus ( $\mu\text{g/L}$ ) plotted as a function of ordinal date showing lack of a persistent seasonal trend in observations over the 10 year period of data collection (2000 – 2009) at both monitoring sites (Stave Lake and Hayward Reservoirs). ....	20
Figure 7. Plot of yearly average nitrate levels ( $\mu\text{g/L}$ ) in Stave Lake and Hayward reservoirs for each year of the monitor (2000 – 2009). The error bars mark the 95% confidence limits about the computed yearly means. ....	21
Figure 8. Nitrate levels ( $\mu\text{g/L}$ ) plotted as a function of ordinal date showing a persistent seasonal trend in observations over the 10-year period of data collection (2000 – 2009) at the Stave Lake and Hayward Reservoir sampling sites. ....	22
Figure 9. Plot of 1% Photosynthetically Active Radiation (PAR) compensation depths (m) as a function of ordinal date collected over a 10-year period (2000 to 2009) showing differences in annual trend between Stave Lake and Hayward reservoirs. Vertical lines highlight the periods where there appeared to be a seasonal change in response; the first was May 15, the second November 1. ....	24
Figure 10. Plots of solar radiation values provided by the Greater Vancouver Regional District from four different stations in the vicinity of the Stave Falls Project against measured solar irradiance data collected on site over a 10-year period (2000 – 2009). T09 = Rocky Point Park, Port Moody, T12 = Chilliwack Airport; T32 = Douglas College, Coquitlam; T34 = Abbotsford Airport. ....	26

Figure 11. Plot of daily accumulated photosynthetic active radiation ( $PAR_{Surface}$ ) estimated for Stave Lake and Hayward Reservoirs for the period Jan 1, 2000 to Dec 31, 2009. The PAR data were calculated from solar radiation data provided by the Greater Vancouver Regional District (GVRD) at 4 locations in the vicinity of the study area. The  $PAR_{Surface}$  values are assumed to be just under the water surface and take into account reflective losses. ....27

Figure 12. Plot of depth integrated water temperature (water surface to a depth of 8m) as a function of ordinal date showing seasonal trends between sites on Stave Lake and Hayward reservoirs.. ..... 28

Figure 13. Plot of daily average inflow discharge to Stave Lake Reservoir over time for the duration of the monitoring program. Data were provided by BC Hydro..... 30

Figure 14. Plot of total inflow volume to Stave Lake and Hayward Reservoirs comprising of regulated (Alouette facility and Stave Falls facilities respectively) and non-regulated (local inflows) for each year of the monitoring program (2000 to 2009). Data were calculated from daily average inflow discharge values provided by BC Hydro.....31

Figure 15. Plot of daily average reservoir elevation in Stave Lake Reservoir over time for the duration of the monitoring program. Data were provided by BC Hydro..... 31

Figure 16. Plot of daily average reservoir elevation in Hayward Reservoir over time for the duration of the monitoring program. Data were provided by BC Hydro..... 32

Figure 17. Plot of daily average inflow discharge to Hayward Reservoir over time for the duration of the monitoring program. Data were provided by BC Hydro..... 32

Figure 18. Depth integrated periphyton production growth plotted as a function of ordinal date showing seasonal trends as well as between-site differences. .... 35

Figure 19. Examples of periphyton growth rates plotted as a function of PAR collected at various water depths. A. Two examples from the Stave North site where the hyperbolic saturation equation was found to provide an excellent fit to the plotted data. B. An example where the hyperbolic saturation equation did not fit well to the data, yet still provided a statistically significant coefficient of determination ( $R^2$ ). The example in B. highlights two common features when fit was poor; much higher growth than expected at low light condition, and/or lower than expected growth at moderate to high light intensities. It should be noted that instances of poor fit were generally rare. .... 39

Figure 20. Plot of mean annual maximum growth coefficients ( $\pm$  95% confidence limits) as determined from fitting a hyperbolic saturation equation to daily growth data as a function of PAR. The 95% confidence limits are narrower for Stave Lake because of larger number of sites. .... 41

Figure 21. Scatterplot of the PAR intensity at which growth is 50% of maximum ( $PAR_{A50}$ ) as a function of average surface PAR during each periphyton growth period..... 44

Figure 22. Scatterplots of periphyton growth rates as a function of average surface PAR intensity for each of four sampling locations on the Stave Lake and Hayward Reservoirs. Only the lower quartile of PAR data are plotted, highlighting the fact that as PAR approaches zero, periphyton growth continues, suggesting the presence of organisms capable of heterotrophic growth ..... 46

Figure 23. Functional form of Eq. 15 to 18 used to describe periphyton growth as a function of PAR intensity in the Stave Lake and Hayward Reservoirs. The effect of water temperature is illustrated by plotting the equations with two different temperatures spanning the range that would typically be experienced in the reservoir system ..... 47

Figure 24. Scatterplots of periphyton growth rate as a function of average photosynthetic active radiation experienced at each growth plate over the course of each periphyton growth period. Data span the 10-year monitoring period. Separate scatterplots are provided for each sampling site. The solid lines show the best fitting non-linear regression equations for each site (Eq. 15 to 18) assuming an average temperature of 14.6°C and site mean PAR<sub>A50</sub> values..... 48

Figure 25. Plot of predicted versus measured periphyton biomass values (mg/m<sup>2</sup>) collected from artificial substrate placed at various depths at three sites in Stave Lake Reservoir and one site in Hayward Reservoir. The predicted values were derived by using a recursive growth algorithm that models biomass change over time using a daily time step. Periphyton growth rates were allowed to vary depending on prevailing light intensity and water temperature conditions using Eq. 15 to 18. The duration of each model run was set to the corresponding periphyton growing periods recorded during the monitoring period. The diagonal red line represents the line of equality..... 51

Figure 26. Plots of simulated periphyton biomass (1000 kg), an indicator of periphyton growth potential, as a function of reservoir depth for pre-WUP (1985 to 1995) and WUP (1999 to 2009) reservoir conditions. Plots A and B show the outcomes of periphyton growth simulations ending Oct 31, the same as the ELZ metric. Plots C and D show the results of a shorter simulation period; ending Aug 30 ..... 53

Figure 27. Plot of ELZ habitat area and depth-integrated periphyton biomass as a function of lower ELZ boundary elevation for all years of simulation (1985 to 2009). ..... 57

Figure 28. Reservoir elevation (m) over time for the pre-WUP period showing how it differed to the WUP period shown in Figure 15..... 58

Figure 29. Periphyton growth potential in Stave Lake Reservoir (derived by empirical ELZ modelling) as a function of reservoir elevation range for the period between Mar 1 and Oct 31 for all years of periphyton growth simulation (both pre- and current-WUP)..... 68

Figure A30 Chlorophyll a data plotted against Ash Free Dry Weight data that were collected simultaneously at three sites in Stave Lake Reservoir and a single site at Hayward Reservoir over a period of three years starting March 2000. ....A2

Figure A31. Comparison of paired Ash Free Dry Weight and Chl a data between upper (1,2) and lower (8-10) sampling plates at all sites in Stave Lake and Hayward reservoirs; 2000-2003.....A3

Figure B32 Primary Production estimated by 14C uptake plotted against AFDW from samples collected simultaneously at randomly chose growth plates for the Stave Lake and Hayward systems, 2007 – 2009.....B4

## Introduction

### Background

Over a 2-year period ending in 1999, BC Hydro carried out a Water Use Planning (WUP) process for the Stave Falls Project with the objective of better balancing facility operations driven by hydro-electric power generation with other social and environmental values of water use (Failing 1999). The WUP planning process was interest-driven, the representatives of which were brought together to form a consultative committee (CC), was focused mainly on potential changes to the operation of existing facilities. The CC relied heavily on what data could be gathered within the 2 year WUP time frame, and used trade off analysis at its core for decision making. A broad range of interests were considered in the trade off analyses, one of which was reservoir productivity and more specifically, the effect of water level fluctuation on the productivity of the littoral zone in each of the Hayward and Stave Lake reservoirs. It was generally believed by fisheries interests that the littoral zone in Stave Lake Reservoir had been (and continues to be) seriously impacted by water level fluctuations, which historically approached or exceeded 10 m in amplitude, and was no longer functioning. It was further hypothesised that the loss of this fully-functional littoral zone had significantly impacted the overall biological (carbon) production of the ecosystem (Failing 1999). However, no past data had ever been collected to assess the extent and/or nature of this impact, nor was there any data that could be used to link a loss or gain in littoral production to a system wide impact on productivity. Despite this lack of information, the relative importance of this issue was considered high among participants (consultative committee or CC members), in the WUP process so much so that it was included as a key trade-off issue in decision-making (Failing 1999).

To carry out the trade-off process, a performance measure (PM) or indicator was required to track relative differences in littoral habitat productivity as operating constraints were varied at both the Stave Falls and Ruskin dams. The adopted PM was derived based on a simple conceptual model of periphyton growth on fixed (epilithic) substrate, but viewed in terms of a daily time step where water level was allowed to fluctuate (Wetzel 2001). The PM, termed the 'Effective Littoral Zone' or ELZ, quantified the area of aquatic shoreline habitat that received adequate photosynthetic active radiation (PAR) to promote photosynthesis for periphyton growth and at the same time, remained continuously wetted to prevent mortality from desiccation. A detailed description of how the measure was calculated can be found in Appendix 2 of the CC report (Failing 1999). Although the ELZ performance measure was used throughout the development of the WUP, its accuracy as a measure of productive littoral habitat was untested. This proved to be a particular concern when simulation modeling found that even small increases in littoral habitat area, as defined by the ELZ measure, could only occur with significant losses in power generation. Because of this uncertainty, the CC found it difficult to justify any operational change that would intentionally increase littoral habitat, despite general consensus that such changes were likely to be beneficial.

At the conclusion of the WUP process, the CC had reached a consensus on a broad range of operational changes and/or adjustments (collectively referred to as the 'Combo 6' operating strategy) for possible implementation over the next ten years (Table 1; Failing 1999, BC Hydro 2003). There were many reasons that lead to this outcome, but the one pertinent to this report was the potential to increase functional littoral habitat area, albeit small in magnitude and highly variable from year to year. This increase was not intentional. Rather it was the consequence of several operating constraints put in place to satisfy other objectives. The CC viewed this potential for littoral gain as an opportunity to test the ELZ

**Table 1. Summary of operational constraints that form the Combo 6 operating alternative recommended by the WUP CC (BC Hydro 2003).**

<b>Constraint</b>	<b>Implementation Dates</b>	<b>Description</b>
1	Oct 15 - Nov 30	<b>Minimum tailwater elevation 1.8m.</b> Initially 1.7m minimum tailwater elevation rest of year, but later changed to 1.8m year round.
2	Oct 15 - Nov 30	<b>Limited Fall Block Loading.</b> Ruskin output is subject to weekly block loading where generation has a set output for a 7-day period. When the discharge from Ruskin is < 100 m <sup>3</sup> /s, the discharge must remain constant for a minimum of 7 days after each change in discharge and each new block load on the plant must be greater than the previous block load. When the weekly block load flow > 100 m <sup>3</sup> /s, peaking operations at Ruskin above 100 m <sup>3</sup> /s is permitted.
3	Feb 15 - May 15	<b>Limited Spring Block Loading.</b> Ruskin is subject to daily block loading, defined as a maximum of one plant load change each day. When the daily block load flow > 100 m <sup>3</sup> /s, peaking at Ruskin is permitted provided a minimum flow of 100 m <sup>3</sup> /s is maintained for the day.
4	Oct 15 - Nov 30, Feb 15 - May 15	<b>Flow Ramping the Spring and Fall Block Loading.</b> The rate of flow reduction from Ruskin, when discharge is < 100 m <sup>3</sup> /s, will be less than 35 m <sup>3</sup> /s at intervals > 10 minutes. When discharge is greater than 100 m <sup>3</sup> /s, rate of flow change will be < 113 m <sup>3</sup> /s at intervals > 30 minutes.
5	Jan 1 - Mar 31	<b>Archaeological Drawdown.</b> Stave Lake Reservoir drawdown below the licensed minimum reservoir level of 73.0 m require for a minimum of 6 week, one out of 3 years on average. The lowest elevation above which access will be provided is 72 m.
6	May 15 - Sep 7	<b>Recreation Season Targets on Stave Lake Reservoir.</b> Preferred elevation of Stave Lake Reservoir for recreational activities is between 80.0 and 81.5 m. During this period, the level of Stave Lake Reservoir will be targeted at 76 m or higher, and will be targeted between 80.0 and 81.5 m for a minimum of 53 days.
7	Oct 15 - Nov 30, Feb 15 - May 15	<b>Hayward Reservoir Operations.</b> During the spring and the fall block load periods, the normal minimum operating level at Hayward Reservoir will be 39.5 m. At other times, the normal minimum operating level at Hayward Lake Reservoir will be 41.08 m.

as a valid indicator of littoral productivity, as well as determine whether the expected increase could be linked to other changes in the reservoir ecosystem. As a result, a monitoring program designed to track changes in littoral productivity over time was incorporated into the consensus operating strategy. The overarching objective of the monitor was to determine whether littoral production varied between seasons and years as a function of reservoir operation (i.e., the extent and duration of water surface elevation fluctuations) and whether these changes could be effectively captured using the ELZ metric calculations. The monitor started in year 2000 and lasted 10 years to year 2009, though data was not collected in all years. This report summarises and analyses the times series of littoral production data, documents findings as they relate to impact hypotheses that were proposed by the CC and addresses key management questions for consideration during a WUP review process scheduled for 2016/17.



## Management Questions

The consultative committee identified four key management questions to be addressed in the monitoring of littoral productivity in the Stave Lake and Hayward reservoirs (BC Hydro, 2005). These were:

- a) What is the current level of littoral productivity in each reservoir, and how does it vary seasonally and annually as a result of climatic, physical and biological processes, including the effect of reservoir fluctuation?
- b) If changes in littoral productivity are detected through time, can they be attributed to changes in reservoir operations as stipulated in the WUP, or are they the result of change to some other environmental factor?
- c) A performance measure was created during the WUP process so as to predict potential changes in littoral productivity based on a simple conceptual model. The Effective Littoral Zone (ELZ) performance measure was used extensively in the WUP decision making process, but its validity is unknown. Is the ELZ performance measure accurate and precise, and if not, what other environmental factors should be included (if any) to improve its reliability?
- d) Does the 'Combo 6' operating alternative improve reservoir littoral productivity as was expected in the WUP? Is there anything that can be done to improve the response, whether it be operations-based or not?
- e) To what extent would reservoir operations have to change to i) illicit a littoral productivity response, and ii) improve current littoral and overall productivity levels?

## Impact Hypotheses

A total of 11 impact hypotheses were identified by the CC for consideration in this monitor (BC Hydro 2005). They were expressed as a series of null hypotheses (i.e., hypotheses of no difference or correlation) to be tested separately for each reservoir. The first five impact hypotheses were related to the extent with which prevailing nutrient concentrations may limit productivity in the littoral zone and more specifically, to take into account the confounding role of nutrient limitation on the outcome and interpretation of the monitor. The impact hypotheses were listed as follows:

- H<sub>0</sub>1: Average reservoir concentration of Total Phosphorus (TP), an indicator of general availability of phosphorus is not limiting to littoral primary productivity.
- H<sub>0</sub>2: Relative to the availability of phosphorus as indicated by level of total dissolved phosphorus (PO<sub>4</sub>), the average reservoir concentration of nitrate (NO<sub>3</sub>) is not limiting to littoral primary productivity.
- H<sub>0</sub>3: Water retention time ( $\tau_w$ ) is not altered by reservoir operations that vary from year to year such that it significantly affects the level of TP as described by Vollenweider's (1975) phosphorus loading equations (referred to here as TP( $\tau_w$ )).
- H<sub>0</sub>4: Water temperature, and hence the thermal profile of the reservoir, is not significantly altered by reservoir operations that vary from year to year.
- H<sub>0</sub>5: Changes in TP as a result of reservoir operations (through changes in  $\tau_w$ ) are not sufficient to create a detectable change in littoral algae biomass as measured by littoral levels of chlorophyll *a* (Chl<sub>a</sub>) and or ash free dry weight (AFDW).

The remaining impact hypotheses pertained directly to the management questions listed above and were stated as follows:

- H<sub>0</sub>6: Overall primary production (as measured by <sup>14</sup>C inoculation and/or as inferred from ash free dry weight data) of Stave reservoir is less than that of Hayward Reservoir.
- H<sub>0</sub>7: Pelagic primary production dominates in Stave reservoir while littoral production dominates in Hayward reservoir.
- H<sub>0</sub>8: Stable reservoir levels do not lead to maximum littoral development as measured by <sup>14</sup>C inoculation and/or inferred from ash free dry weight data.
- H<sub>0</sub>9: Water level fluctuations that raise the euphotic zone (defined here as the depth at which photosynthetically active radiation (PAR) is 1% that of the water surface) from lower elevations does not lead to a collapse of littoral primary production (as measured by <sup>14</sup>C inoculation and/or inferred from ash free dry weight data) that occurred near the prior 1% PAR depth.
- H<sub>0</sub>10: Littoral zone productivity, as measured by <sup>14</sup>C inoculation and/or inferred from ash free dry weight data, remains unchanged as reservoir water level stability increases.
- H<sub>0</sub>11: Changes in littoral productivity (as measured by <sup>14</sup>C inoculation and/or inferred from ash free dry weight data) can be expressed primarily in terms of changes in areal extent as defined by upper and lower boundary elevations. Within these boundaries, primary production does not vary in proportion to accumulated PAR exposure under wetted conditions.

## Objective and Scope

The overarching objective of this monitor was to collect and analyse the data necessary to test the impact hypotheses listed above and hence, address the five management questions identified by the CC. The following aspects defined the general scope of the study:

- a) The study area consisted of Stave Lake and Hayward Lake Reservoirs.
- b) Data were collected at four sites; three on Stave Lake Reservoir to address the potential for significant spatial differences, and one on Hayward Lake Reservoir to serve as a stable reservoir control.
- c) The program was carried out in two phases, an initial 3 year high-intensity sampling program followed by a less intense annual sampling program. Though not stipulated in the original terms of reference for the monitor, two other studies were carried out; one specially examining the effects of dewatering of periphyton survival (Bruce et al., 2011), and the other to specifically quantify the effects of different PAR intensities on periphyton survival (Bruce and Beer, 2014).
- d) The monitor was started in 2000, though some data collection occurred prior to this date as a pilot study. These earlier data however, were not included in the present meta-analysis as they did not fully conform to the methods used in the following survey work. Annual monitoring was completed in 2009, after which study efforts were directed towards resolving key uncertainties regarding the effects of dewatering and low light intensities on the survival of periphyton communities.

- e) The monitor focused only on those variables associated with, or indicative of littoral primary productivity, a parameter assumed to be a critical driver for overall reservoir productivity (J. Stockner, Ecologic Environmental, P Comm.).

## Methods

### Study Area

The Stave Falls power project consists of three reservoirs, four dams and three powerhouses (Figure 1) and is located roughly 15 km west of Maple Ridge BC. The uppermost reservoir, Alouette Lake Reservoir, feeds into Stave Lake Reservoir via a diversion tunnel located at its northern end. Outflows from Alouette Lake Reservoir are directed either through a powerhouse or a bypass tunnel that can be used in conjunction with the powerhouse to help regulate Alouette Lake Reservoir elevations. Use of the powerhouse however, has been infrequent in recent years due to reliability issues, thus the majority of outflows have been through the bypass tunnel. Stave Lake Reservoir can be viewed as being comprised of two basins; an upper basin that includes a deep-water lake (Stave Lake) fed by the outflows of Alouette Reservoir and the majority of the large tributaries in the watershed (including upper Stave River); and a lower basin that consists mainly of flooded river channel and is therefore much shallower than the upper basin. Both Alouette Lake and Stave Lake Reservoirs have the capability to store and release water for power generation and downstream flood control. Hence, Stave Lake Reservoir has highly variable water levels that can change seasonally in response to local inflows, power generation demands, and recreational requirements, while Hayward is more stable. The lower basin leads to Stave Falls Dam, which releases water to Hayward Reservoir. Like the lower basin of Stave Lake Reservoir, Hayward Reservoir is largely a flooded river channel with little capacity for storage. However, because of its length, it can be fairly deep at its downstream end and for the purposes of this study, was considered to be 'lake-like'.

This monitoring program was focused primarily on the hydrology and productivity of Stave Lake and Hayward Reservoirs. The hydrology of Alouette Lake Reservoir was taken simply as another source of inflow to the Stave Lake Reservoir, though its water quality may be unique due to its reservoir ecology and long running fertilization program (Harris *et al*, 2010). Of the two systems under study, Stave Lake Reservoir was considered the treatment system with its broad range of water level fluctuations - sometimes exceeding 8 m (but with the capacity for deeper drawdowns), while Hayward Reservoir was deemed the control system. Historically, water levels in Hayward Reservoir were relatively stable (variance < 1.5m) with periodic but short-duration drawdowns to carry out maintenance activity (generally every 2 years). However, starting in 2006, maximum reservoir elevation was dropped from roughly 42.7 m to 41.3 m to mitigate seismic concerns related to Ruskin Dam's aging infrastructure. A consequence of this operational change was a more stable reservoir elevation outside the typical drawdown periods (variance < 0.5m).

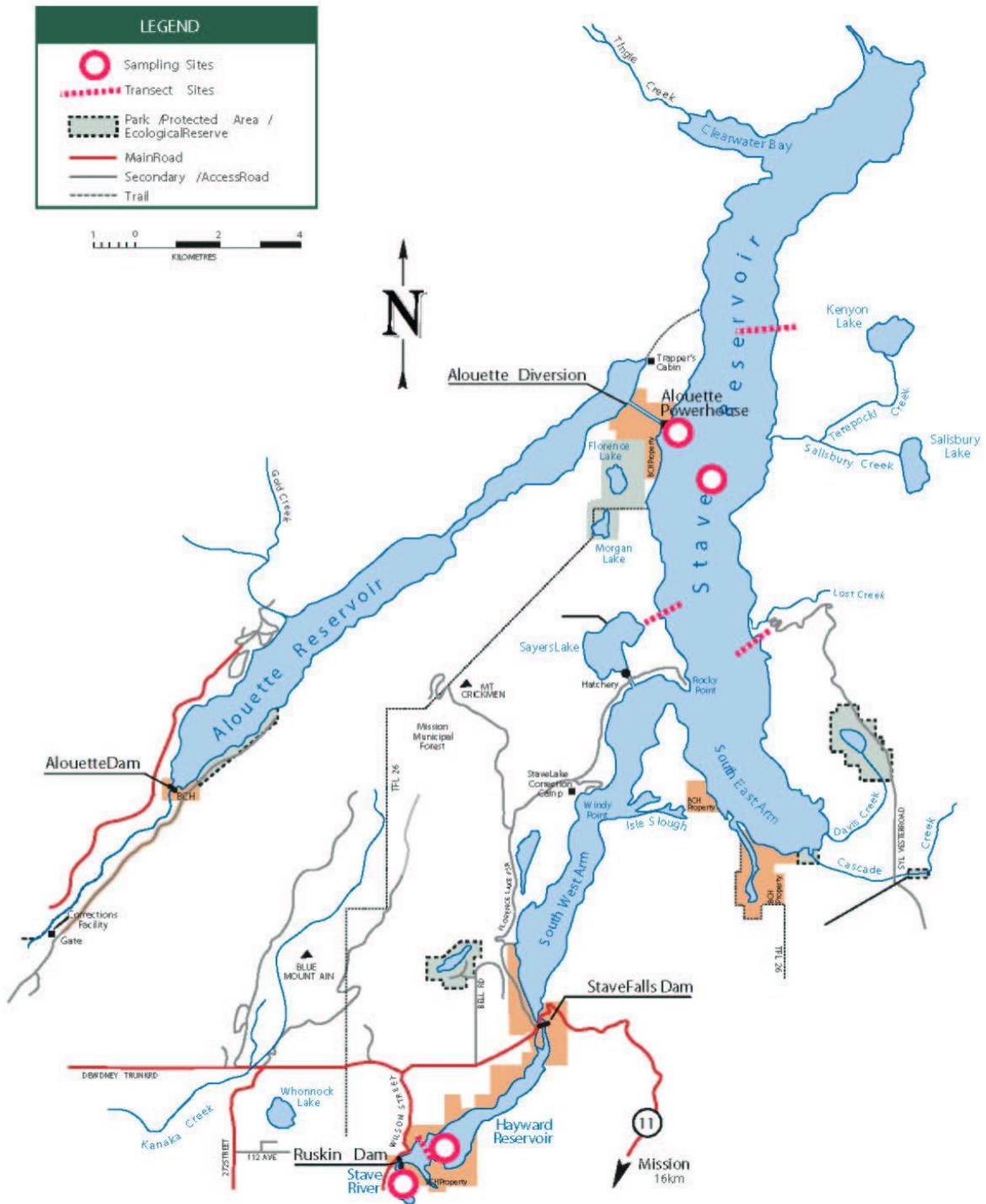


Figure 1. Map of Stave Lake and Hayward Lake Reservoirs showing monitor sampling locations. Red circles identify the location of water quality sampling sites while the dashed red line denotes the location of periphyton sampling transects.

## General Study Design

The general approach to the littoral zone monitor was predicated on a simple conceptual model of periphyton growth that assumed; 1) growth was proportional to light (i.e., PAR) intensity; 2) light intensity decreased exponentially with water depth; 3) at 1% of surface PAR intensity (i.e., compensation depth), there was insufficient light to sustain growth and biomass of periphyton would decrease over time; 4) at maximum PAR intensity near the water surface, growth was inhibited due to light saturation; and finally 5) when dewatered, periphyton dried out, were exposed to intense UV light and in turn experienced near complete mortality. Thus, for periphyton growing near the surface at a fixed depth and with a constant water surface elevation, the community would be expected to grow daily at a near maximum rate in response to a relatively consistent exposure to a high PAR values. In deeper waters, available light would decrease and in turn result in slower rates of growth. At the 1% light compensation depth, net growth would effectively be zero (i.e., the rate of growth occurs at the same rate of natural mortality). Obviously, no periphyton growth would occur above the water surface, and those communities found in such a situation would be expected to rapidly perish.

In a constant water level environment, the euphotic zone (the depth to which periphyton communities would be expected to grow) would be fixed given the conceptual model assumptions, and its bottom extent would be defined by the 1% light compensation depth. In a variable water level environment, the 1% compensation depth would vary in line with water surface elevation, causing the euphotic zone to vary in elevation over time (i.e. move up and down with water elevation changes). During drawdown periods, the euphotic zone would drop in elevation, allowing new periphyton communities to grow at deeper depths, but as water levels rise, these communities would eventually become starved of light and hence disappear over time. Similarly, with rising water levels, new areas above the water surface would be wetted allowing new communities to establish. With dropping water levels, however, these established communities would become stranded, are commonly de-watered, and eventually succumb to desiccation and the damaging effects of UV radiation. The area of littoral habitat that remains continuously wetted while receiving sufficient PAR to sustain growth has been defined here as the effective littoral zone or ELZ. When the amplitude of water level fluctuations is negligible, the ELZ would be expected to near its maximum value. As amplitude increases however, the ELZ would be expected to narrow and eventually disappear altogether when it exceeds the 1% light compensation depth.

Tests of these predictions formed the basis of the monitor's experimental design where Stave Lake Reservoir was the variable water level treatment and Hayward Reservoir the relatively stable or control treatment. In each reservoir system periphyton growth was measured on artificial substrate suspended 1 m above the reservoir bottom. These were placed along at least one transect line perpendicular to the shoreline at roughly 2 m depth intervals. Periphyton was measured at 10 sites along the length of the transect line in Stave Lake Reservoir, while there were only at 8 sites in Hayward Reservoir. Three transect lines were installed in Stave Lake Reservoir in order to estimate between-site variance, while only one transect line was installed in Hayward Reservoir, largely due to the limited area that was free of large woody debris and deep enough to accommodate the number of periphyton sampling sites. All transect lines were located in areas where shoreline slope was generally less than 30% grade. This helped ensure stability of the sampling apparatus over time (early attempts at setting up sampling sites found that the apparatus would migrate downslope over time in steeper shoreline habitat) and provided roughly 3 m of horizontal spacing between sampling sites so that they did not interfere with one another. The artificial plates were typically given 6 to 8 weeks for a measurable periphyton film to form prior to sampling. All

periphyton samples were collected in a single day, along with other ancillary water chemistry and physical data to characterise the growth environment.

These data in turn formed the foundation from which a more empirical form of the ELZ metric was derived. The ELZ metric developed and used during the WUP process was a conceptual construct and lacked empirical validation. The process of developing an empirically based ELZ metric was viewed as an opportunity to test the validity of the various ELZ model assumptions (the driver for many of the impact hypotheses listed above) and whether together as an ELZ metric, forms a meaningful measure of littoral productivity for decision making purposes. To assess the latter, the ELZ metric used in the WUP process ( $ELZ_{WUP}$ ) was recalculated for the pre-WUP base-case operating strategy, the expected operations with implementation of the WUP recommended “Combo 6” strategy, vs. the actual operations following implementation of the ‘Combo 6’ strategy. The outcome from these calculations was then compared to the same outcomes calculated using the empirically based ELZ metrics to determine if the expected post-WUP benefits could have been realized with ‘Combo 6’ implementation and whether this is supported in the empirical data collected. Through the process of carrying out these analyses, impact hypotheses were addressed and in turn, the management questions. Detailed descriptions of all the methodologies and analytical procedures used are provided in the sections that follow.

## Water Chemistry

Only three water chemistry related variables were considered in the present monitor: Total Phosphorus (TP,  $\mu\text{g/L}$ ), Total Dissolved Phosphorus (TDP,  $\mu\text{g/L}$ ) and Nitrate ( $\text{NO}_3$ ,  $\mu\text{g/L}$ ) levels. These were all collected as part of another monitoring program being carried out simultaneously focused on pelagic rather than littoral productivity. It was assumed that these pelagic data would adequately reflect littoral conditions so that seasonal and inter-annual trends could be taken into account during analysis of the littoral production data, as well as test impact hypotheses  $H_01$  to  $H_05$ .

All water chemistry data were collected at either one of two sites (Figure 1). The first was in Stave Lake Reservoir in the upper basin located in the center of the reservoir midway between the North and South periphyton transect sites. The other was in Hayward Reservoir, also at its center, but roughly 100 m upstream of the Hayward periphyton transect site. The sites were sampled every 6 to 8 weeks starting in March/April and ended October/November. The objective was to collect a minimum of 6 samples per site per year, all coinciding with the time of periphyton data collection. Actual sampling dates varied from year to year depending on prevailing weather conditions, and crew availability or boat access. In both reservoirs, the sole boat launch was not always usable depending on reservoir elevation.

Water quality samples at each of the sample sites were collected by a vertical, non-metallic Van Dorn sampler at 1, 3 and 5 m depths below the water surface. The three  $\sim 500$  ml samples were poured into a large (2 L) dark bottle and then mixed to get a single representative sample for the site. All sub-samples used to test for individual water quality parameters were drawn from this mixed epilimnetic sample.

Little field processing was required to prepare the TP sample for transport and laboratory analysis. Test tubes and caps (one per site) were first rinsed with the sampled water before being filled, capped and labelled. At no time was the mouth of the bottle or the inside of the cap touched to avoid contamination. Once filled, the sample test tubes were placed in a cooler on ice and then refrigerated until analysed within a two-day period. Once per field trip, two sample bottles of double distilled water (DDW) were prepared as blanks for comparison purposes.

Preparations for TDP and  $\text{NO}_3$  samples were more involved. The mixed epilimnetic water subsamples were field filtered using a 47 mm filtering manifold equipped with an ashed GF/F filter. Prior to filtering, the filter was rinsed with 180 ml of DDW, and then rinsed again with 180 ml of the sampled epilimnetic water. Plastic 120 ml sample bottles were then rinsed by filtering 60 ml of the mixed epilimnetic water into each bottle, which was capped and shaken. All filtrate to this point was discarded. The rinsed sample bottles were then filled with filtered epilimnetic water, capped tightly, and immediately frozen. Once per field trip, two sample bottles of DDW were prepared as blanks for comparison purposes.

All samples were immediately sent to SPAChemtest (DFO Laboratory at Cultus Lake, BC) for chemical analysis in order to maintain consistency throughout the 10year monitor.

Between-site comparisons were initially done using simple linear regression techniques to examine the nature of the relationship between the two sites, if any. This was followed by two-way factorial Analysis of Variance (ANOVA) to explore between year differences in nutrient levels at both sites collectively, as well as yearly trends at each site individually (i.e., site x year interactions). Where necessary, data were log transformed to ensure normality and homoscedasticity in the dataset. Sample size tended to differ for each of the factorial groupings, thus a computational approach that assumed an unbalanced design was used (Tabachnic and Fidell, 1983). Evidence for seasonal trends was explored subjectively by plotting the nutrient data on an ordinal date scale.

## Physical Characteristics

### Light

Photosynthetically active radiation (PAR) was measured at 1-metre intervals to a depth at which PAR was < 1% of surface readings. A LiCor Li-250 light meter (surface measurements) with an Li-192SA submersible quantum sensor (under water measurements) were used to collect the data, all of which were recorded in units of  $\mu\text{mol}/\text{m}^2/\text{s}$ . A light weight was used to keep the sensor vertical while taking deep water measurements, and care was taken to ensure that the boat did not cast a shadow over the sensor. A single light profile was collected mid-reservoir from Stave Lake and Hayward sampling sites during each nutrient sampling trip (Figure 1). Additional profiles were collected in some years in the vicinity of the periphyton sampling transects in Stave reservoir, including a site opposite the Alouette powerhouse. As a result, over the course of the monitoring period, vertical light profiles were collected at 4 different sites in Stave Lake Reservoir, but not in all years. Vertical profiles of PAR were log transformed and then regressed against water depth to estimate the light extinction coefficient 'k' (slope of the regression) and surface PAR radiation (intercept of the regression). The surface radiation estimates were then compared to measured values obtained by the LiCor Li-250 light meter to confirm accuracy as well as develop an equation to transform the full spectrum solar irradiation to values to PAR. All analyses, which included use of regression and ANOVA techniques, were focused primarily on the individual light extinction coefficient data. In cases where normality or homoscedasticity assumptions could not be met, the coefficients were transformed to 1% light compensation depths (m) by solving each regression equation for water depth assuming a 99% loss in intensity from measured surface PAR readings.

The surface irradiance measurements were also compared to global solar radiation values that were continuously collected by LiCor pyranometers (LI-200SA) at four different locations in the vicinity of the study area by the Greater Vancouver Regional District (GVRD). These were:

- T09 – Rocky Point Park, Port Moody
- T12 – Chilliwack Airport
- T32 – Douglas College, Coquitlam

### T34 – Abbotsford Airport

The data provided were in the form of hourly average radiation values (wavelengths from 400 to 1100 nm) reported in units of  $W \cdot m^{-2}$ . The four sites were needed as there were many gaps in the data set given. This ensured full coverage for the entire monitoring period. Regression analysis was used to determine which of the data sets best predicted solar conditions at the Stave Lake and Hayward locations, as well as the best strategy to deal with data gaps. The objective of this analysis was to develop a daily time series of solar radiation values that could be used as a potential predictor variable for periphyton growth. The hourly solar radiation values were calibrated to reflect Stave and Hayward conditions using the regression equations, transformed to a surface PAR using a regression equation equating surface light readings to surface PAR, and then summed across each 24-hour period to yield a time series of daily accumulated PAR values for the duration of the monitoring program. Analysis of this dataset consisted primarily of time plots and yearly comparisons.

The surface PAR data were then used to derive accumulated PAR over the course of each growth period at a given site by calculating PAR at each of the periphyton growth plate elevations using the derived extinction coefficients in

$$PAR_{Plate\_z,d} = PAR_{Surface,d} * e^{-kz} \quad (\text{Eq. 1})$$

Where  $PAR_{Plate\_z,d}$  is the PAR intensity at a given growth plate on day 'd' found at depth 'z' below the water surface, and  $-k$  is the seasonal average extinction coefficient for the reservoir of interest. For the purposes of this modeling exercise, plates above the water surface had their PAR totals reset to 0, assuming that dewatering for one or more days would result in 100% mortality all periphyton growth, and that growth would only resume when re-submerged. The  $PAR_{Plate\_z}$  data were summed across each day of growth to derive an accumulated total PAR value which was then divided by the number of growing days, yielding an average PAR intensity for the plate of interest;

$$PAR_{Plate\_z} = (\sum^t PAR_{Surface,d} * e^{-kz}) / t \quad (\text{Eq. 2})$$

These data were then used to explore relationships with periphyton growth rates, as well as in models to predict depth integrated production for comparison with observed values.

### Water Temperature

Water temperatures at each of the transect sites was only measured in years 2002 and 2003. In subsequent years (2005 onward) measurements were only taken at a single mid-reservoir site in Stave Lake Reservoir, and a single site on Hayward reservoir. The data were collected at 1 m intervals, but only to depths ranging from 8 to 25 meters, sometimes missing the thermocline depth that delineates the lower extent of the summer epilimnion. In most cases, water temperature was relatively constant throughout the range of depths measured, even during the summer. As a result, analysis was limited to depth-averaged temperatures that extended only to a maximum depth of 8 m, ensuring consistency in measurement protocol between all sites and years. All temperature data were collected by an Oxy-guard Handy portable water temperature meter that measured temperature to the nearest 0.2°C.

For the present analysis, only the data collected from 2005 onward were considered for analysis as this represents the longest times series of consistently collected data In Stave Lake Reservoir. The water temperature sampling site tended to vary in location, sometimes being more closely in line with the Stave North transect and other times the Stave South. Site selection however, was often driven by time constraints and prevailing sampling conditions, though attempts were made to evenly split sampling effort. Nevertheless, data were not evenly distributed between all years and sites and in fact, some



year/site combinations were not sampled at all. Consequently, between-site and between-year comparisons were only analysed using separate single factor ANOVAs. Analysis of site and year interactions was not possible. Seasonal trends were analysed by simply plotting depth averaged temperature as a function of ordinal date. Trends with other independent variables were explored using regression techniques that involved data transformation when required to ensure normality and homoscedasticity of residuals.

There were long gaps in the water temperature dataset as a result of the interval sampling protocol. To fill these data gaps, regression analysis was used to develop predictive equations from the available solar radiation data with the objective of developing a time series of daily surface water temperatures spanning the entire monitoring period. The time series was then used to calculate average water temperatures during each of the periphyton incubation periods so it, along with the observed temperature data, can be assessed as potential predictor variables for periphyton growth. Details of this exploratory analysis are presented in the results section.

## Hydrology

All hydrology data were provided by BC Hydro in the form of daily average values for total inflow to Stave Lake reservoir, the change in reservoir elevation, total inflow to Hayward reservoir and corresponding change in reservoir elevation. Data analysis consisted of yearly comparisons to summarize differences through time, as well as time plots of daily average values to highlight between-reservoir differences. Water retention rate was calculated on an annual basis by first determining reservoir volume ( $\text{m}^3/\text{s-days}$ ) at the yearly median water elevation and then dividing it by the yearly sum of daily average discharges ( $\text{m}^3/\text{s-days}$ ). The reservoir volume data were provided by BC Hydro.

In addition to these summary statistics, average inflow discharge to each reservoir was calculated for each periphyton growth incubation period (lasting between 24 and 77 days) for use in trend analyses, while the effects of water level fluctuation were evaluated by calculating and comparing the standard deviation about each average inflow discharge. A more effective test of the effects of water level fluctuation was done by incorporating daily reservoir elevation as part of a daily periphyton growth simulation model akin to the ELZ (see below).

## Periphyton

Periphyton growth was measured by repeatedly sampling periphyton biomass grown on artificial substrate placed at regular depth intervals along permanently established transect lines (Figure 1). The artificial substrate consisted of Plexiglas plates scuffed with sand paper to create a roughened surface that facilitated periphyton attachment. The plates were also scored into 100  $\text{cm}^2$  quadrants to standardise sampling. All Plexiglas plates were mounted on inverted, Styrofoam filled trays that were in turn attached to cinder block anchors by steel cable (Figure 2). This allowed the plates to float horizontally above the anchor blocks by about 1 m, keeping them well above the loose bottom sediments that were sometimes kicked up during the plate retrieval process. The plates were held on to the floating trays by a pair of spring clamps that they could easily be removed by scuba diver, placed into a purpose-built Plexiglas case and brought to the surface for sampling. Use of the case ensured that none of the accumulated periphyton would slough off while on route to the surface. Once sampled, the entire plate was scraped clean of accrued material using a glass slide and brought back to the anchor location to start the next growth phase.

The Plexiglas plates were placed at 2 m ( $\pm 0.5$  m) depth intervals along each transect line beginning at the 'full pool' elevation. The deepest plate was placed 1 m below the 1% light compensation depth at

the normal “low pool” elevation. Three transect lines were established on Stave Lake reservoir (Stave North, Stave South and Stave West), and only one line on Hayward reservoir (Figure 1). A total of 10 anchored sampling plates spanning 20 vertical meters of shoreline were installed per transect on Stave Lake Reservoir, while only 8 plates were required in Hayward Reservoir due to its shallower depth and infrequent drawdowns.

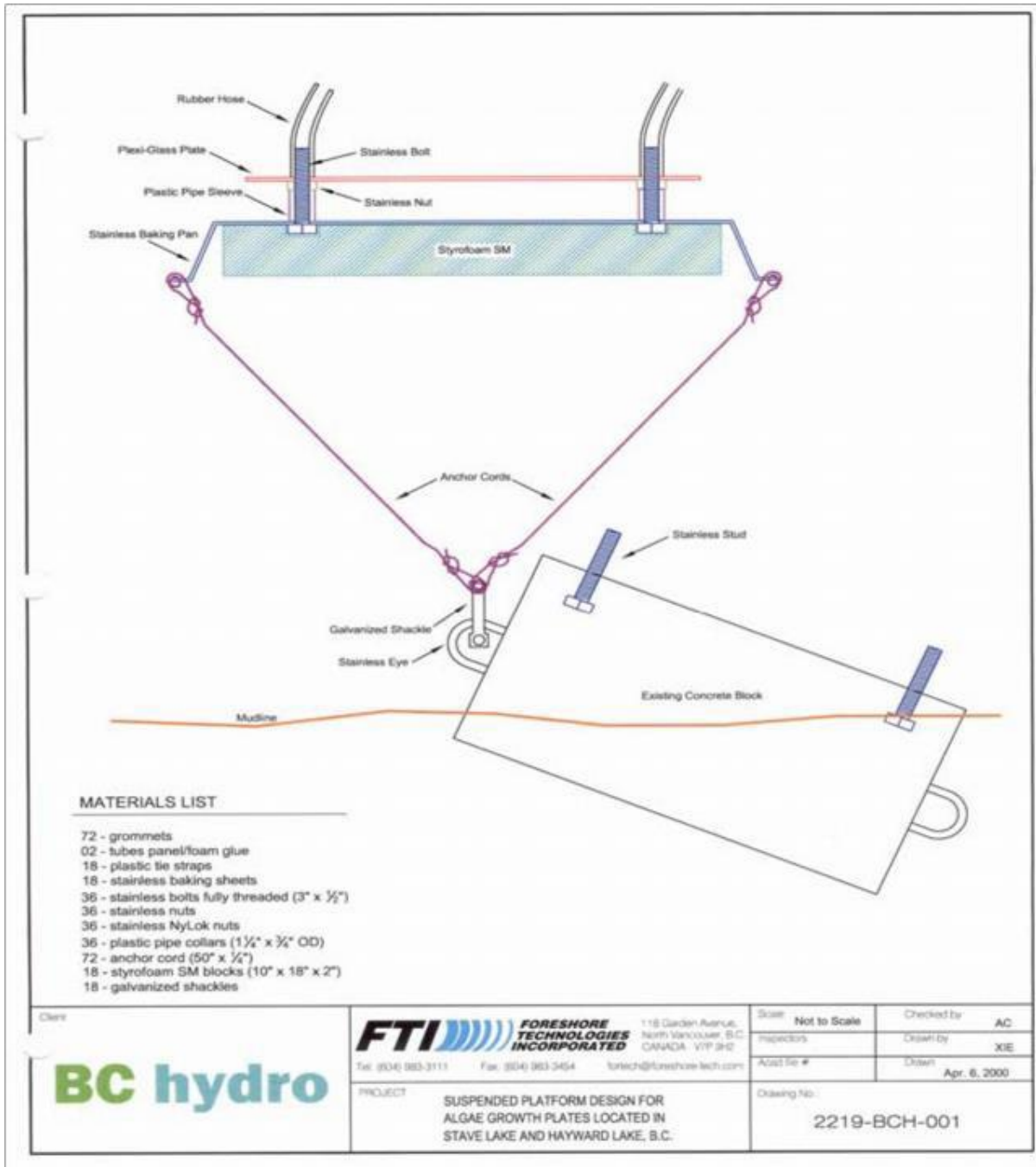


Figure 2. Schematic diagram of periphyton growth plate set up consisting of a scuffed Plexiglas plate as the artificial growth substrate, floating tray holding the plate well above bottom sediments, and a large concrete anchor block.

The Plexiglas plates were sampled every 6 to 8 weeks starting March/April. All samples at all sites were collected on the same day of sampling to ensure between-site comparability. No samples were collected during the winter months after the 1<sup>st</sup> week of December. However, the sampling plates were left in place till the spring of next year where they were scraped clean or replaced with new ones as required to launch the new sampling year. Though a subsample of these initial periphyton scrapings were processed to determine AFDW, the data were excluded from analysis due to the extended growth period that was inconsistent with the rest of the year's sampling.

Periphyton samples were collected by scraping clear a 10 cm by 10 cm area of each Plexiglas plate with a glass slide and transferring the material into a labeled plastic jar using a stream of lake water. The samples were labeled, stored in a cooler and taken to the laboratory for immediate processing at the end of the sampling session. Additional samples were also collected for Chl<sub>a</sub> analysis and <sup>14</sup>C Radio assay. Sampling procedures and analytical results associated with these samples can be found in Appendices A and B respectively.

In the laboratory, the periphyton samples were filtered at low vacuum pressure into a pre-weighed, pre-ashed, 0.45 µm, 47 mm glass fibre filter (GFF). The filter sample was placed in an aluminium weigh boat and dried in an oven at 100°C for 12-24 hours to ensure all moisture was eliminated from the filter sample. The oven-dried filter sample was then weighed and recorded as dry-weight ( $DW_{oven}$ ). The oven-dried filter samples were then ashed at 500°C in a muffle furnace for a minimum of 5 hours and then re-weighed ( $DW_{muf}$ ). Ash free dry weight (AFDW) was calculated as the difference between the  $DW_{oven}$  and  $DW_{muf}$  and expressed in terms of the mass of organic matter per unit area ( $mg/m^2$ ).

Incubation periods between biomass sampling events varied considerably over the course of the monitor. The shortest period was 24 days, while the longest was 78 days (this excluded the over wintering incubation samples that were discarded at the start of each sampling year) and the median duration was 40 days. To account for the different durations when comparing the biomass data, the original terms of reference simply required the biomass values be divided by the incubation period to yield a measure of productivity ( $mg/m^2/day$ ) However, the work of Bruce and Beer (2010) showed that the periphyton biomass tended to increase exponentially over time, with no evidence of slowing down even after 12 weeks of growth. This, combined with the broad range of incubation periods, was found to introduce unacceptable error when computing biomass production. To increase accuracy and hence allow for more robust between-site or between-year comparisons in littoral periphyton production, the AFDW data was instead used in the following equation, which estimated the rate of exponential growth ( $b$ ) based on two data points:

$$b = \ln((x_t + x_o)/x_o)/t \quad (\text{Eq. 3})$$

where  $x_t$  is the AFDW biomass of periphyton at the end of a growth period lasting  $t$  days, and  $x_o$  is the starting biomass at time  $t = 0$ . It should be noted that 'b' represents the intrinsic biomass growth rate of the periphyton community being measured and has units of proportion per day. Unfortunately, the methods used in this monitoring program did not include a provision to directly measure a starting biomass ' $x_o$ '. It was however, assumed to be  $100 \mu g/m^2$  based on the study of periphyton growth by Bruce and Beer (2010) which showed that starting biomass on similarly treated artificial substrate typically ranged from  $50$  to  $160 \mu g/m^2$ . This value was also added to  $x_t$  to account for the fact that the starting biomass always comprised of residual organisms trapped on the roughened surface of the artificial growth substrate after it was scraped clean of periphyton during the AFDW sampling procedure. It was assumed that the starting biomass was the same for all plates and all sampling periods. Finally, the transformation

was only done on those AFDW samples where the corresponding sampling plates were continuously submerged during the growth period. This avoided the confounding effects of substrate dewatering that sometimes resulted from fluctuations in reservoir elevation. The outcome of this transformation process was a dataset of growth rates that could be directly compared between sites and years, as well as a function of water depth and solar irradiance.

Water chemistry and other physical variables describing the growth environment during each incubation period were not available for all sampling depths. To assess their effects of periphyton growth, the biomass data were first integrated (summed) across all water depths to obtain a depth-integrated biomass value, which was then used in Eq. 3 to yield a measure of depth integrated growth. The starting biomass ( $x_0$ ) needed for this calculation was obtained by multiplying the  $x_0$  for individual plates ( $100 \mu\text{g}/\text{m}^2$ ) by the number of plates that were continuously submerged during the growth period of interest. The estimates of depth integrated periphyton growth rates were then analysed for relationships with water chemistry and other physical attributes measured at the time of sampling using multiple correlation techniques. In the analysis, it was assumed that the water chemistry, light compensation depth and temperature data collected at the time of biomass sampling reflected growing conditions throughout the incubation period. In addition to these data, the average and standard deviation of water surface elevations were calculated for each reservoir across each incubation period. Because a reconstructed time series was available, average surface PAR levels and average water temperatures during the incubation period were also added to the analysis. Between-site and between-year differences were explored using ANOVA, and annual trends were explored using simple time plots.

Analysis of the periphyton data at all water depths required that they be examined in terms of a functional relationship, much like the PAR data that were analysed in terms of extinction coefficients (Eq. 2). From the conceptual ELZ model described Failing (1999), the functional relationship initially considered most applicable was the maxima function of the form  $y = Ax \cdot e^{-nx}$ , which characterises a curve shape that is bell-like and skewed towards the origin. This was considered analogous to the expected periphyton growth curve where growth would be near zero at the water's surface due to photo inhibition, increase exponentially as the inhibitory effects abate with increasing water depth, reach a peak at a depth where PAR is at an optimum level, and then fall in intensity as light levels drop exponentially with further increases in water depth. Though this function was successfully fitted to most depth vs periphyton growth data sets, it tended to grossly under estimate periphyton growth near the surface. In fact, a review of all depth vs periphyton growth data sets found little evidence of photo-inhibition – a key premise for the use of this functional form (see discussion below). Furthermore, cases that were suggestive of photo inhibition tended to occur at all times of the year where one would only expect it in mid-summer. In addition, all of these cases could be explained by the effects of periodic dewatering during the growing phase between sampling dates. As a result, the maxima function was abandoned and a hyperbolic saturation function was used instead.

In adopting the saturation function, water depth could not be directly used as a predictor variable. Rather light intensity was more appropriate. A saturation function is typically used to describe the Michealis-Menten kinetics of enzymatic chemical reactions where initially, reaction rates increase as a function of input chemical concentration, but the rate of rise decreases as enzymes become increasingly saturated. Eventually the enzymes are fully saturated and no further increase in reaction rates are possible, regardless of the quantity of input chemical. This process was considered to be characteristic of the relationship of periphyton growth and light intensity (Wetzel 2001), where in low light intensities, growth increases rapidly as intensity rises, but as light intensity begins to saturate the photosynthetic

processes, further increases in growth rates begin to slow down. Eventually a point is reached where further increases in light intensity have little effect on growth rate. The equation describing the saturation equation was of the form;

$$y = Ax/(B + x) \quad \text{Eq. 4}$$

where in the present case A = maximum periphyton growth rate regardless of light intensity, B = the PAR intensity at which periphyton growth was 50% of maximum, x = PAR intensity, and y = predicted periphyton growth rate. Fitting the hyperbolic saturation equation to the water depth vs periphyton growth data sets required two data transformations. The first was a conversion of average water depth during each growth period to a measure of average PAR intensity. This was done using equations 2 and 3 above. The next transformation was to take the inverse of the measured growth rate (determined using Eq. 4) and multiplying it by the corresponding PAR intensity value. The result is a linear relationship between light intensity and the transformed growth variable that can be solved using simple linear regression. Maximum growth rate 'A' was obtained by taking the inverse of the regression slope, and the light intensity where growth was 50% of maximum (B) was obtained by dividing the intercept by the slope. This was done for all paired water depth and periphyton growth data sets. The result was a set of two new parameters that could be examined for relationships to the water chemistry and physical environment data, as well as for between site or between year differences using ANOVA techniques.

To minimize the confounding effects of water level fluctuation, only those plates that were continuously submerged for the entire between sample growth periods were used in the analyses above. As well, it was assumed that the effects of PAR intensity over the course of the growth period were additive and therefore reasonably summarized by an average PAR intensity value that could be considered independent of water level fluctuation (this assumption should be tested, but is considered outside the scope of the present analysis). To incorporate the effects of water level fluctuation, results of the saturation equation analyses were used to construct a typical saturation curve for a given site and then used in a recursive algorithm where periphyton biomass was predicted on a daily time step and then compared to the data set of observed biomass values using regression techniques. High correlations indicated a robust periphyton growth model that successfully tracked the effects of reservoir operations. The recursive algorithm assumed 100% mortality if a plate was dewatered for a day (Bruce and Beer 2010), and assumed a starting biomass of 100 mg/m<sup>2</sup> when plates were newly wetted.

## ELZ Modelling

Two ELZ models are tested in this study. The first of these, a "conceptual" ELZ model, was developed during the WUP process based on general concepts of periphyton growth. It was used during the WUP process to explore the consequences of variable reservoir elevations on littoral development and ultimately as a performance measure in trade-analysis with other values. The other is developed as part of the present study and is empirically derived from the water quality, physical attributes, hydrology and periphyton growth data collected as part of the WUP ELZ monitoring program. The latter model is referred to as the "empirical" based ELZ model.

The conceptual ELZ model/performance measure used during the WUP assumed a constant 8 m deep euphotic zone that rose and fell daily with reservoir elevation (Failing 1999). For each day of reservoir operation between March 1 and October 30 (bracketing the period of greatest periphyton growth in the reservoir), each 0.1 m depth interval between El 63 m and El 85.5 m that was wetted and within the 8 m euphotic zone was assigned a binary value of 1, indicating that there was the potential for littoral periphyton growth. A depth interval that did not fit this criterion were assigned a value of 0. These

binary values were added to the sum of previous depth specific values computed to date. For those 0.1 m depth intervals that became dewatered on the day of interest, the assigned value for growth potential was reset to zero assuming 100% mortality of dewatered periphyton. At the end of each year, the depth-specific sums were integrated across all water depths. The depth-specific sums were then divided by the grand total to obtain a proportional value that can be integrated across a range of depths. The results were then summed across all depths to create a cumulative depth distribution function from which the 10<sup>th</sup> and 90<sup>th</sup> percentile values could be obtained. The depth at which these statistics were found were then used to define the elevation boundaries of the effective littoral zone. From a relationship that gives the hectare area of shoreline habitat that has a gradient less than 15° at 0.1m intervals (provided by BC Hydro), the total area of ELZ habitat was estimated by summing the depth specific shoreline habitat areas between the ELZ elevation boundaries. The end result is an estimate of shoreline habitat area with a slope less than 15% (the limit at which sediments can accumulate as epipellic soil and periphyton mats don't slough, J. Stockner, Pers. Comm.) that received adequate light for photosynthesis and remained wetted sufficiently so as not to significantly impact periphyton biomass growth during the reservoir's main growing season; i.e., the ELZ metric measured in units of hectares.

This computation was repeated for each year of simulated or actual reservoir elevation data. The individual data sets used in the ELZ calculation were as follows:

Pre-WUP<sub>Obs</sub> : Measured reservoir elevations in Stave and Hayward Lakes for years 1984 to 1995 (provided by BC Hydro)

Pre-WUP<sub>Sim</sub> : Simulated "base case" reservoir elevations in Stave and Hayward Lakes for years 1969 to 1995 (WUP Simulation dataset, Failing 1999)

WUP<sub>Obs</sub> : Measured reservoir elevations in Stave and Hayward Lakes for years 1999 to 2014 (provided by BC Hydro)

WUP<sub>Sim</sub> : Simulated "Combo 6" reservoir elevations in Stave and Hayward Lakes for years 1969 to 1995 (WUP simulation dataset, Failing 1999)

The yearly ELZ calculations were summarised in terms of median values for each data set, along with corresponding 5<sup>th</sup> and 95<sup>th</sup> percentile values.

Calculation of the empirically derived ELZ metric followed the same procedures as the conceptual version, but with a few changes. Rather than assign a value of 1 for each day and depth-specific interval, an AFDW biomass value is assigned based on the predictive growth relationships developed from the monitoring data. Because there were three monitoring sites in Stave Lake, three site specific biomass values were calculated and then averaged before assignment. Also, because AFDW biomass is tracked in this version of the ELZ metric, the depth specific biomass data can be multiplied directly to the depth specific shoreline area data to yield an estimate of periphyton standing crop (kg/ha) at the end of each year of calculation. Like the conceptual ELZ metric, this integration procedure was only carried out between the 10 and 90<sup>th</sup> percentile boundaries of the ELZ so that the two versions can be directly compared. Comparisons between the various ELZ outcomes was done primarily by plot comparisons using summary statistics such as the median and 95th percentile data.

## Results

### Water Chemistry

Over the course of the 10-year monitoring period, a total of 51 water chemistry observations were made at each site. There were some instances however, when the laboratory results were deemed inconclusive and a missing value was entered. This was most often the result of improper sample storage during transport to the lab, or an excessive delay between sample collection and laboratory analysis. These occurrences were rare however, and scattered throughout the dataset. Given the number of samples collected, the loss of these data was not considered to have a significant impact on overall analytical outcomes.

It should be noted that no water chemistry data was collected in 2004, and only two sets of observations were made in 2003 and 2005.

### Total Phosphate (TP)

Total Phosphate concentrations averaged 2.2 µg/L in Stave Lake Reservoir over the course of the 10-year monitoring period (SD = 0.99, n = 46). During that same period in Hayward Reservoir, TP was found to be slightly higher with an average TP concentration of 2.9 µg/L (SD = 1.41, n = 46). Though there was a statistically significant positive correlation between the two sites, shared variance was low ( $R^2_{Adj} = 0.160$ ,  $P = 0.0045$ ). The positive correlation indicated that the difference between reservoirs tended to be consistent across all sampling days, and could be predicted by the following regression equation:

$$(TP_{\text{Hayward}} = 0.636 * TP_{\text{Stave Lake}} + 1.566) \quad \text{Eq. 1}$$

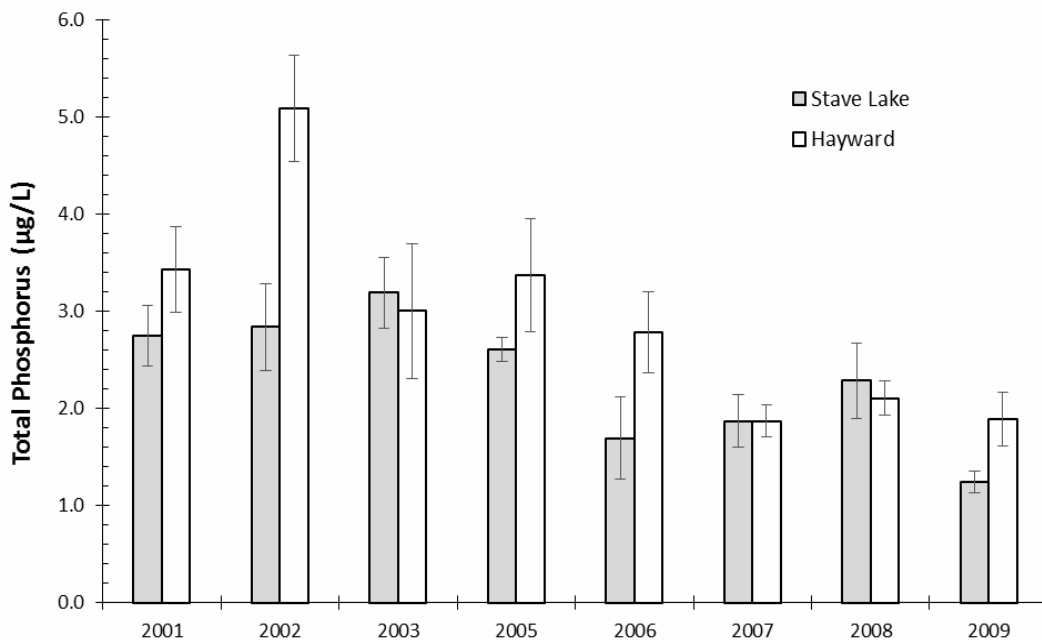


**Figure 3. Plot of yearly average total phosphorus levels (µg/L) in Stave Lake and Hayward Reservoirs for each year of the monitor (2000 – 2009). The error bars mark the 95% confidence limits about the computed yearly means.**

**Table 2. Results of a two way, unbalanced factorial ANOVA on the Total Phosphate data ( $\mu\text{g/L}$ ) collected at two sites (Stave Lake and Hayward Reservoirs) over a 10 year period (2000 – 2009).**

ANOVA					Alpha	0.05
	<i>SS</i>	<i>df</i>	<i>MS</i>	<i>F</i>	<i>p-value</i>	<i>sig</i>
Site	6.896	1	6.896	8.597	0.0044	yes
Years	58.649	7	8.378	10.445	0.0000	yes
Interaction	14.243	7	2.035	2.537	0.0212	yes
Within	60.962	76	0.802			
Total	144.932	91	1.593			

Average TP varied significantly between years (Table 2), showing a declining trend over time that was apparent in both reservoirs (Figure 3). There were also significant differences between sites, though they were not consistent across all years. In some years, TP values between sites were very similar to one another. This was reflected in a significant ANOVA interaction term (Table 2). A plot of TP as a function of ordinal date showed that there was no persistent seasonal trend in the data, regardless of site (Figure 4).

#### Total Dissolved Phosphate

Total dissolved phosphate levels averaged  $1.4 \mu\text{g/L}$  ( $SD = 0.77$ ,  $n = 44$ ) and  $1.6 \mu\text{g/L}$  ( $SD = 1.04$ ,  $n = 44$ ) over the 10-year monitoring period at the Stave Lake and Hayward Reservoir sites respectively.

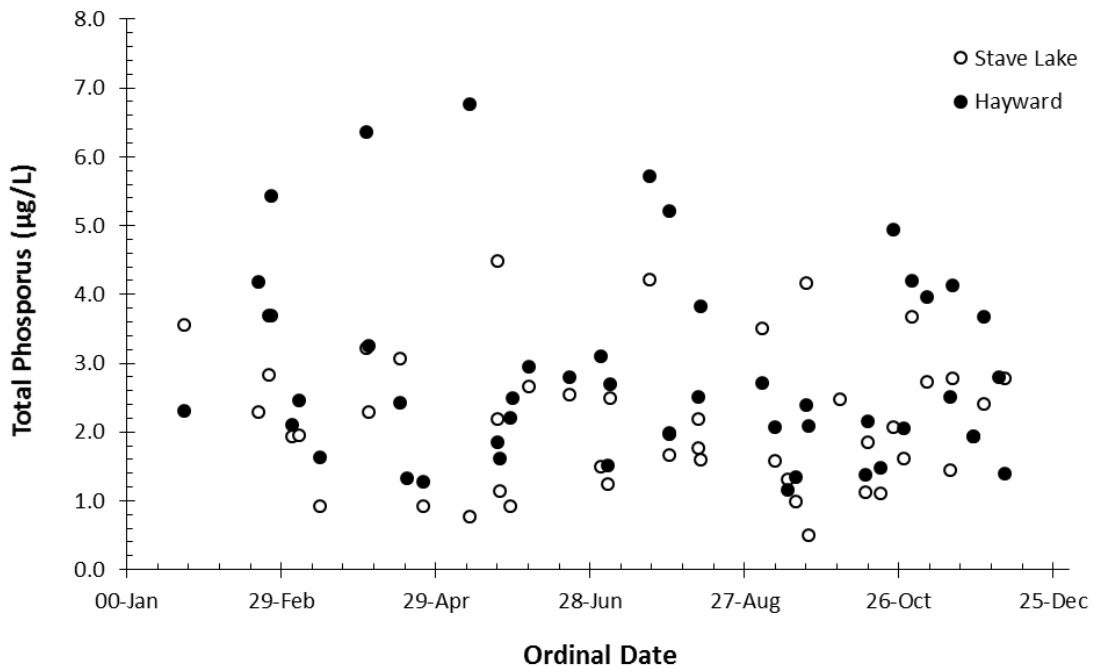


**Figure 4. Total phosphorus ( $\mu\text{g/L}$ ) plotted as a function of ordinal date showing lack of a persistent seasonal trend in observations over the 10-year period of data collection (2000 – 2009). This was apparent at both monitoring sites (Stave Lake and Hayward Reservoirs), though there was a tendency for Hayward levels to be higher than those at Stave Lake.**



Regression analysis was able to show that the two sites were highly correlated ( $R^2_{Adj} = 0.499$ ,  $P < 0.0001$ ). The slope ( $s = 1.02$ ,  $F_{1, 78} = 0.075$ ,  $P < 0.001$ ) was near unity (95% CI = 0.709 to 1.331) and the intercept (0.13,  $t = 0.542$ ,  $P = 0.59$ ) was not significantly different from 0, suggesting that the TDP concentrations at each site tended to be very similar. The relatively low regression coefficient of determination however indicated that there was considerable sampling error in the measurements.

This was confirmed by two-way ANOVA (Table 3), which found no significant difference between samples sites regardless of sample year (Figure 5). There was however a significant declining trend in TDP over the course of the monitoring period that was similar to that found in the TP data. In general, TDP levels in that last 4 years of the monitor was roughly 50% that of the first 4 years (Figure 6). A plot of TDP concentration as a function of ordinal date showed that there was no persistent seasonal trend in the data at either site (Figure 6).

**Table 3. Results of a two way, unbalanced factorial ANOVA on the Total Dissolved Phosphate data ( $\mu\text{g/L}$ ) collected at two sites (Stave Lake and Hayward Reservoirs) over a 10 year period (2000 – 2009).**

ANOVA					Alpha	0.05
	<i>SS</i>	<i>df</i>	<i>MS</i>	<i>F</i>	<i>p-value</i>	<i>sig</i>
Site	1.089	1	1.089	1.424	0.2366	no
Years	18.573	7	2.653	3.472	0.0029	yes
Interaction	2.964	7	0.423	0.554	0.7904	no
Within	55.027	72	0.764			
Total	77.154	87	0.887			

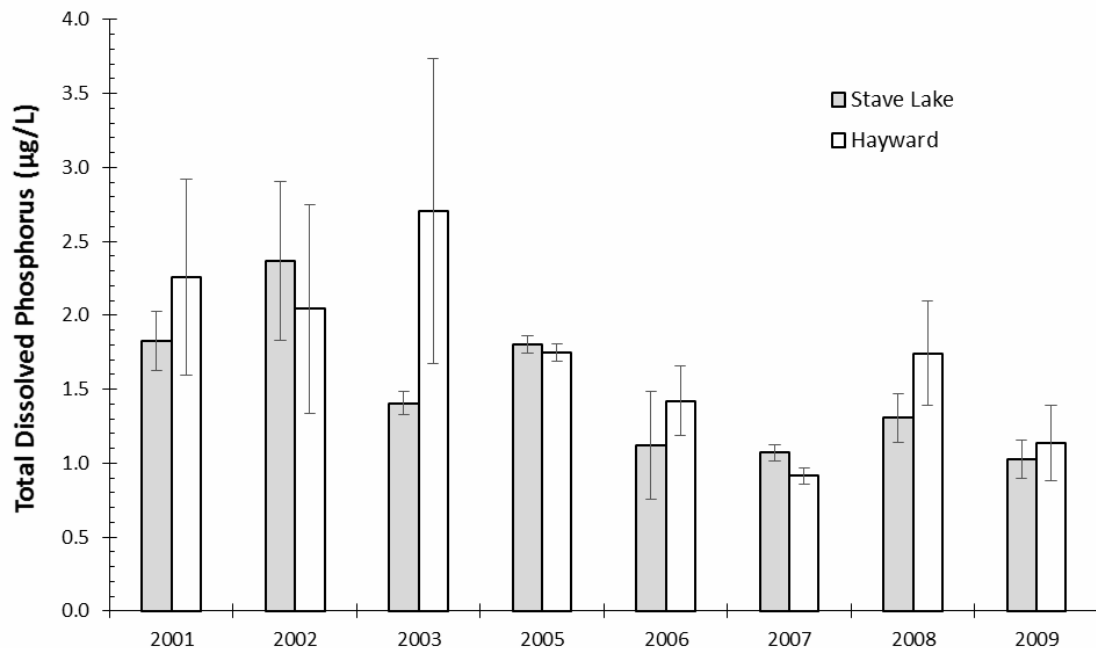


**Figure 5. Plot of yearly average total dissolved phosphorus levels ( $\mu\text{g/L}$ ) in Stave Lake and Hayward Reservoirs for each year of the monitor (2000 – 2009). The error bars mark the 95% confidence limits about the computed yearly means.**

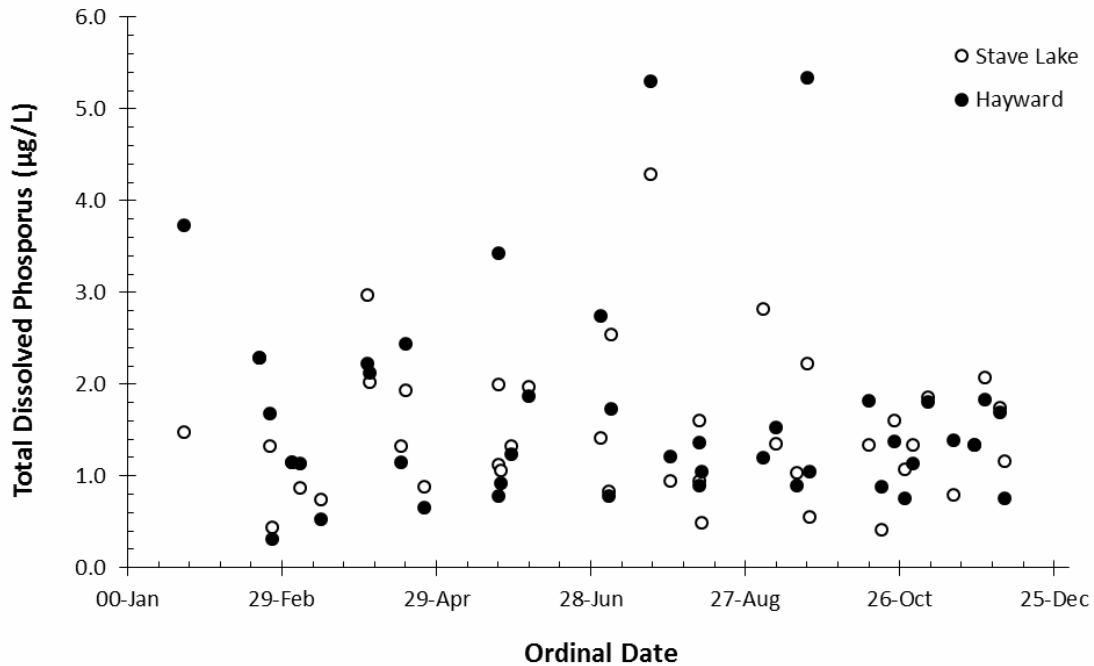


**Figure 6. Total dissolved phosphorus (µg/L) plotted as a function of ordinal date showing lack of a persistent seasonal trend in observations over the 10 year period of data collection (2000 – 2009) at both monitoring sites (Stave Lake and Hayward Reservoirs).**

A statistically significant but weak correlation between TDP and TP ( $r = 0.533$ ,  $P < 0.001$ ) was uncovered through regression analysis. Analysis of covariance on the log transformed data (used to normalise the distribution of regression residuals) found the slopes and intercepts of the relationship were similar between the Stave Lake and Hayward sites ( $F_{1, 78} = 0.075$ ,  $P = 0.785$ ,  $F_{1, 78} = 0.102$ ,  $P = 0.751$  respectively). It would appear that dissolved phosphorus concentrations at the Stave Falls site passed through the lower sections of the reservoir and on through the Hayward system largely unchanged.

### Nitrate

Nitrate levels at the Stave Lake and Hayward sites found to be highly correlated ( $R^2_{Adj} = 0.964$ ,  $P < 0.0001$ ) and very similar to one another (slope = 0.91,  $P < 0.0001$ , intercept = 7.64,  $P = 0.0111$ ). Over the 10-year monitoring period,  $NO_3$  averaged 103.9 µg/L (SD = 36.8,  $n = 48$ ) at the Stave Falls site and 106.3 µg/L (SD = 39.9,  $n = 48$ ) at the Hayward site. The lack of a significant difference was confirmed by two-way factorial ANOVA which found this trend to be consistent across all years of monitoring (Table 4). There was however a significant declining trend in  $NO_3$  over time that was similar in character to other nutrient related water chemistry data (Figure 7).

A plot of  $NO_3$  as a function of ordinal date uncovered what appeared to be a strong and persistent seasonal trend with peak  $NO_3$  levels ranging from 120 to 170 µg/L occurring in late winter, a gradual decline in levels over the course of spring and summer periods where it reached a late summer/early fall low ranging 30 to 90 µg/L, and a rapid increase in levels during early winter to late winter highs (Figure 8). Throughout the cycle,  $NO_3$  values tended to stay within  $\pm 25$  µg/L range.

**Table 4. Results of a two way, unbalanced factorial ANOVA on the nitrate levels ( $\mu\text{g/L}$ ) collected at two sites (Stave Lake and Hayward Reservoirs) over a 10year period (2000 – 2009).**

ANOVA					Alpha	0.05
	<i>SS</i>	<i>df</i>	<i>MS</i>	<i>F</i>	<i>p-value</i>	<i>sig</i>
Site	238.093	1	238.093	0.175	0.6771	no
Years	29272.940	7	4181.849	3.068	0.0065	yes
Interaction	188.500	7	26.929	0.020	1.0000	no
Within	109033.019	80	1362.913			
Total	138636.103	95	1459.327			

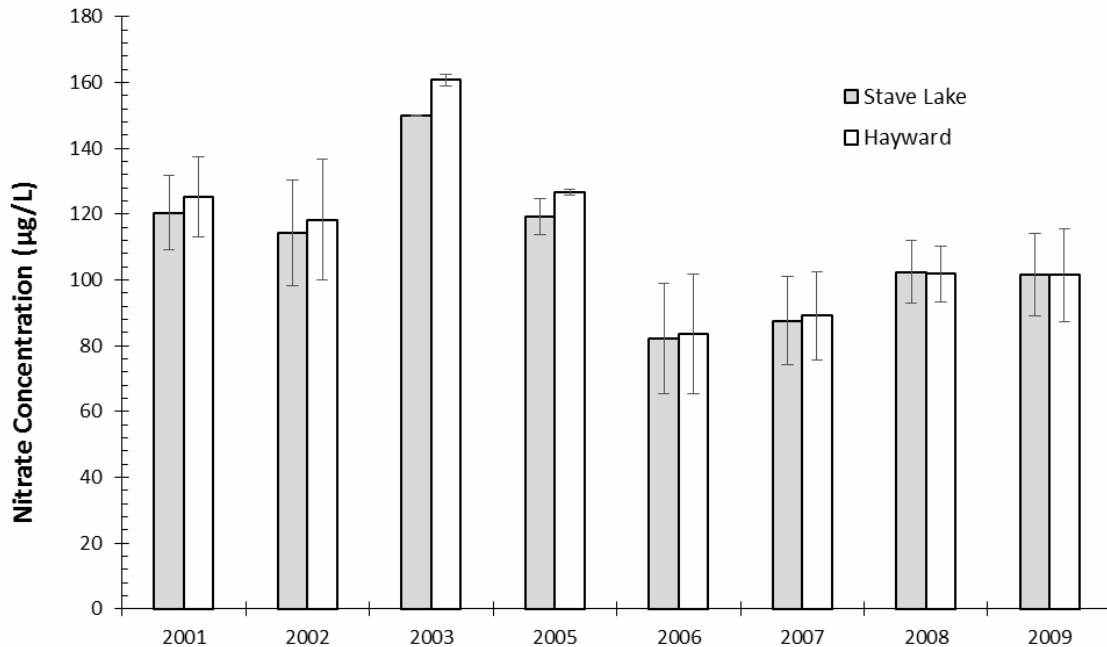


**Figure 7. Plot of yearly average nitrate levels ( $\mu\text{g/L}$ ) in Stave Lake and Hayward reservoirs for each year of the monitor (2000 – 2009). The error bars mark the 95% confidence limits about the computed yearly means.**

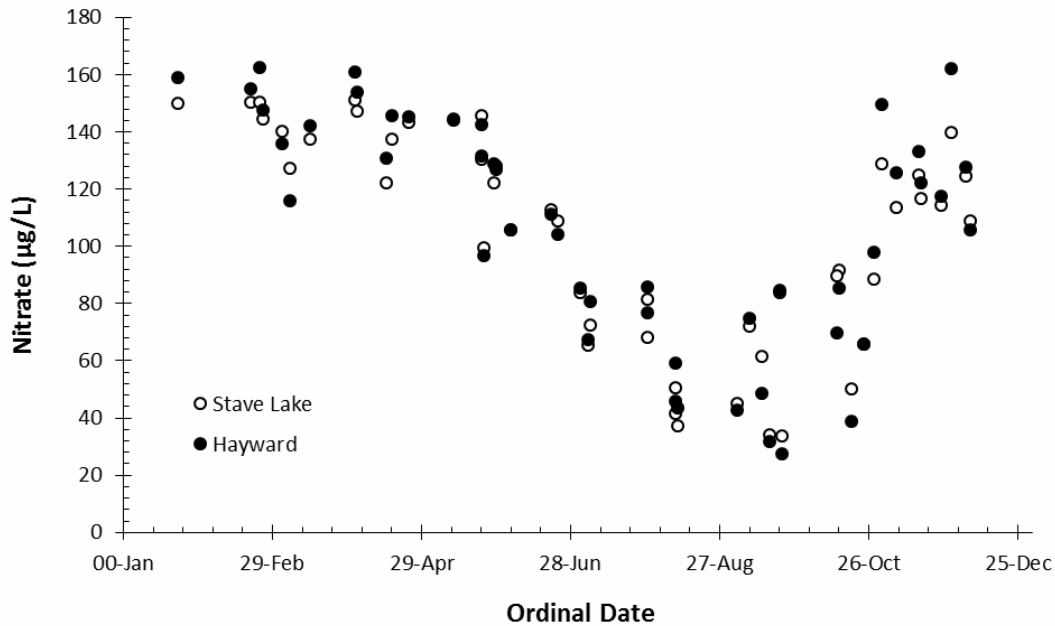


**Figure 8. Nitrate levels ( $\mu\text{g/L}$ ) plotted as a function of ordinal date showing a persistent seasonal trend in observations over the 10-year period of data collection (2000 – 2009) at the Stave Lake and Hayward Reservoir sampling sites.**

## Physical Characteristics

### Light

A total of 145 vertical light profiles were collected over the course of the 2000 to 2009 monitoring period, but they were not evenly distributed across all years or sites. The grand mean of all PAR extinction coefficients was  $-0.39$  with a coefficient of variation of 20% ( $SD = 0.08$ ). This corresponds to a grand mean 1% PAR compensation depth of 11.9 m with a 17% coefficient of variation ( $SD = 2.1$ ). The distribution of light extinction coefficients however, was positively skewed while that of the depth compensation data approached normality. As a result, the depth compensation data were used to assess between site and year differences rather than the extinction coefficients. For ELZ modelling purposes, the compensation data and summary statistics were converted back to extinction coefficients so that PAR intensities could be readily calculated for different depths.

Single factor ANOVA (assuming unequal samples sizes) found that there were significant differences in 1% compensation depth between sites (Table 5). Multiple comparisons using the Games Howell (1976) method found that compensation depths were similar between sites within Stave Lake Reservoir, but were consistently shallower in Hayward Reservoir by at least 1 m. The average compensation depth for all sites in Stave Lake across all years was 12.4 m, while that in Hayward Reservoir was 11.1 m. There appeared to be considerable between-year variability in compensation depth when averaged across all sites, but ANOVA found that these differences were not statistically significant (Table 6). The lowest yearly average compensation depth was in 10.8 m which occurred in 2005, while the highest was 13.2 m in 2009. Also, there was no apparent temporal trend to the annual data. Rather, between-year variation appeared to be random in nature. Unfortunately, there were too many missing values to carry out a two-way ANOVA to determine whether between-site differences were consistent across all years.

**Table 5. Results of a single factor ANOVA of the 1% Photosynthetically Active Radiation (PAR) compensation depth data collected at four sites in Stave Lake and a single site at Hayward reservoir (H) testing for significant between year differences (2000 – 2009).**

ANOVA: Single Factor							Alpha	0.05
<i>Groups</i>	<i>Count</i>	<i>Sum</i>	<i>Mean</i>	<i>Variance</i>	<i>SS</i>	<i>Std Err</i>	<i>Lower</i>	<i>Upper</i>
2000	6	76.656	12.8	0.684	3.418	0.821	10.664	14.888
2001	20	238.491	11.9	2.670	50.729	0.450	10.983	12.866
2002	26	298.542	11.5	5.033	125.817	0.395	10.670	12.295
2003	27	330.568	12.2	2.190	56.934	0.387	11.447	13.039
2005	10	108.123	10.8	2.932	26.390	0.636	9.373	12.252
2006	14	156.169	11.2	8.333	108.325	0.538	9.993	12.317
2007	15	180.517	12.0	4.654	65.160	0.520	10.920	13.149
2008	12	134.978	11.2	2.915	32.064	0.581	9.970	12.527
2009	15	197.393	13.2	5.843	81.796	0.520	12.045	14.274

ANOVA								
<i>Sources</i>	<i>SS</i>	<i>df</i>	<i>MS</i>	<i>F</i>	<i>P value</i>	<i>F crit</i>	<i>RMSSE</i>	<i>Omega Sq</i>
Between Gr	60.9860	8	7.6233	1.8829	0.0675	2.0071	0.3858	0.0464
Within Grou	550.6323	136	4.0488					
Total	611.6183	144	4.2473					

**Table 6. Results of a single factor ANOVA of the 1% Photosynthetically Active Radiation (PAR) compensation depth data collected at four sites in Stave Lake (Stave North, SN; Stave opposite the Alouette Powerhouse, SP; Stave South, SS; and Stave West, SW) and a single site at Hayward reservoir (H) over a 10-year period (2000 – 2009).**

ANOVA: Single Factor							Alpha	0.05
<i>Groups</i>	<i>Count</i>	<i>Sum</i>	<i>Mean</i>	<i>Variance</i>	<i>SS</i>	<i>Std Err</i>	<i>Lower</i>	<i>Upper</i>
H	58	641.5	11.1	4.641	264.513	0.258	10.544	11.576
SN	36	440.8	12.2	3.599	125.953	0.327	11.580	12.908
SP	10	128.2	12.8	2.265	20.386	0.621	11.412	14.220
SS	29	359.8	12.4	2.769	77.535	0.364	11.660	13.153
SW	14	174.7	12.5	4.506	58.579	0.525	11.345	13.611

ANOVA								
<i>Sources</i>	<i>SS</i>	<i>df</i>	<i>MS</i>	<i>F</i>	<i>P value</i>	<i>F crit</i>	<i>RMSSE</i>	<i>Omega Sq</i>
Between Groups	65.588	4	16.397	4.257	0.003	2.435	0.342	0.081
Within Groups	546.966	142	3.852					
Total	612.554	146	4.196					

A plot of PAR compensation depth as a function of ordinal date found that for the Stave Lake sites, there was no obvious seasonal trend (Figure 9) except possibly in November/early December when average compensation depth appeared to be lower than the rest of the year (10.7 m vs 12.4 respectively). This November 'dip' was more apparent in the Hayward data where average compensation depth was closer to 8.8 m (Figure 9). The between site difference however was not statistically significant ( $t = -1.847$ ,  $P = 0.10$ ). During the summer growth period (May 15 to Oct 30), compensation depth was similar in both systems, though Hayward values tended to be slightly lower (12.6 vs 11.9 m respectively,  $t = -1.997$ ,  $P = 0.047$ ). This similarity between sites however did not apply to the late winter-early spring period where there was a considerable divergence in response. In Stave Lake Reservoir, compensation depth averaged 12.3 m during the months of February to mid-May, which was similar to values observed during the rest of the year. In Hayward Reservoir, however, the average compensation depth was closer to 9.3 m; almost 3 m less than that at the Stave Lake site ( $t = -4.219$ ,  $P = 0.0004$ ).

Surface irradiance ( $I_s$ ) measured at the water's surface at each site was found to be highly correlated with surface PAR levels estimated by regression analysis using Eq. 1 and the vertical PAR profile data ( $r = 0.963$ ,  $P < 0.0001$ ). The distribution of data however was heteroscedastic with variance increasing systematically with surface irradiance. Following log-log transformation of the data, the best fit regression equation describing the relationship between the two metrics was the following power function:

$$I_s = 1.21 \cdot (\text{PAR}_{\text{Surface}})^{0.996} \quad (R^2_{\text{Adj}} = 0.989, P \ll 0.0001) \quad \text{Eq. 5}$$

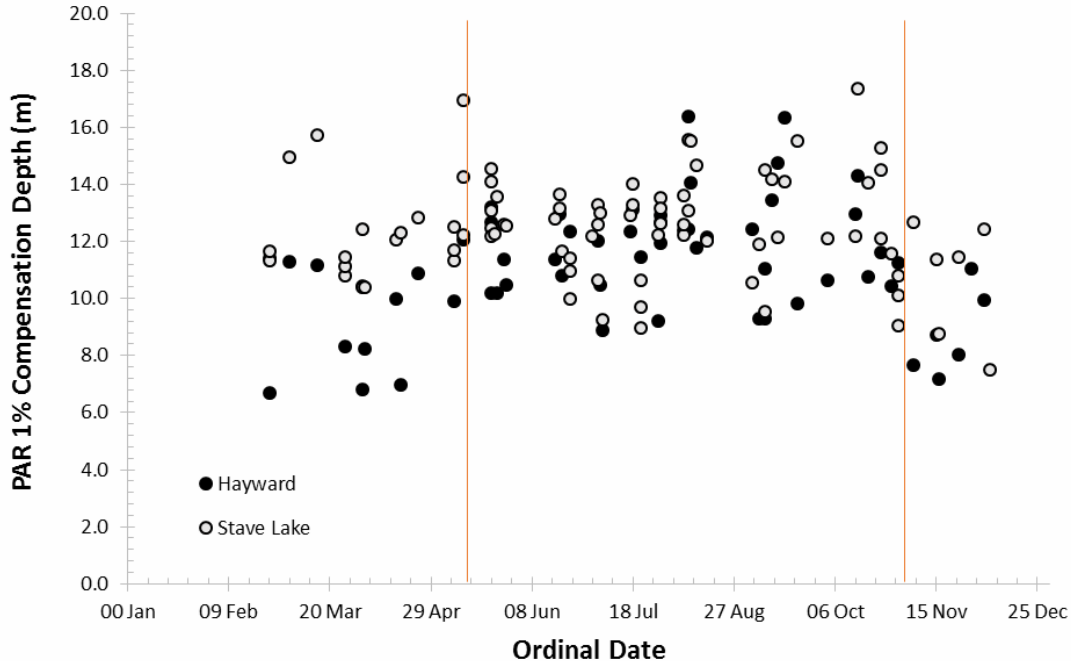


**Figure 9. Plot of 1% Photosynthetically Active Radiation (PAR) compensation depths (m) as a function of ordinal date collected over a 10-year period (2000 to 2009) showing differences in annual trend between Stave Lake and Hayward reservoirs. Vertical lines highlight the periods where there appeared to be a seasonal change in response; the first was May 15, the second November 1.**

The exponent of Eq. 5 was found not to differ significantly from 1, suggesting that surface readings taken by the LiCor Li-200SA pyranometers were consistently 21% higher than the estimates derived from LiCor Li-250 meter with the Li-192SA submersible quantum sensor. This likely represents a calibration difference between the two instruments as the LiCor Li-200SA measures the full spectrum of visible light, while the LiCor Li-250 meter is limited to the PAR spectrum (400 – 700 nm). Also a likely factor, was the reflection of light off the water's surface (Wetzel 2002).

Scatterplots of hourly average global solar radiation data collected at the same time as the surface irradiance measurements found a high degree of correspondence in all four data sets (Figure 10). The relationships however were not linear and tended to be complex in nature. In all cases best fit regressions required use of the functional form  $y = (Ax + B)^n$  to create a pattern of normalized residual values. Each had very similar curve shapes, and in turn coefficients of determination ( $R^2 = 0.654, 0.670, 0.739$  and  $0.681$  for sites T09, T12, T32, and T34 respectively). Because the relationships were so similar, the hourly solar radiation data were averaged across sites to create a single time series of data for regression analysis, which lead to the following predictive equation;

$$I_s = (0.0125x + 3.3654)^{2.74} \quad \text{Eq. 6}$$

where  $I_s$  = surface irradiance ( $\mu\text{moles}/\text{m}^2/\text{s}$ ) at either of the reservoir sites and  $x$  = average global solar radiation ( $\text{W}/\text{m}^2$ ) of the four local datasets. The coefficient of determination was  $R^2 = 0.719$  ( $P \ll 0.0001$ ), suggesting a reasonably good fit, though variance increased proportionately with the predicted mean irradiance values.

Equation 6 was used to convert all average hourly solar radiation readings to that of surface irradiance values for each of the reservoir study sites. These were in turn converted to estimated surface PAR readings by dividing irradiance data by 1.21 (using Eq. 5, assuming that the exponent in the equation was equal to 1). Finally, the hourly data were summed across each 24-hour period to provide a daily total of surface PAR values just under water's surface at each site ( $\text{PAR}_{\text{Surface}}$ ) taking into account reflective losses. The result was a times series of estimated daily total  $\text{PAR}_{\text{Surface}}$  values at the Stave Lake and Hayward Reservoir sites starting Jan 1, 2000 and ending Dec 31, 2009 (Figure 11). These  $\text{PAR}_{\text{Surface}}$  data were found to be highly variable, but tended to be range bound in a sinusoidal pattern that reflected a yearly cycle. The highest  $\text{PAR}_{\text{Surface}}$  values occurred in mid-summer (Jun 21), approaching a maximum of  $9058 \mu\text{moles}/\text{m}^2/\text{s}$ , but were just as likely to be as low as  $870 \mu\text{moles}/\text{m}^2/\text{s}$  on the same ordinal date. The lowest range of values occurred on Dec 21, where PAR was found to be anywhere between 150 and  $550 \mu\text{moles}/\text{m}^2/\text{s}$ . This time series of data was in turn used to estimate average  $\text{PAR}_{\text{Surface}}$  during each of the periphyton growth periods, as well as for modelling purposes.

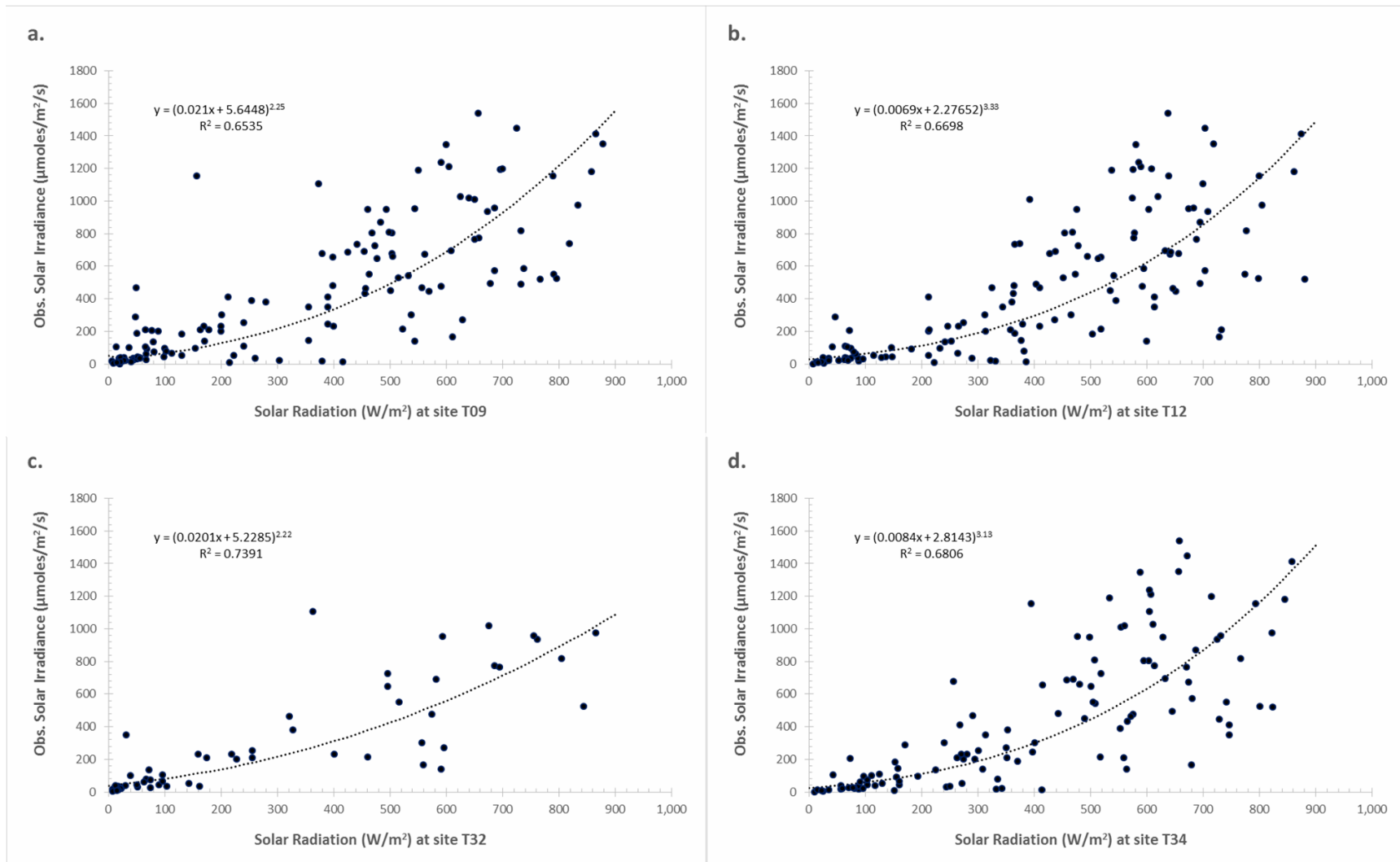


**Figure 10.** Plots of solar radiation values provided by the Greater Vancouver Regional District from four different stations in the vicinity of the Stave Falls Project against measured solar irradiance data collected on site over a 10-year period (2000 – 2009). T09 = Rocky Point Park, Port Moody; T12 = Chilliwack Airport; T32 = Douglas College, Coquitlam; T34 = Abbotsford Airport.



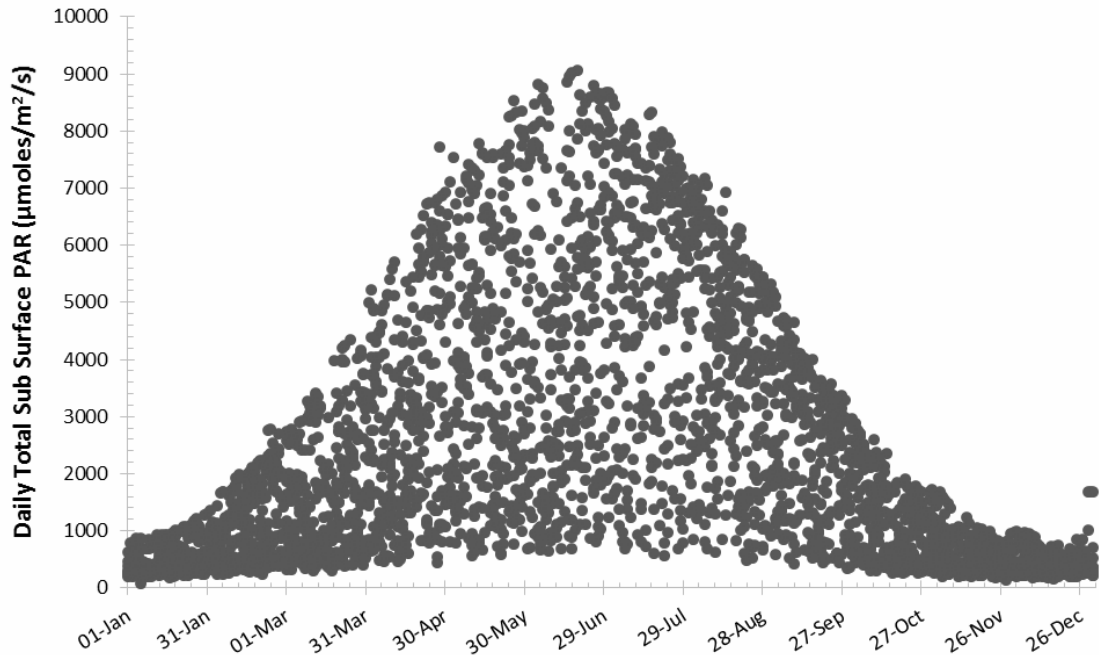


**Figure 11.** Plot of daily accumulated photosynthetic active radiation ( $PAR_{Surface}$ ) estimated for Stave Lake and Hayward Reservoirs for the period Jan 1, 2000 to Dec 31, 2009. The PAR data were calculated from solar radiation data provided by the Greater Vancouver Regional District (GVRD) at 4 locations in the vicinity of the study area. The  $PAR_{Surface}$  values are assumed to be just under the water surface and take into account reflective losses.

## Water Temperature

Water temperature measurements collected at all sites across all years (2005 to 2009) ranged from 3.5 to 24.8°C. Depth integrated values ranged from 3.6 to 22.0°C with gradients that spanned less than 2°C in 76% of the instances. In 18% of the instances, the temperature gradient between the water surface and a depth of 8 m ranged from 2 to 4 °C. Maximum observed temperature gradient was 7.4°C.

Analysis of variance found no significant differences in depth integrated temperature among the Stave North, Stave South and Hayward transect sites ( $F_{2,62} = 0.320$ ,  $P = 0.728$ ). Average values were 14.4, 13.5, and 15.1 °C for each site respectively. There were no significant between-year differences either ( $F_{4,59} = 0.593$ ,  $P = 0.670$ ), though yearly average values tended to vary by 2.2°C. Average values were 14.6, 15.9, 12.7, 14.5, and 14.4 °C for the years 2005 to 2009 respectively. A plot of individual depth integrated temperature values as a function of ordinal date revealed a strong seasonal trend in the data (Figure 12). Temperatures reached peak values in mid-July approaching 21°C. The lowest recorded values occurred during winter (3.5°C), and began to rise to their summer highs in late March/early April. Seasonal trends between Stave Lake and Hayward sites overlapped one another, which was consistent with the ANOVA results that found no between-site differences.

Regression analysis found that depth integrated water temperature at each site was highly correlated with PAR during the preceding periphyton growth period ( $r = 0.887$ ,  $P < 0.001$  for all sites and

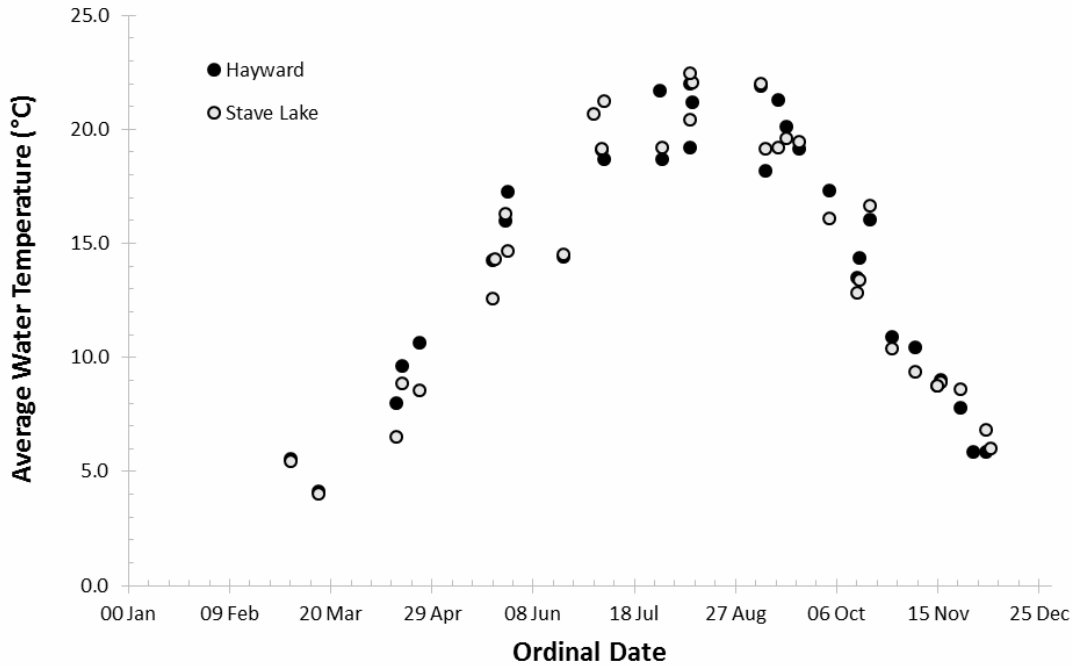


**Figure 12. Plot of depth integrated water temperature (water surface to a depth of 8m) as a function of ordinal date showing seasonal trends between sites on Stave Lake and Hayward reservoirs.**

years). While on average the duration of these periods was 40 days there were times when the period was longer or shorter. To determine whether duration was indeed a factor influencing the strength of the correlation, average PAR was calculated for periods ranging from 25 to 95 days prior to the measurement date for each of the temperature data on record. This was done at 5 day intervals, and the results regressed against water temperature. The outcome of the analysis found a continuously increasing coefficient of determination from 25 days of irradiance ( $r^2 = 0.657$ ) to a peak value at 75 days ( $r^2 = 0.966$ ,  $P \ll 0.0001$ ), followed by a continuously decreasing trend with longer durations. Overall, this regression analysis found that depth integrated water temperature ( $T_{Avg}$ ) at all sites and sample dates could be predicted from average PAR intensity the previous 75 days ( $PAR_{75d}$ ) to within  $\pm 1.8^\circ\text{C}$  90% of the time using the following equation:

$$T_{DI} = 0.00374 \cdot PAR_{75d} + 2.94 \quad (\text{Eq. 7})$$

A comparison of regression slopes between sites found no significant difference ( $0.00382 \pm 0.00023$  and  $0.00374 \pm 0.00030$  95% Confidence Intervals (CI) for the Stave Lake and Hayward sites respectively). However, there was a tendency for water temperature in Hayward reservoir to be  $0.8^\circ\text{C}$  higher than at the Stave Lake site. The difference though, was not statistically significant ( $t = 0.825$ ,  $P = 0.415$ ).

Regression analysis with other physical variables, in particular inflow discharge to each reservoir, found no other significant relationships with water temperature. The only exception was at the Hayward site where a significant negative correlation was found with the average inflow discharge during each periphyton growth period ( $r = 0.370$ ,  $P = 0.031$ ). Like the PAR data, these periods varied considerably and a systematic approach to regression analysis was carried out to determine whether duration was a significant factor. Inflow discharge was averaged for periods lasting 25 to 95 days at 5 day intervals and

each regressed to the residuals of the PAR model from Eq. 3. Results of the analysis found that the coefficient of determination peaked at 30 days ( $r^2 = 0.167$ ,  $P = 0.022$ ), and fell gradually as duration increased. Combining the 30-day average inflow data ( $Q_{30d}$ ) with the 75-day average solar irradiance ( $S_{75d}$ ) as independent variables that predicted depth integrated water temperature ( $T_{DI}$ ) at Hayward Reservoir resulted in the following equation ( $r^2 = 0.965$ ,  $P \ll 0.0001$ ):

$$T_{DI} = 0.00343 \cdot PAR_{75d} - 0.01131 \cdot Q_{30d} + 5.422 \quad (\text{Eq. 8})$$

This equation was able to predict Hayward water temperature to within  $\pm 1.5^\circ\text{C}$  90% of the time. Having a separate model for Hayward water temperature resulted in an improved regression for Stave Lake water temperatures when a separate model was developed for it ( $r^2 = 0.975$ ,  $P \ll 0.0001$ );

$$T_{DI} = 0.003817 \cdot PAR_{75d} + 2.60 \quad (\text{Eq. 9})$$

This equation was also able to predict water temperature to within  $\pm 1.5^\circ\text{C}$  90% of the time. Both Equations 8 and 9 were used to estimate water temperature at the sites and sampling dates where they were missing, thus filling in these data gaps. As well, a daily water temperature time series was constructed for the entire monitoring period. This data was in turn used to estimate average water temperature during each periphyton growth period ( $T_{Avg}$ ).

## Hydrology

Hydrology data for the Stave Lake and Hayward reservoirs were provided by BC Hydro. The total volume of inflow discharge into Stave Lake Reservoir (local inflows and Alouette Facility discharge) varied from year to year with the highest value ( $4.94 \text{ Gm}^3$ ) occurring in 2007 and the lowest ( $3.71 \text{ Gm}^3$ ) occurring in 2009 (Figure 13). The average for all years was  $4.00 \text{ Gm}^3$ . The hydrology of Stave Lake inflows was dominated by high inflow events that occurred throughout the year, but tended to be more concentrated during the winter months (October to the end of January) (Figure 14). Also occurring each year, was a prolonged period of high inflow due to spring freshet (April to the end of August).

Total inflow to Hayward reservoir was similar to that of Stave Lake. A slightly higher value was expected due to local inflows, but this was not a consistent feature in the annual data (Figure 13). Rather, total inflow to Stave Lake reservoir was frequently higher than in Hayward reservoir. This may have been in part due to the use of storage in Stave Lake Reservoir, but the discrepancy could also have been due to estimation errors introduced by the process of averaging instantaneous measurements of inflow to create daily average values (which increases with inflow volatility). As well, flow estimation errors in general tend to be higher in larger reservoirs<sup>1</sup>.

Inflows to Hayward reservoir were far less volatile due to its predominantly regulated source (i.e., Stave Falls Powerhouse). Periods of greater volatility were due either to high local inflows relative to Stave Falls Powerhouse outflows, or spills from Stave Falls Dam. These were relatively infrequent compared to the highly volatile inflows of Stave Lake reservoir (Figure 15).

The comparatively stable inflows to Hayward reservoir was largely due to the use of reservoir storage in Stave Lake, which attenuated the effects of pulsing inflows. As a result, reservoir elevation in

---

<sup>1</sup> A key component in estimating reservoir inflow is the change in reservoir storage. In larger reservoirs, a 1 cm error in elevation measurement (due for example to wave action) represents a much larger volume of water than in a smaller reservoir.

Stave Lake Reservoir varied considerably each year (Figure 16). The pattern of daily reservoir elevation varied from year to year, though there tended to be some convergence in mid-summer elevations to provide stable reservoir conditions for recreation. Maximum elevations varied little across all years of the monitoring program, averaging 81.7 m (CV = 0.3%) and did not exceed 82 m. Minimum yearly elevations were far more variable, ranging from 71.9 to 76 m in response to inflow conditions, downstream outflow requirements and power demand. The reservoir fluctuations typically ranged from 5.8 to 9.9 m depending on the year, providing a broad range of reservoir conditions to examine its effect on littoral periphyton productivity.

Hayward Reservoir elevation was far less variable than Stave Lake, reflecting its status as a run-of-the-river system (Figure 17). However, it was not free of variability. There were several key trends of interest. The first was an approximate 1.4 m drop in maximum elevation that occurred in 2006 (42.7 to 41.3 m) that was carried over to the end of the monitoring period. This change was in response to dam safety concerns related to its age and seismic stability (B Wilson, BC Hydro, personal comm.). Another key feature was the periodic deep reservoir drawdowns that occurred every second year starting 2001 (Table 7). In each case, reservoir elevation was drawn down to between 32.5 and 34.5 m for periods lasting from 1 and 3 weeks to carry out dam maintenance work (B Wilson, BC Hydro, personal comm.). These deep drafts likely had a significant impact on periphyton growth and needed to be taken into account when analysing the periphyton growth data. Finally, for most of the monitoring period, there were persistent fluctuations in elevation that had an amplitude no more than 1.25 m depending on time of year. The most stable periods on record were midsummer and mid-winter during the last three years of the monitoring program where fluctuations were typically < 0.25 m in amplitude.

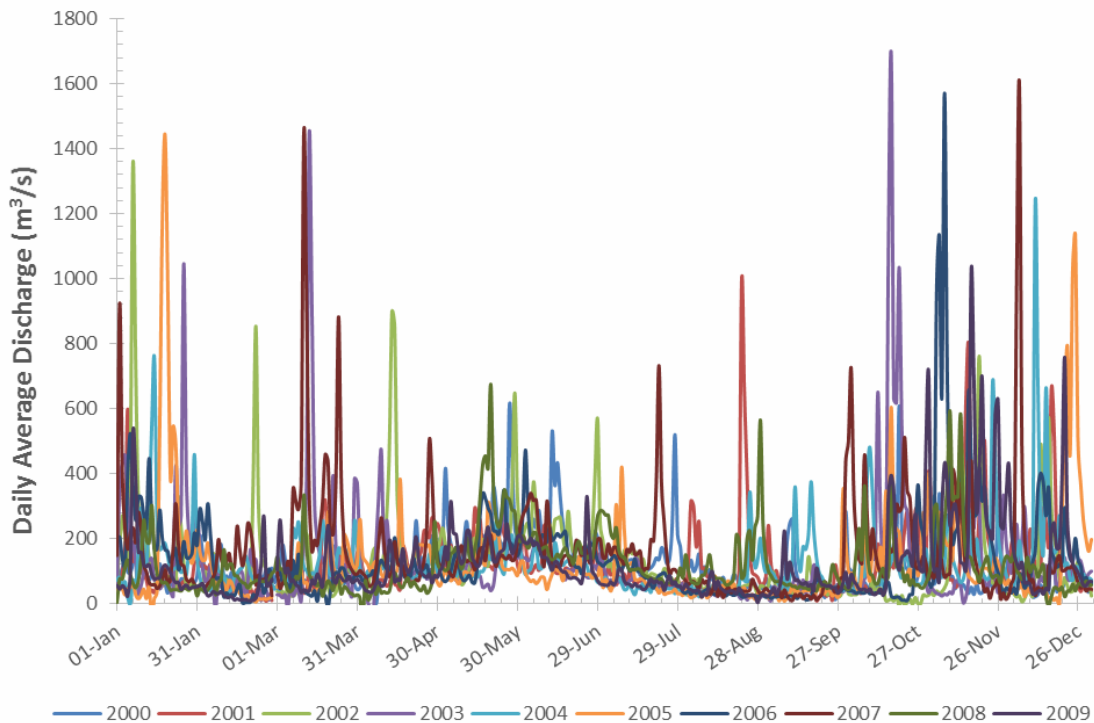


**Figure 13. Plot of daily average inflow discharge to Stave Lake Reservoir over time for the duration of the monitoring program. Data were provided by BC Hydro.**

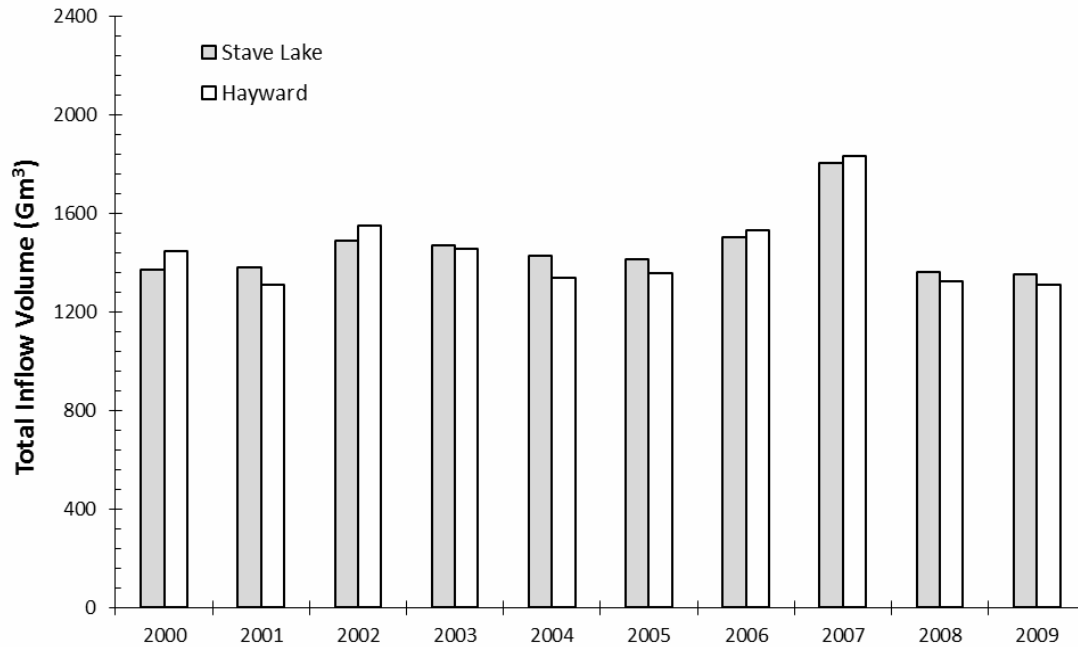


**Figure 14. Plot of total inflow volume to Stave Lake and Hayward Reservoirs comprising of regulated (Alouette facility and Stave Falls facilities respectively) and non-regulated (local inflows) for each year of the monitoring program (2000 to 2009). Data were calculated from daily average inflow discharge values provided by BC Hydro.**

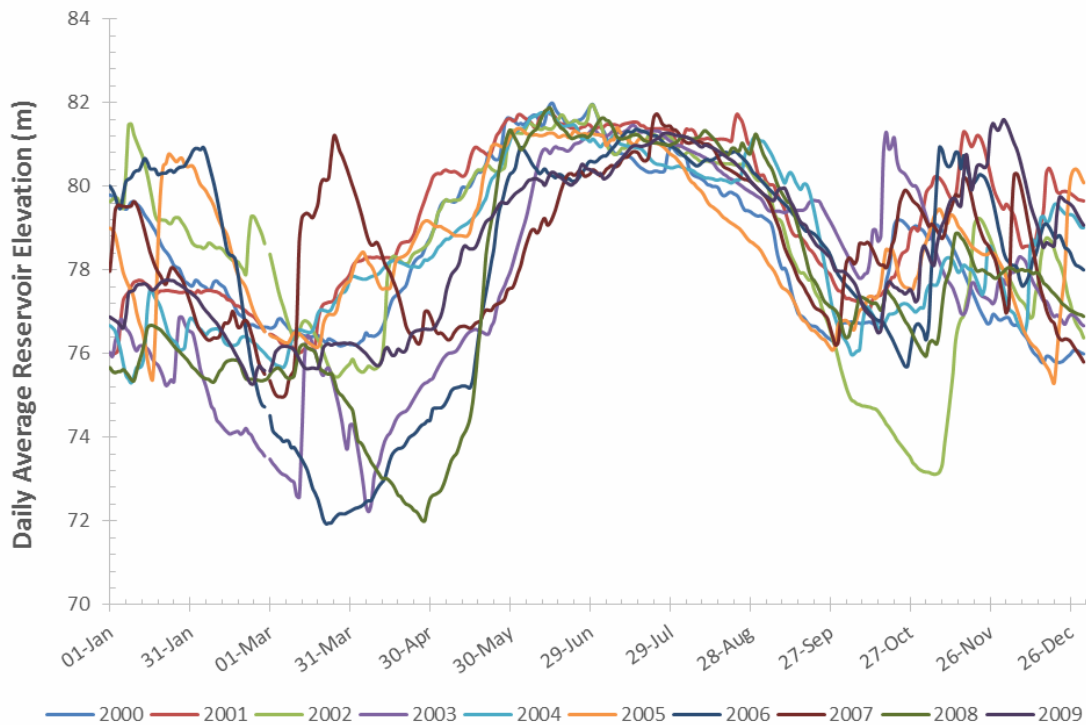


**Figure 15. Plot of daily average reservoir elevation in Stave Lake Reservoir over time for the duration of the monitoring program. Data were provided by BC Hydro.**

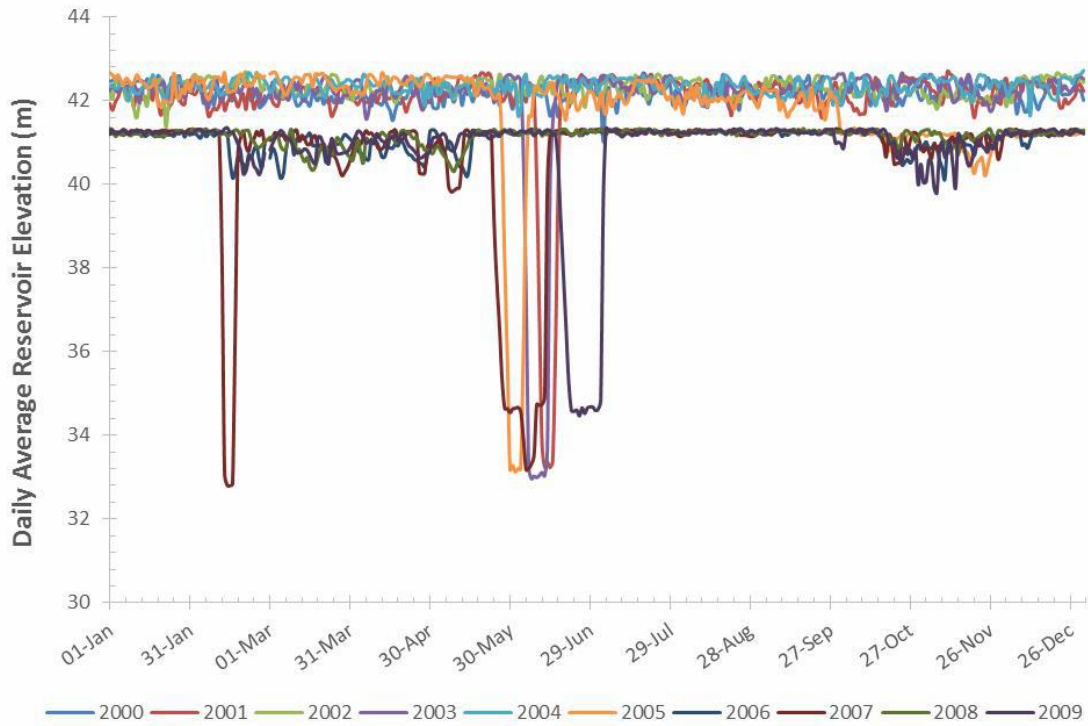


**Figure 16.** Plot of daily average reservoir elevation in Hayward Reservoir over time for the duration of the monitoring program. Data were provided by BC Hydro.

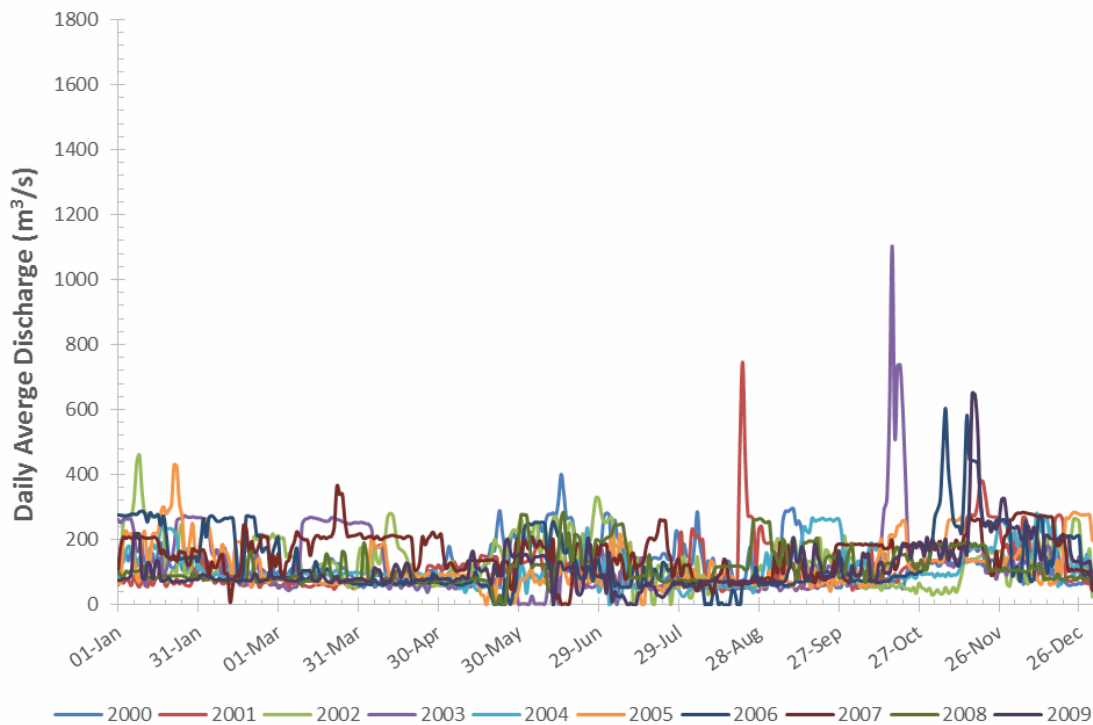


**Figure 17.** Plot of daily average inflow discharge to Hayward Reservoir over time for the duration of the monitoring program. Data were provided by BC Hydro.

**Table 7. Yearly summary statistics of reservoir elevation for Stave Lake and Hayward reservoirs during the 10-year littoral periphyton growth monitoring program. Data were provided by BC Hydro.**

Year	Stave Lake Elevation (m)				Hayward Elevation (m)			
	Min	Median	Max	Range	Min	Median	Max	Range
2000	75.79	78.29	81.99	6.19	41.02	42.19	42.62	1.61
2001	75.99	79.50	81.80	5.80	33.24	42.20	42.70	9.47
2002	73.12	78.65	81.95	8.83	41.37	42.31	42.69	1.32
2003	72.23	77.66	81.47	9.24	32.97	42.28	42.67	9.70
2004	75.30	78.19	81.77	6.46	41.64	42.37	42.72	1.09
2005	75.30	78.58	81.39	6.09	33.13	42.13	42.68	9.55
2006	71.94	79.07	81.36	9.43	40.13	41.20	41.33	1.21
2007	74.97	78.64	81.73	6.77	32.80	41.22	41.33	8.53
2008	72.00	77.21	81.88	9.87	40.31	41.23	41.34	1.03
2009	75.28	78.58	81.60	6.32	34.47	41.21	41.35	6.89

Water residence time in Stave Lake Reservoir averaged 33.5 days over the course of the monitoring period, but ranged from 27.7 to 40.9 days depending on the year. This is in contrast to Hayward Reservoir where residence time averaged 1.5 days and varied by no more than 0.7 days from year to year.

### Periphyton Growth

A total of 1995 Ash Free Dry Weight (AFDW) samples were collected over the course of the 10-year monitoring period. Values ranged from 100 to 63,050 mg/m<sup>2</sup> and had a grand mean of 2,047 mg/m<sup>2</sup>. In 105 of the cases, AFDW was below the detectable limits of 1 mg/100 cm<sup>2</sup> for the 2000 to 2003 sampling period and 0.1 mg/100 cm<sup>2</sup> for 2005 onward. These cases were recorded as missing values rather than assume no growth (i.e., a weight of 0 g). As well, there were another 228 cases where the sampling plates were above the water line and could not be sampled.

A comparison of the Ash Free Dry Weight (AFDW) data with coincident samples tested for Chl<sub>a</sub> concentration found a high degree of correlation between the two variables (Appendix A), verifying that AFDW was indeed a suitable indicator of periphyton biomass at all water depths. This was also confirmed with coincident samples inoculated with <sup>14</sup>C to determine instantaneous productivity by <sup>14</sup>C radio assay (Appendix B). Though the correlation was not as strong as that with Chl<sub>a</sub>, the <sup>14</sup>C radio assay work did show that the AFDW samples were comprised of live organisms and not simply a collection of organic debris associated with sedimentation. As would be expected, the higher the AFDW, the higher the concentration of Chl<sub>a</sub> or assimilated <sup>14</sup>C.

Depth-integrated AFDW ranged from 800 to 82,900 mg/m<sup>2</sup> and had a grand mean of 16,986 mg/m<sup>2</sup>. When converted using Eq. 1, these values corresponded to periphyton growth rates of 1.25 to 0.150 day<sup>-1</sup> and a grand mean growth rate of 0.075 day<sup>-1</sup>. Of the 206 possible depth-integrated growth rate observations, 7 were entered as missing values because of an insufficient number of plate data to ensure an unbiased estimate (fewer than 4 plates and 5 plates for Hayward and Stave Lake

**Table 8. Results of a two-way unbalanced factorial ANOVA on depth integrated periphyton growth rate collected at four sites (Stave North, Stave South, and Hayward) and over a 10-year period (2000 to 2009). In Table A., year 2000 was dropped from the analysis so that all sites could be compared for differences as no data was collected at the Stave West Site. In Table B., the Stave West site was excluded from the analysis so that year 2000 data could be incorporated into the analysis.**

A. Periphyton Growth Rate - Yr 2000 excluded					Alpha	0.05
	<i>SS</i>	<i>df</i>	<i>MS</i>	<i>F</i>	<i>p-value</i>	<i>sig</i>
Year	0.00880	7	0.00126	3.24083	0.00314	yes
Site	0.02114	3	0.00705	18.17322	0.00000	yes
Interaction	0.00507	21	0.00024	0.62301	0.89682	no
Within	0.05778	149	0.00039			
Total	0.09337	180	0.00052			

B. Periphyton Growth Rate - Stave West Site excluded					Alpha	0.05
	<i>SS</i>	<i>df</i>	<i>MS</i>	<i>F</i>	<i>p-value</i>	<i>sig</i>
Year	0.01009	8	0.00126	2.88035	0.00560	yes
Site	0.00940	2	0.00470	10.73352	0.00005	yes
Interaction	0.00379	16	0.00024	0.54050	0.92060	no
Within	0.05515	126	0.00044			
Total	0.07934	152	0.00052			

reservoirs respectively). This was either the result of sampling during a deep drawdown period or the loss of plate data due to sample processing issues.

Two-way ANOVA showed that growth rates varied significantly between sites and across years (Table 8). There was no significant interaction between the two factors, indicating that the between site differences in growth rate were consistent across all years. Overall, Hayward Reservoir had the highest primary production growth rate with a grand mean of 0.090 day<sup>-1</sup>. This was followed by the Stave North and Stave South sites with average growth rates of 0.078 and 0.070 day<sup>-1</sup> respectively. The Stave West site had the slowest growth rate with 0.061 day<sup>-1</sup>. Across years, average growth rates ranged from 0.062 to 0.085 day<sup>-1</sup> with the lowest rate occurring in 2007. The highest was in 2009. A plot of growth rate as a function of ordinal date showed strong seasonal trends at all sites (Figure 18). In general, growth rates tended to peak in late summer (late July) through to the end of fall (mid-October), and were at their lowest during the start of winter (early December) through to the beginning of summer (late May). Also, apparent in the plots were the between-site differences in average growth rate identified in the ANOVA.

Correlation analysis found that the depth integrated periphyton growth rate in Hayward Reservoir did not vary in concert with any of the water chemistry or other physical attribute data collected at site, except for average reservoir inflow which had a low but statistically significant correlation coefficient (Table 9). The relationship was only able to explain 9% of the variance in Hayward depth-integrated growth rates. The correlation coefficient also suggested that the relationship was a negative one, where growth rates tended to be slightly higher during periods of lower inflow discharge. Regression analysis



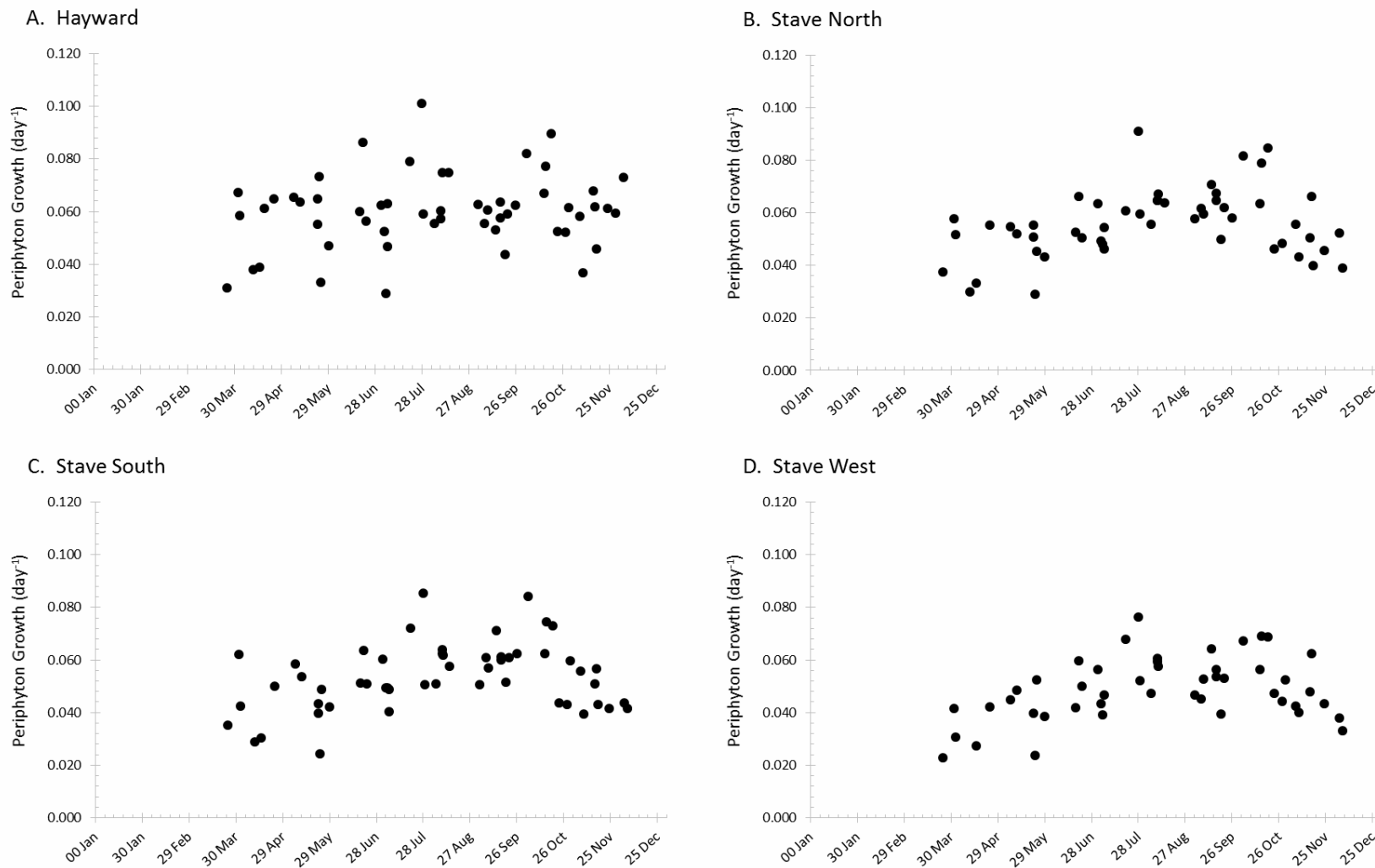


**Figure 18.** Depth integrated periphyton production growth plotted as a function of ordinal date showing seasonal trends as well as between-site differences.

**Table 9. Results of correlation analyses of various water chemistry and physical attributes on depth integrated periphyton growth data collected at four sites over a 10 year period (2000 - 2009). Shaded areas highlight correlation coefficients that were found to be statistically significant at  $\alpha = 0.05$  given the sample size of paired values (n).**

	Hayward		Stave North		Stave South		Stave West	
	<i>n</i>	<i>r</i>	<i>n</i>	<i>r</i>	<i>n</i>	<i>r</i>	<i>n</i>	<i>r</i>
Average Elevation	51	-0.091	50	0.159	52	0.229	46	0.262
Standard Deviation	51	0.050	50	-0.222	52	-0.239	46	-0.306
Nitrate (NO <sub>3</sub> )	37	-0.110	38	-0.472	39	-0.507	38	-0.609
Total Phosphorus (TP)	35	0.255	35	-0.293	36	-0.294	35	-0.421
Total Dissolved Phosphorus (TDP)	35	0.142	33	-0.312	34	-0.196	33	-0.293
Light Compensation Depth	38	0.155	29	0.370	25	0.128	12	-0.091
Average Surface PAR	51	0.177	50	0.297	52	0.289	46	0.272
Water Temperature	51	0.079	50	0.587	52	0.375	-	-
Average Water Temperature	51	0.237	50	0.645 <sup>1</sup>				
Average Reservoir Inflow	51	-0.302 <sup>1</sup>	50	-0.574 <sup>2</sup>	52	-0.560 <sup>2</sup>	46	-0.408 <sup>1</sup>

<sup>1</sup> Dominant variable in a forward stepwise regression analysis

<sup>2</sup> Significant secondary variable in a forward stepwise regression analysis

showed that, for inflows spanning 50 to 250 m<sup>3</sup>/s, periphyton growth rates ranged from 0.104 day<sup>-1</sup> to 0.84 day<sup>-1</sup> respectively.

At the Stave North site, depth integrated periphyton growth was significantly correlated with a large number of variables (Table 9). Average water temperature during each incubation period had the highest correlation coefficient, followed by the water temperature recorded at the time of sampling, average inflow rate during the incubation period and nitrate concentrations. Also, statistically significant were correlations with light compensation depth and average surface PAR levels. It should be noted that all of these variables were highly correlated with one another. To identify the most influential ones, forward stepwise regression analysis was done using average water temperature as the starting variable. As expected, the water temperature variable was able to explain 41.7% of the variance in growth rates at the site. When the residuals of this regression were examined for correlations with the remaining variables, none were found to be statistically significant except for average inflow discharge to Stave Lake Reservoir. This confirmed that the most of the correlations observed initially were spurious in nature and due to their common relationship with the water temperature variable. Inflow discharge, though correlated with average water temperature ( $r = -0.435$ ), did appear to have an independent relationship with growth rate, explaining an additional 13.9% of the variable's variance. With the two variables combined, a total of 55.6% of the variance in depth integrated periphyton growth rate at the site was accounted for.

A similar pattern of correlation coefficients was observed at the Stave South site, where average water temperature during the incubation period was the variable most strongly correlated with depth integrated growth, followed by average inflow discharge and nitrate levels (Table 9). Average surface PAR was also statistically significant, as was water temperature observed at the time of sample collection. Forward stepwise regression with average water temperature as the starting variable was able to confirm that the correlations with nitrate levels, average surface PAR and water temperature at the time of

sampling were spurious in nature, and that the average water temperature variable was able to explain 42.7% of the variance in periphyton growth rates at the site. Like, the Stave North site, average inflow discharge appeared to have an independent relationship with growth, which was able to explain another 13.5% of the growth rate variance. Together, the two variables were able to explain a total of 56.2% of the variance in Stave South depth-integrated growth rates.

At the Stave West site, a slightly different pattern of correlations was observed (Table 9). As with the other Stave Lake Reservoir sites, average water temperature had the highest correlation coefficient. Rather than be followed by average inflow rates, nitrate and total phosphorus levels had the next highest degree of correlation, suggesting that water quality (more specifically nutrient levels) was important at the site. This was then followed by average inflow discharge to the reservoir, and the variance in reservoir surface elevations. When these variables were examined in a forward stepwise regression with average water temperature as the starting variable, like the previous sites, most of the correlations with initial set of regression's residuals were not statistically significant, including the inflow discharge metric. This was not the case for total phosphorus levels however. This variable was able to explain an additional 12.2% of the variance on periphyton growth rates at the site. With the 42.7% of variance explained by water temperature, the two variables were able to explain a total of 54.9% of the variance in depth-integrated periphyton growth at the Stave West Site.

When viewed collectively, it was clear in the correlation results that average water temperature played a dominant role in regulating growth rates, particularly at the Stave Lake sites. In all cases, the direction of correlation was positive, indicating that growth rates increased with average water temperature. Given the well-known relationship between water temperature and the photosynthetic efficiency of algae, as well as algal growth in general (Wetzel 2001), the relationship was likely causal in nature. Also, playing a significant, but lesser role, was inflow discharge to each reservoir. In the latter case, the direction of correlation was negative, suggesting that as inflow discharge increased, growth rates decreased. Whether there was a causal link to periphyton growth is unclear, though it is possible that the inflow variable may be related to water retention times in the reservoir, which can in turn impact the residence time of nutrients in the reservoir. The fact that the total phosphorus levels was found to be a significant factor at the Stave West site suggested that this may be indeed be the case. However, the direction of the correlation was negative, indicating that growth decreased as levels of total phosphorus increased. This is opposite of what would typically be expected. Furthermore, the correlation between total phosphorus levels and inflow discharge, though positive, was not statistically significant ( $r = 0.239$ ,  $P = 0.139$ ).

As expected periphyton growth at all sites and sampling dates varied considerably as a function of water depth. In general, growth was higher in plates nearer to the water surface than those at depth. The nature of this relationship however, did not fully coincide with the depth attenuation of PAR intensity as would be expected given the premise of the ELZ model. It was assumed that growth close to the water surface would be inhibited due to photosynthetic inhibition, reach a peak value several meters below the surface (where light attenuation removed the inhibitory effects), and then drop off exponentially as PAR intensity dropped with depth. Individual plots of growth rate as a function of average PAR intensity during the growth phase of each biomass sample failed to provide consistent evidence of photo inhibition when PAR intensities were at their highest. In most cases, growth tended to follow more of a hyperbolic saturation relationship

$$Ax/(B + x) \tag{Eq. 6}$$

where growth increased rapidly with PAR intensity and then leveled off to a constant rate with no further increases (Figure 19a). The A coefficient in Eq. 6 was considered a measure of maximum growth rate while the B coefficient was considered to be the PAR intensity at which growth rate is 50% of the maximum. To fit this equation to each depth series of periphyton growth data, the growth data were first transformed by dividing by the corresponding depth series of PAR data and then by taking the natural logarithm of the result. The transformed data were then plotted as a function of PAR at depth, the result of which was a linear relationship where the 'A' coefficient of Eq. 6 could be obtained by taking the inverse of the regression slope, and 'B' coefficient was derived by dividing the regression intercept with the slope. Overall,  $r^2$  values for the hyperbolic saturation regression ranged from 0.363 to 0.999, and was greater than 0.80 95% of the time, and greater than 0.90 89% of the time. Of the 206 regressions across all years and sites, only 28 cases had potential evidence of photo inhibition; where growth appeared to be lower at the highest PAR intensities near the water surface compared to observations at more moderate depths. In most cases, however, it was difficult to distinguish this potential inhibitory effect from possible sampling error. Also problematic was the fact that such down turns in growth occurred as frequently in the early spring or late fall as it would in mid-summer when light intensity would be brightest. Furthermore, these cases were not consistent across all sites. Finally, even at the brightest recorded PAR intensities, there were many instances when growth rates were at also their highest, with no indication of photo inhibition. When viewed collectively, there appeared to be little evidence supporting the notion of systematic photo inhibition in the present study. Cases where growth patterns appeared to characterize a photo-inhibition-like effects may simply have been the consequence of sampling error, fluctuating water levels, or if very close to the water surface, the erosive forces of wave action.

There were nevertheless a number of instances where fit of the hyperbolic saturation equation was considered poor (Figure 19 b). In most cases, the poor fit was due to higher than expected growth at the lowest light intensities rather than at the highest. The cause for this was uncertain and may have been due to sampling error, though heterotrophic (i.e., non-photosynthetic growth) may have been a possible factor (Wetzel 2001, Bruce and Beer, 2015a). It should be noted though, that only two of these poorer fitting regressions were found to be statistically insignificant (Stave North, May 8 2003,  $r^2 = 0.363$ , and Stave West, Mar 26 2005,  $r^2 = 0.425$ ). In both cases, deep drawdowns had occurred during the incubation period that may have severely confounded growing conditions and hence the accumulation of biomass on the sampling plates. Of the two cases, only the Stave North May 8 2003 record was excluded from further analyses due to its extreme outlier designation when carrying out regression analyses (its coefficient 'B' was more than 17 standard deviations from the grand mean). A common effect of high growth rates at depth when trying to fit the hyperbolic saturation equation was a 'B' coefficient that approached 0 (thus computing an average growth rate for the site) or even became negative. In the latter case, the coefficients result in an equation that is nonsensical, even though coefficients of determination were very high. To avoid confounding further analyses, all cases where the 'B' coefficient was less than 1 were excluded from the data set and assigned a missing value designation. In total, there were 6 such cases. Also, excluded from the analysis were all samples that collected at the beginning of each sample year where the plates were left in the lake to overwinter. Though periphyton biomass data were collected on these occasions, the length of time these plates were left to incubate was often more than double or triple of all other incubation periods in the dataset. These data were also incomplete as the overwintering was not done in all years, and often lead to missing or damaged plates. Thus, of the 206 occasions that periphyton growth data were collected during this monitor, only 188 periphyton growth versus PAR-at-depth regressions were deemed suitable for subsequent analyses.

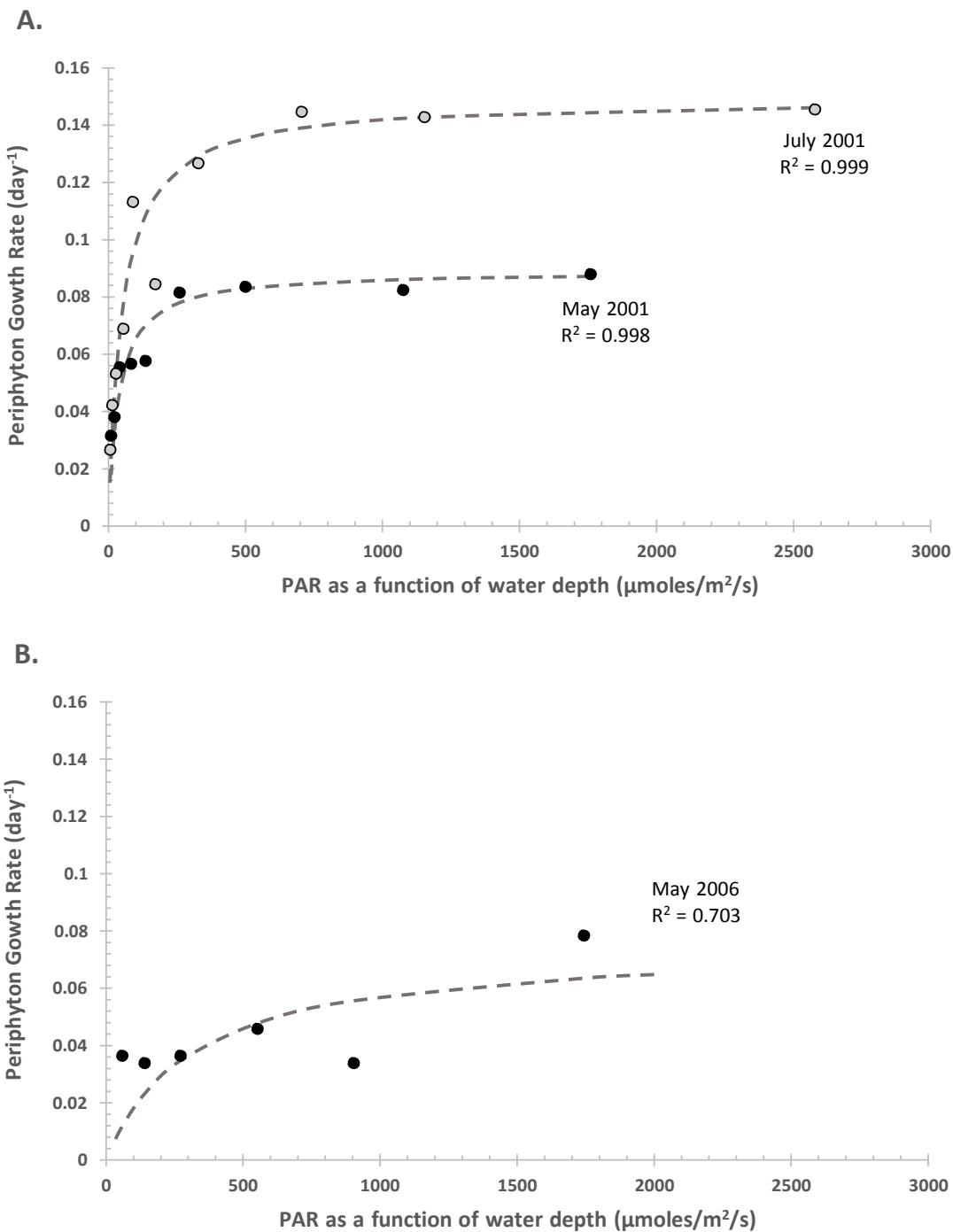


**Figure 19.** Examples of periphyton growth rates plotted as a function of PAR collected at various water depths. **A.** Two examples from the Stave North site where the hyperbolic saturation equation was found to provide an excellent fit to the plotted data. **B.** An example where the hyperbolic saturation equation did not fit well to the data, yet still provided a statistically significant coefficient of determination ( $R^2$ ). The example in B. highlights two common features when fit was poor; much higher growth than expected at low light condition, and/or lower than expected growth at moderate to high light intensities. It should be noted that instances of poor fit were generally rare.

**Table 10. Results of a two-way unbalanced ANOVA on maximum growth rate coefficients “A” derived by fitting a hyperbolic saturation equation [of the form  $Ax/(x+B)$ ] to growth data calculated at various sampling depths plotted against corresponding PAR intensity data (x). Year and site are the two factors of interest and are based on data collected from years 2000 to 2009. The Student Newman-Kuels procedure was used to compare site means and determine which were significantly different.**

Two Way ANOVA - Maximum growth rates					Alpha	0.05
	<i>SS</i>	<i>df</i>	<i>MS</i>	<i>F</i>	<i>p-value</i>	<i>sig</i>
Year	0.020	8	0.003	3.003	0.0036	yes
Site	0.023	3	0.008	9.215	0.0000	yes
Interaction	0.015	23	0.001	0.765	0.7704	no
Within	0.141	168	0.001			
Total	0.198	202	0.001			

Student Newman-Keuls multiple comparisons					Alpha	0.05
<i>Comparison</i>	<i>Difference</i>	<i>SE</i>	<i>q</i>	<i>p-value</i>	<i>sig</i>	
H - SW	0.0283	0.0060	6.6552	0.0000	yes	
SN - SW	0.0242	0.0060	5.7149	0.0002	yes	
SS - SW	0.0155	0.0060	3.6943	0.0097	yes	
H - SS	0.0127	0.0058	3.0868	0.0766	no	
SN - SS	0.0086	0.0058	2.1006	0.1390	no	
H - SN	0.0041	0.0059	0.9918	0.4839	no	

Maximum growth rates (i.e., the ‘A’ coefficient) varied considerably across all sites and years. Values ranged from 0.023 to 0.217 day<sup>-1</sup> and averaged 0.093 day<sup>-1</sup> overall. Analysis of variance identified significant between-site differences in mean growth, as well as significant differences between years. There were however, no significant interaction effects, indicating that between-site differences were consistent across all years (Table 10). Multiple comparisons using the Student Newman-Keuls procedure found no significant differences in average maximum growth rates between the Hayward and Stave North sites (A = 0.106 vs 0.104 day<sup>-1</sup> respectively). This extended to the Stave South site as well, though the average maximum growth rate was noticeably lower (A = 0.093 day<sup>-1</sup>, Table 10). Average maximum growth rate at the Stave West site however, was significantly lower than all other sites (A = 0.077 day<sup>-1</sup>, Table 9).

The between year differences in the maximum growth rate did not appear to follow a particular trend (Figure 20), neither did the pattern of differences appear to coincide with annual trends in the water quality or physical attribute data. The highest annual average maximum growth rate for Stave Lake Reservoir occurred in 2009 (0.081 day<sup>-1</sup>), which was not significantly different from values observed in other years. The only exception was in 2007 where the average growth rate was 0.071 day<sup>-1</sup>. All other between year comparisons were not statistically significant. Average yearly maximum growth rates in Stave Lake Reservoir were consistently lower than corresponding values in Hayward Reservoir (Figure 20), which was consistent with the lack of a significant interaction term noted in the ANOVA results of Table 9. With the exception of years 2003 and 2007, maximum growth rates in Hayward Reservoir were not significantly different from one another, averaging 0.096 day<sup>-1</sup>. The highest average maximum growth rate occurred in 2008 (0.102 day<sup>-1</sup>) while the lowest rates were 0.069 and 0.070 day<sup>-1</sup> in years 2003 and

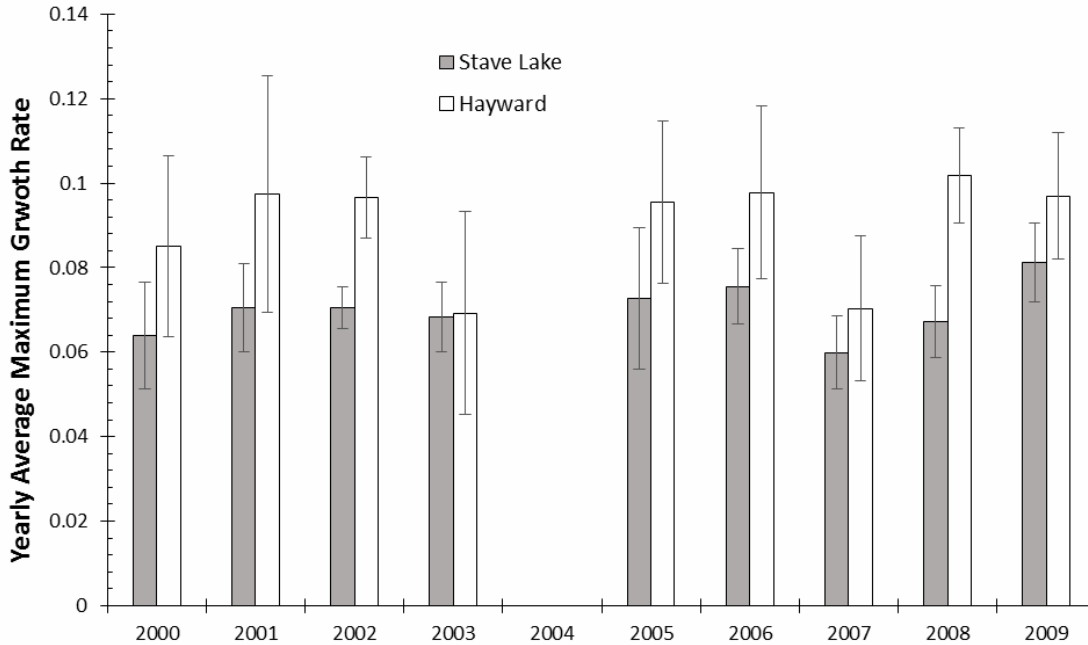


**Figure 20. Plot of mean annual maximum growth coefficients ( $\pm$  95% confidence limits) as determined from fitting a hyperbolic saturation equation to daily growth data as a function of PAR. The 95% confidence limits are narrower for Stave Lake because of larger number of sites.**

2007 respectively. It is interesting to note that in 2007, the year when average maximum growth rates were at their lowest in both reservoirs, measured water temperatures were the coolest on record and average yearly inflow discharges were at their highest. This was consistent with the correlation results on average growth rates described earlier, which showed that both average water temperature and average inflow discharge were potentially influential factors affecting periphyton growth.

Correlation analyses done with depth-integrated average growth rate data were repeated with the maximum growth rates derived from Eq. 6, the results of which are shown in Table 10. In Hayward Reservoir, maximum growth rates were found to be uncorrelated with all water quality and physical attribute metrics. This includes the average reservoir inflow variable which was shown to be significantly correlated to depth-integrated average growth rates, suggesting that this relationship was more tenuous than the coefficient of correlation in Table 9 suggested. The correlation analyses of Table 10 show that little of the variance in Hayward reservoir periphyton growth rates could be accounted for by shared variances in the water quality and physical attribute data. Thus, the best estimate for maximum periphyton growth rate in Hayward reservoir ( $A_H$ ), regardless of reservoir water quality and general condition, was  $0.106 \text{ day}^{-1}$  with a 95% confidence interval of  $\pm 0.008$ .

At the Stave North Site, maximum growth rates were found to be correlated with all three water quality metrics, the two water temperature variables and the average reservoir inflow. The variable with the highest correlation coefficient was average water temperature, which was able to explain 25.6% of the variance in maximum growth rate. A forward stepwise regression analysis using water temperature as the starting variable showed that all other variables except for TDP levels were spurious in nature due to their strong correlation with the temperature variable (i.e., correlation with the regression residuals was not statistically significant). The TDP variable was able to explain another 13.1% of variance in

maximum growth rate. When combined with the water temperature variable, a total of 38.7% of the variance in maximum growth rate ( $A_{SN}$ ) at the Stave North site could be accounted for.

**Table 11. Results of correlation analyses of various water chemistry and physical attributes on maximum periphyton growth rates derived from Eq. 6 collected at four sites over a 10 year period (2000 - 2009). Shaded areas highlight correlation coefficients that were found to be statistically significant at  $\alpha = 0.05$  given the sample size of paired values (n).**

	Hayward		Stave North		Stave South		Stave West	
	<i>n</i>	<i>r</i>	<i>n</i>	<i>r</i>	<i>n</i>	<i>r</i>	<i>n</i>	<i>r</i>
Average Elevation	46	-0.119	49		52	0.240	42	0.380
Standard Deviation	46	0.006	49	-0.151	52	-0.291	42	-0.342
Nitrate (NO <sub>3</sub> )	35	0.189	38	-0.381	38	-0.485	35	-0.627
Total Phosphorus (TP)	33	0.264	35	-0.368	35	-0.268	33	-0.305
Total Dissolved Phosphorus (TDP)	33	0.086	33	-0.445 <sup>2</sup>	33	-0.166	31	-0.184
Light Compensation Depth	35	-0.240	29	0.340	26	0.031	12	0.011
Average Surface PAR	46	-0.243	49	0.114	52	0.221	42	0.479
Water Temperature	46	-0.263	49	0.417	52	0.177	-	-
Average Water Temperature	46	-0.127	49	0.506 <sup>1</sup>	52	0.595 <sup>1</sup>	42	0.690 <sup>1</sup>
Average Reservoir Inflow	46	-0.110	49	-0.433	52	-0.461	42	-0.332

<sup>1</sup> Dominant variable in a forward stepwise regression analysis

<sup>2</sup> Significant secondary variable in a forward stepwise regression analysis

A slightly different subset of variables was correlated with the maximum growth rates measured at the Stave South site (Table 11). The standard deviation of reservoir elevations was found to be significant in this case, and both phosphorus related variables were not. Water temperature measured at the time of sampling was also uncorrelated. Forward stepwise regression analysis revealed that average water temperature was the only statistically significant variable, explaining 35.4% of the variance in maximum growth rates at the Stave South site ( $A_{SS}$ ). All other variables were found to be correlated with the average water temperature metric and therefore spurious in nature.

The same outcome was observed at the Stave West site, though with two additional variables with significant correlations; average reservoir elevation during the incubation period and average PAR intensity (Table 11). Forward stepwise regression analysis showed however, that only average water temperature was statistically significant, explaining 47.5% of the variance in maximum growth rate at the Stave West site ( $A_{SW}$ ). All other variables were correlated with the average water temperature metric and therefore considered spurious.

The correlation analyses above clearly showed that water temperature was a key determinant of maximum growth rate in the Stave Lake Reservoir. Average inflow discharge was a factor, even though it was identified as a potential predictor variable of average depth integrated growth data. The role of TDP or TP as a predictor of periphyton growth was unclear. Both were significant correlates, but only at only at the Stave North site. Also, the direction of the relationship was negative for both variables, indicating better growth during times of lower TP or TDP levels. This is opposite of what is generally expected, particularly in oligotrophic lake systems where higher TP or TDP is commonly associated with higher primary production (Schindler 1978, Wetzel 2001). Also, confounding the relationship between the two phosphorus metrics and Stave Lake periphyton growth was the fact that both were measured at a single, mid-reservoir site, well away from each of the littoral sampling transects. Bruce and Beer (2015b) was able to show that TP and TDP in Stave Lake reservoir varied considerably depending on the location of



**Table 12. Results of correlation analyses of various water chemistry and physical attributes on PAR<sub>A50</sub>, the light intensity at which periphyton growth is 50% of maximum, collected at four sites over a 10-year period (2000 - 2009). Shaded areas highlight correlation coefficients that were found to be statistically significant at  $\alpha = 0.05$  given the sample size of paired values (n).**

	Hayward		Stave North		Stave South		Stave West	
	<i>n</i>	<i>r</i>	<i>n</i>	<i>r</i>	<i>n</i>	<i>r</i>	<i>n</i>	<i>r</i>
Average Elevation	46	-0.278	49	-0.362	52	-0.212	42	-0.159
Standard Deviation	46	0.221	49	0.123	52	0.043	42	-0.150
Nitrate (NO <sub>3</sub> )	35	-0.219	38	-0.027	38	-0.084	35	-0.060
Total Phosphorus (TP)	33	-0.007	35	-0.062	35	-0.151	33	0.123
Total Dissolved Phosphorus (TDP)	33	-0.031	33	-0.195	33	-0.155	31	0.112
Light Compensation Depth	35	0.088	29	0.145	26	0.127	12	0.033
Average Surface PAR	46	0.214	49	0.279	52	0.477	42	0.471
Water Temperature	46	0.188	49	0.512	52	0.210	-	-
Average Water Temperature	46	0.164	49	0.005	52	0.089	42	-0.053
Average Reservoir Inflow	46	0.045	49	-0.080	52	-0.103	42	-0.018

<sup>1</sup> Dominant variable in a forward stepwise regression analysis

<sup>2</sup> Significant secondary variable in a forward stepwise regression analysis

sampling. They concluded that data collected at one site, and in particular at the mid-reservoir sampling site, could not be used to infer TP and TDP at other locations with confidence. Thus, given the inconsistent growth response and uncertainty of TP and TDP concentrations at each site, the phosphorus-based metrics were excluded from the development of predictive maximum growth regression equations.

Maximum growth rate was therefore concluded to be solely related to average water temperature ( $T_{Avg}$ ) in Stave Lake reservoir and independent reservoir condition in Hayward reservoir. Simple linear regression resulted in the following set of predictive equations for Stave Lake reservoir:

$$A_{SN} = 0.0614 + 0.0029 * T_{Avg} \quad (\text{Eq. 10})$$

$$A_{SS} = 0.0446 + 0.0036 * T_{Avg} \quad (\text{Eq. 11})$$

$$A_{SW} = 0.0440 + 0.0026 * T_{Avg} \quad (\text{Eq. 12})$$

In addition to the maximum growth coefficient described above, the hyperbolic saturation equation also required a coefficient defining the PAR intensity at which growth was 50% of maximum ( $B$ , in our case re-defined here as  $PAR_{A50}$ ). Like the 'A' coefficients, this was calculated for each day of sampling. Values were highly variable, ranging from - 113.2 to 465.0  $\mu\text{moles}/\text{m}^2/\text{s}$  and overall averaged 74.7  $\mu\text{moles}/\text{m}^2/\text{s}$  across all sites and years. ANOVA found that there were significant between-site differences ( $F_{3, 191} = 6.258$ ,  $P < 0.001$ ), but not across all years ( $F_{8, 191} = 1.524$ ,  $P = 0.151$ ). A comparison of site means using the Student Newman-Keuls procedure found that values were similar between the Stave North and Stave South sites (85.0 vs 105.4 respectively,  $q = 1.957$ ,  $P = 0.168$ ), as they were between the Stave West and Hayward sites (56.7 vs 49.0 respectively,  $q = 0.722$ ,  $P = 0.755$ ). However, the two pairs of sites were not significantly different from each other ( $q = 3.426$ ,  $P = 0.043$ ). Though the differences in  $PAR_{A50}$  were statistically significant, when compared to the overall range of PAR values observed ( $PAR_{Max} = 6148 \mu\text{moles}/\text{m}^2/\text{s}$ ), they appeared to be negligible (less than 0.5% of the PAR range).

Correlation analysis found little correspondence between the  $PAR_{A50}$  data with most of the water quality and physical environment variables (Table 12). The only exception was a consistent correlation with average surface PAR intensity ( $PAR_{Surr}$ ) among Stave Lake reservoir sites. In all cases, the coefficient

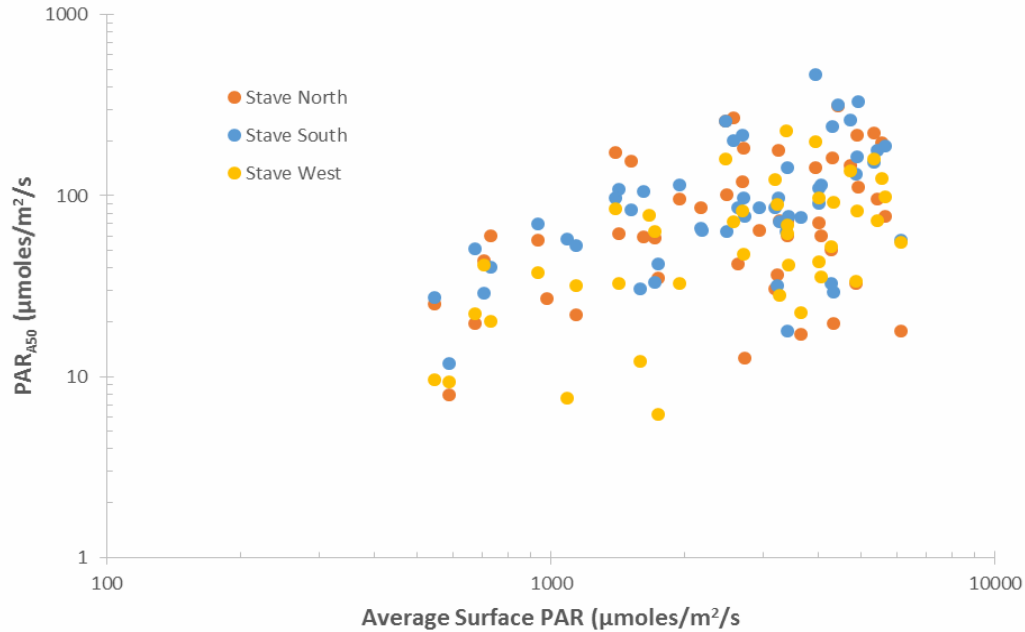


**Figure 21.** Scatterplot of the PAR intensity at which growth is 50% of maximum ( $PAR_{A50}$ ) as a function of average surface PAR during each periphyton growth period.

of correlation was positive, indicating that  $PAR_{A50}$  tended to increase with PAR intensity. A scatter plot of the PAR data showed a high degree of overlap in the relationship between sites (Figure 21), allowing the data to be pooled for regression analysis. Following a log transformation of both variables to normalize the distribution of data, the best fit regression model was found to be the following power function equation:

$$PAR_{A50} = 0.41 \cdot PAR_{Surf}^{0.65} \quad (R^2_{Adj} = 0.241, P \ll 0.0001) \quad (\text{Eq. 13})$$

It should be noted that four outlier values were excluded from the data set as each was more than three standard deviations away from the geometric mean. The exclusion of these data had little impact on sample size ( $n = 139$ ), yet significantly improved the regression. Furthermore, for the Stave North site, forward stepwise regression with  $PAR_{Surf}$  as the starting variable was able to show that the addition of the average water surface elevation and water temperature variables did not significantly contribute to the regression  $R^2_{Adj}$ . Both of these variables were highly correlated with  $PAR_{Surf}$  ( $r = 0.900$  and  $0.455$  respectively), indicating that the correlations with  $PAR_{A50}$  at the North Stave site was spurious in nature. Finally, for the Hayward site,  $PAR_{A50}$  was set to  $49 \mu\text{moles}/\text{m}^2/\text{s}$  and was assumed not to vary as a function of  $PAR_{Surf}$ .

Combining the A and B coefficients as described by Eq. 10 to 13 resulted in the following periphyton growth (G) hyperbolic saturation equations for each site:

$$G_H = 0.106 \cdot PAR / (49 + PAR) \quad (\text{Eq. 14})$$

$$G_{SN} = (0.0614 + 0.0029 \cdot T_{Avg}) \cdot PAR / (PAR_{A50} + PAR) \quad (\text{Eq. 15})$$

$$G_{SS} = (0.0446 + 0.0036 \cdot T_{Avg}) \cdot PAR / (PAR_{A50} + PAR) \quad (\text{Eq. 16})$$

$$G_{SW} = (0.0440 + 0.0026 \cdot T_{Avg}) \cdot PAR / (PAR_{A50} + PAR) \quad (\text{Eq. 17})$$

Inherent in the hyperbolic saturation equations was an explicit assumption that as PAR approached near darkness (i.e., PAR = 0), growth rates would also approach near zero levels. This however, rarely occurred. In almost all instances, when PAR was less than 40  $\mu\text{moles}/\text{m}^2/\text{s}$ , there was a measurable biofilm collected from each sampling plate indicating at least some periphyton growth. When the lower quartile of data was plotted out, it was clear that the intercepts of each regression was well above zero at all sites (Figure 22). ANCOVA found that the slope of the PAR vs growth regression was not significantly different between sites ( $F_{3,381} = 0.378$ ,  $P = 0.769$ ), and when combined was estimated to be 0.0005, a value well below the slopes observed at higher light intensities (i.e., Eq. 10 to 12). Though slopes were similar, there were significant between-site differences in intercepts ( $F_{3,384} = 23.856$ ,  $P \ll 0.001$ ). Using a common slope for all sites, the Tukey–HSD multiple comparisons procedure found that all Stave sites has similar intercept values (0.022, 0.023, and 0.026 for the Stave North, South and West sites respectively) and all were significantly less than that observed at the Hayward site (0.032). The average value for all Stave sites was 0.024. Thus, the data suggested that there was a base level of productivity that occurred which was independent of light intensity and therefore chemo-autotrophic or heterotrophic in nature. It was also possible that some of this observed “productivity” may simply have been the result of accumulating planktonic sediments. It should be noted however, that the results of  $^{14}\text{C}$  analyses found that all these samples contained live individuals capable of measurable respiration (Appendix B).

To account for this base level of periphyton growth in the hyperbolic saturation equations above, it was subtracted from the maximum growth rate coefficients and treated as a separate input variable. This base level of growth likely varied as a function of water temperature (Wetzel 2001). However, it was not possible to characterise this relationship with the data available. It should be noted though that low light conditions only occurred at the deepest depths sampled (16 to 20 m), which typically experienced less seasonal fluctuation in temperature than surface waters. Assuming that this base level growth occurred at all sampling locations, combining this base level of periphyton growth with the hyperbolic saturation equations Eq. 11 to Eq. 14 resulted in the following modified growth rate equations;

$$G_H = 0.032 + 0.080 \cdot \text{PAR} / (58 + \text{PAR}) \quad (\text{Eq. 15})$$

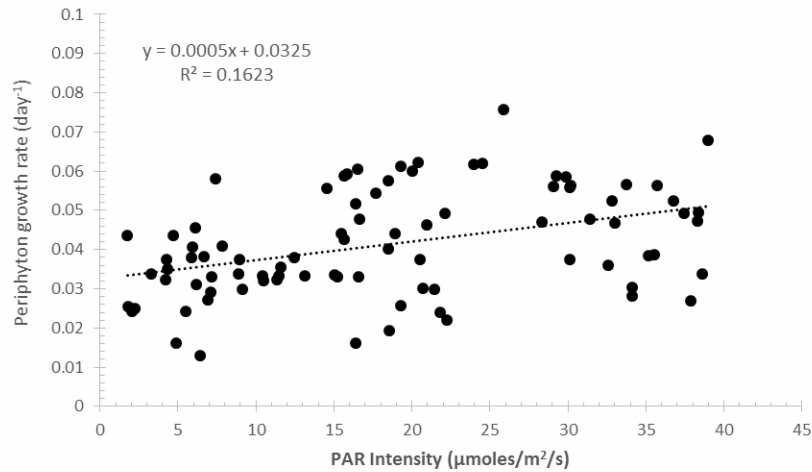
$$G_{SN} = 0.022 + (0.0394 + 0.0029 \cdot T_{\text{Avg}}) \cdot \text{PAR} / (\text{PAR}_{A50} + \text{PAR}) \quad (\text{Eq. 16})$$

$$G_{SS} = 0.024 + (0.0206 + 0.0036 \cdot T_{\text{Avg}}) \cdot \text{PAR} / (\text{PAR}_{A50} + \text{PAR}) \quad (\text{Eq. 17})$$

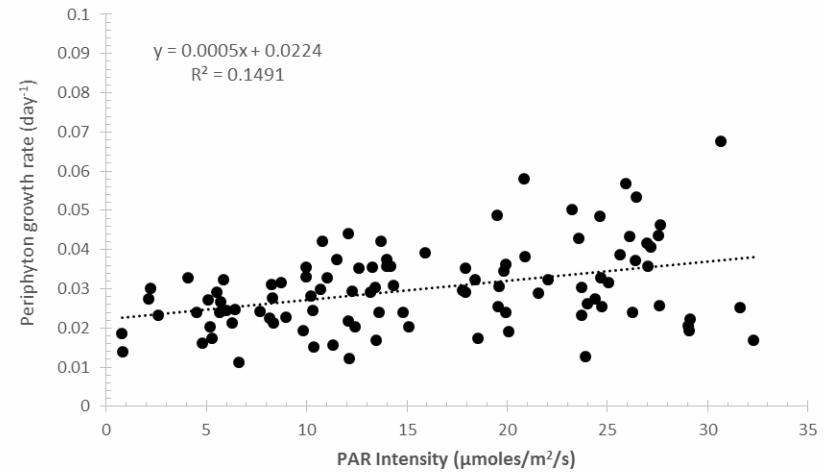
$$G_{SW} = 0.026 + (0.0440 + 0.0026 \cdot T_{\text{Avg}}) \cdot \text{PAR} / (\text{PAR}_{A50} + \text{PAR}) \quad (\text{Eq. 18})$$

The resulting sinusoidal form of these equations is plotted out in Figure 23 illustrating some of their key features, including the effect of water temperature. Equations 15 to 18 are plotted out in Figure 24 along with their corresponding scatterplot of observed values, illustrating the general fit of these equations. In each case,  $T_{\text{Avg}}$  was set to 14.6°C (the grand mean of all observations) and  $\text{PAR}_{A50}$  was set to the site mean rather than use predicted values from Eq. 13 and the  $\text{PAR}_{A50}$  data.

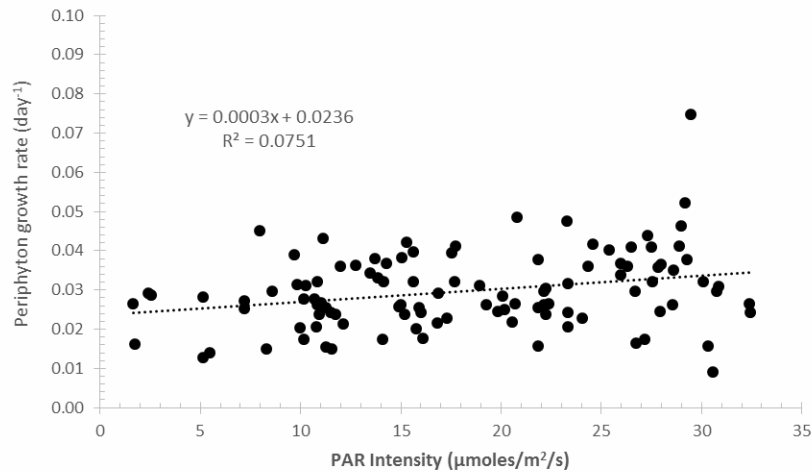
A. Hayward



B. Stave North



C. Stave South



D. Stave West

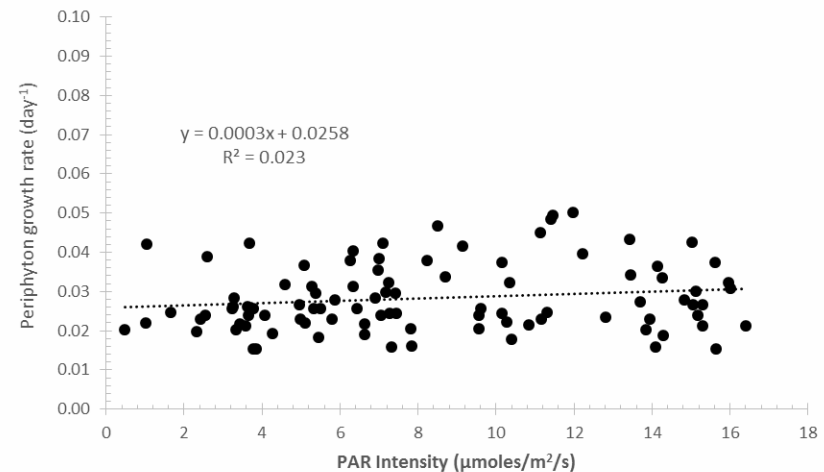


**Figure 22.** Scatterplots of periphyton growth rates as a function of average surface PAR intensity for each of four sampling locations on the Stave Lake and Hayward Reservoirs. Only the lower quartile of PAR data are plotted, highlighting the fact that as PAR approaches zero, periphyton growth continues, suggesting the presence of organisms capable of heterotrophic growth.

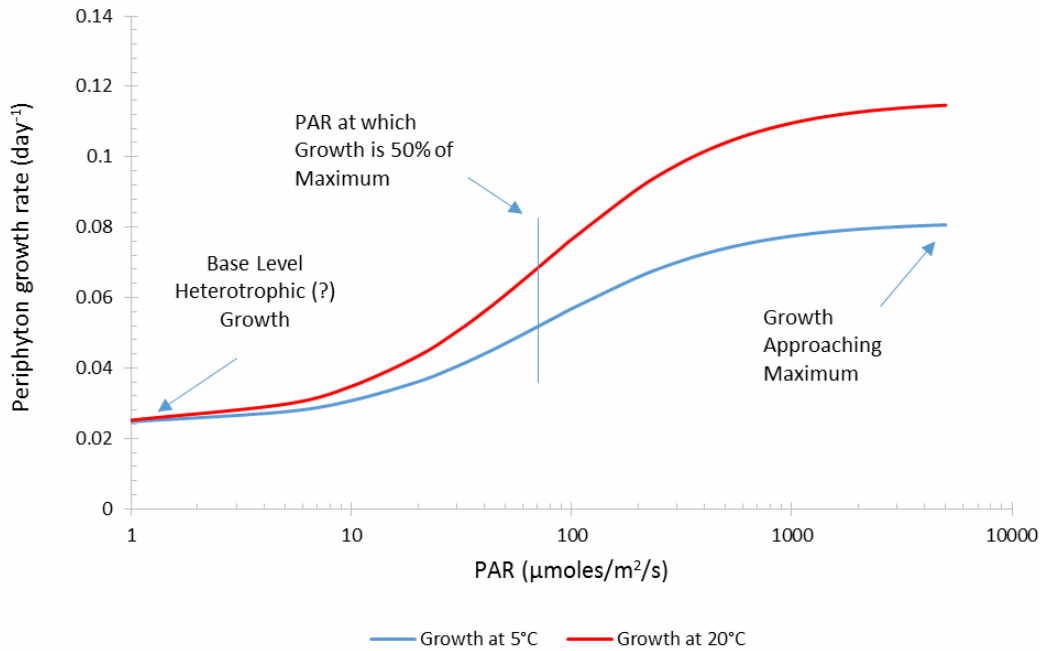


**Figure 23. Functional form of Eq. 15 to 18 used to describe periphyton growth as a function of PAR intensity in the Stave Lake and Hayward Reservoirs. The effect of water temperature is illustrated by plotting the equations with two different temperatures spanning the range that would typically be experienced in the reservoir system.**

While attempting to fit these equations to the data, it became apparent that the procedure used to accommodate base growth also required a shift in  $PAR_{A50}$ . The required shift was determined by trial and error where  $PAR_{A50}$  was incrementally increased to a point where the correlation coefficient between modeled and measured values reached a maximum value. The starting  $PAR_{A50}$  for this procedure was the average value for each site, ignoring the regression with  $PAR_{Surface}$ . Furthermore,  $T_{Avg}$  for all Stave Falls sites was set to 14.6°C, the grand mean of all observations. Both steps simplified the optimization procedure, which resulted in  $PAR_{A50}$  shifts that ranged from 55 to 85  $\mu\text{moles}/\text{m}^2/\text{s}$  among the Stave Falls sites and 57  $\mu\text{moles}/\text{m}^2/\text{s}$  for the Hayward site. These shifts in  $PAR_{A50}$  were taken into account in Eq. 15 to 18 by modifying the equation for  $PAR_{A50}$  as follows:

$$PAR_{A50} = S + 0.41 \cdot PAR_{Surface}^{0.65} \quad (\text{Eq. 19})$$

where  $S = 57, 55, 78$  or  $85 \mu\text{moles}/\text{m}^2/\text{s}$  for sites H, SN, SS and SW respectively.

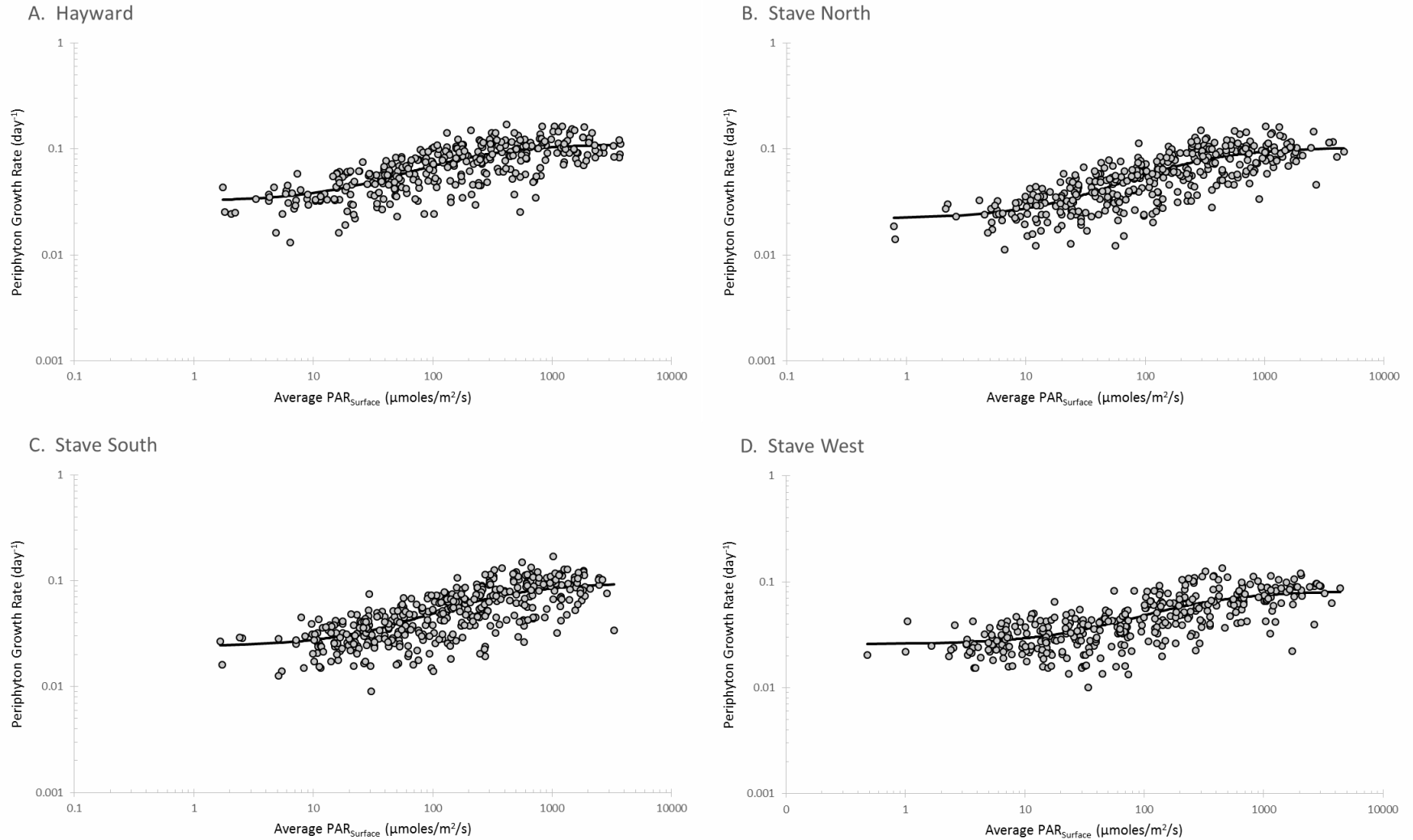


**Figure 24. Scatterplots of periphyton growth rate as a function of average photosynthetic active radiation experienced at each growth plate over the course of each periphyton growth period. Data span the 10-year monitoring period. Separate scatterplots are provided for each sampling site. The solid lines show the best fitting non-linear regression equations for each site (Eq. 15 to 18) assuming an average temperature of 14.6°C and site mean PAR<sub>A50</sub> values.**

It should be noted that the equations above predict an average growth rate over a period of 25 to 77 days for those sampling plates that were continuously submerged for the entire period of growth. Thus the only effect of varying water levels captured in the equations so far is the influence of the changing PAR intensities where plates in shallower waters receive greater PAR than those at greater depth. To incorporate the effects of plate dewatering, periphyton biomass must be calculated on a daily basis. Thus it must be assumed that the hyperbolic saturation growth equations Eq. 15 to 18 can be used to calculate growth rate on a daily basis. By assuming 100% mortality when a plate is dewatered, and estimating light intensity as a function of water depth using the light extinction coefficients calculated earlier, the effect of daily water level changes can also be taken into account. This was done using the following recursive algorithm to track periphyton growth over time at a given plate ( $B_{d,p}$ , in this case, for the Stave North site):

```

FOR d = 0 to t
  FOR p = 0 to 10
    IF  $z_p > WSE_d$  THEN
      Let  $B_{d,p} = 0$ 
    ELSE
      IF  $B_{d,p} = 0$  THEN
        Let  $B_{d,p} = 100 \mu\text{g}/\text{m}^2$ 
      ELSE
        Let  $B_{d,p} = B_{d-1,p} + B_{d-1,p} * G_{SN,d,p}$ 
      ENDIF
    ENDIF
  NEXT P
NEXT d

```

Where,

$d$  = day

$t$  = duration of growth period (days)

$P$  = plate number

$z_p$  = elevation of plate 'p' (m)

$WSE_d$  = water surface elevation on day 'd'

$G_{SN,d,z} = 0.024 + (0.046 + 0.0023 * T_d) \cdot PAR_{d,z} / (PAR_{A50} + PAR_{d,z})$  (from Eq. 16 and 19)

$PAR_{d,z} = PAR$  intensity at  $El_p = PAR_{Surface,d} * e^{-k \cdot z}$  (From Eq. 3)

$k$  = light extinction coefficient

$T_d$  = average epilimnion water temperature on day 'd'

There are several items of note in the algorithm above. Firstly, the biomass value represents the weight of periphyton scraped off of each plate, with a residual amount left on each plate for subsequent re-colonization; in this case, it was assumed to be  $100 \mu\text{g}/\text{m}^2$ . Secondly, daily surface PAR values were estimated from solar irradiation data collected at several locations in the lower mainland, as were the daily water temperature data (Eq. 4 or 5 depending on the site). These were not measured values. Finally, different growth equations were used depending on site location. Results of the periphyton biomass growth algorithm are presented in Figure 25 as comparisons between predicted and measured biomass values for each site.

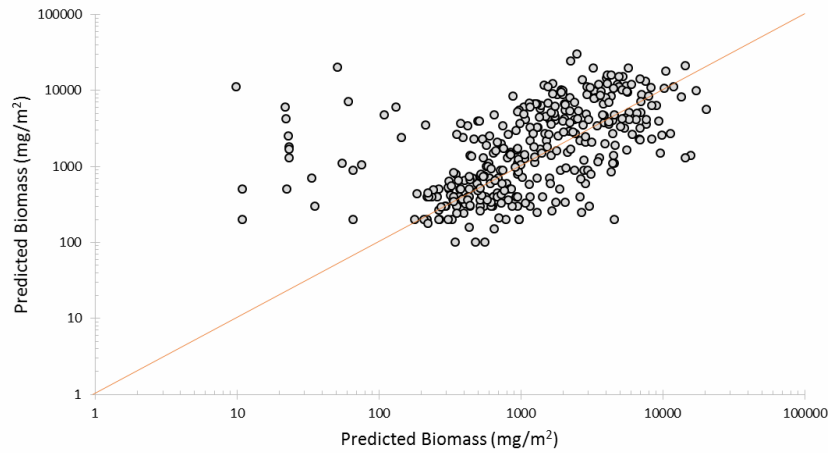
In all cases, the recursive algorithm employing the site-specific growth models was successful in predicting biomass concentrations that were comparable to measured values at different plate depths. Coefficients of determination between predicted and measured values however were modest in magnitude, ranging from 0.252 at the Hayward site to a high of 0.665 at the Stave North site. The low  $R^2_{Adj}$  value at the Hayward site was likely due to the high number of outlier biomass predictions when observed values were less than 100 g/m<sup>2</sup>. In all cases, the measured biomass values were much greater than predicted. A review of these outlier predictions found that all occurred at the upper most growth plate and when Hayward reservoir was held relatively constant with an average elevation of El 42.2 m. Elevation of the upper plate was 42.1 m. Thus, for each outlier prediction, average reservoir elevation during the growth period was typically within 10 cm of the plate surface. The standard deviation of reservoir fluctuations averaged 19 cm (maximum 29 cm), which was almost twice that of the elevation difference. Thus, it would appear that the upper plate in Hayward reservoir was repeatedly dewatered and then re-submerged during the growth period. The duration of these dewatering periods often lasted several days or more, so the growth recursive algorithm would have predicted near complete periphyton mortality in these upper plates. These upper plates however, were likely close enough to the surface that when dewatered, wave action could have been sufficient to keep the plates wet. Within-day variations in reservoir elevation may also have been contributing factor, re-submerging the plate for short periods each day. Regardless of the mechanism, the predicted mortality when the near surface plate was dewatered for short periods of time did not occur. Rather the periphyton colonies appeared to continue growing as if continuously submerged. Removing these outlier predictions from the Hayward dataset resulted in an improved regression ( $R^2_{Adj} = 0.437$ ). It should be noted that there were other instances where average reservoir elevations were close to the plate elevation, resulting in much higher measured biomass values than predicted, and were not restricted to the Hayward site. These occurrences however were comparatively rare and therefore did not warrant exclusion from the dataset.

Regression analysis of the paired predicted vs measured values at each site showed that the slopes and intercepts were similar to one another, indicating a relatively consistent model performance across all sites:

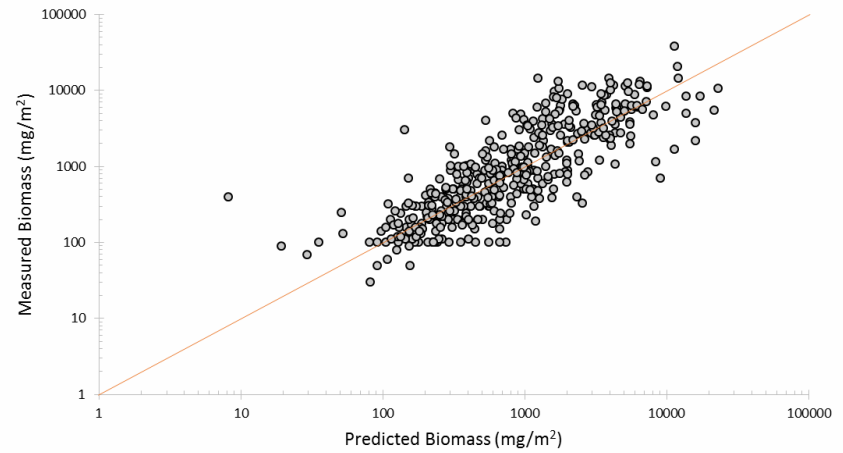
Hayward	$Biomass_{Obs} = 0.719 \cdot Biomass_{Pred}^{0.797}$	$(R^2_{Adj} = 0.437, P \ll 0.0001)$
Stave North	$Biomass_{Obs} = 0.302 \cdot Biomass_{Pred}^{0.908}$	$(R^2_{Adj} = 0.665, P \ll 0.0001)$
Stave South	$Biomass_{Obs} = 0.338 \cdot Biomass_{Pred}^{0.880}$	$(R^2_{Adj} = 0.582, P \ll 0.0001)$
Stave West	$Biomass_{Obs} = 0.527 \cdot Biomass_{Pred}^{0.815}$	$(R^2_{Adj} = 0.536, P \ll 0.0001)$



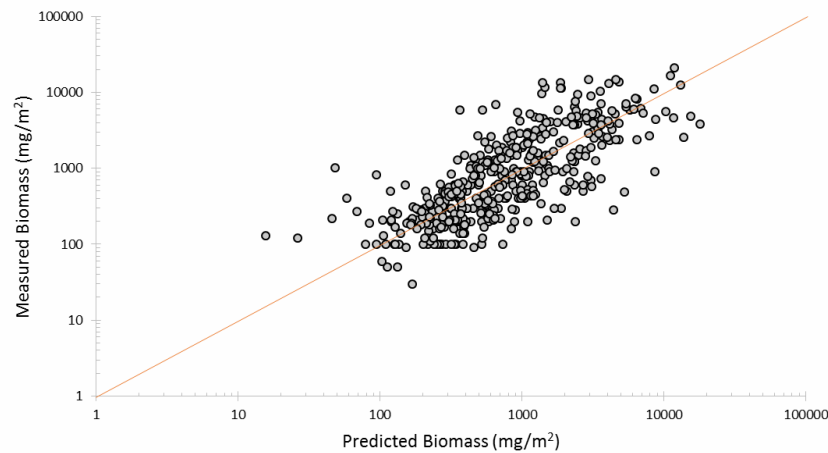
A. Hayward



B. Stave North



C. Stave South



D. Stave West

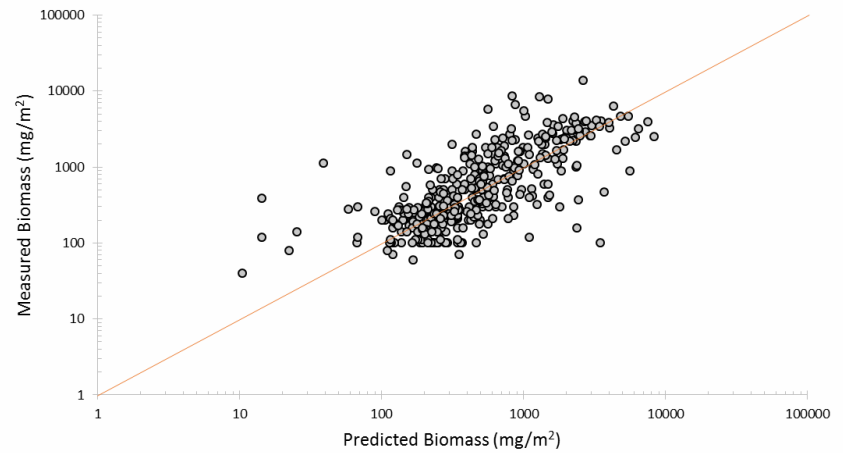


**Figure 25.** Plot of predicted versus measured periphyton biomass values ( $\text{mg}/\text{m}^2$ ) collected from artificial substrate placed at various depths at three sites in Stave Lake Reservoir and one site in Hayward Reservoir. The predicted values were derived by using a recursive growth algorithm that models biomass change over time using a daily time step. Periphyton growth rates were allowed to vary depending on prevailing light intensity and water temperature conditions using Eq. 15 to 18. The duration of each model run was set to the corresponding periphyton growing periods recorded during the monitoring period. The diagonal red line represents the line of equality.

The slope and intercept coefficients however indicated that predictions from the recursive algorithm tended to overestimate actual biomass at the lower range of measured values, and underestimated values at the higher end. The cause for this bias is uncertain, but is believed to be the result of using the depth-averaged water temperature variable when predicting growth daily growth rates in Eq. 16 to 18. Assuming that the majority of low biomass values typically occur at depth, actual water temperatures would likely be cooler than the depth averaged value, hence resulting in slightly lower growth rate than would be predicted by the growth equations. The reverse would be the case for plates near the water surface, where most of the higher biomass estimates would typically occur due to the higher  $PAR_{Surface}$  values. Water temperatures at these plate locations would tend to be warmer than the depth-average, thus resulting in slightly higher growth rates than would be predicted. In the case of predictions at Hayward site, not incorporating a temperature variable in the Hayward model (Eq. 15) may have implicitly caused a similar effect by effectively assuming a constant water temperature with depth when this was not actually the case, particularly during the summer.

## Effective Littoral Zone Modelling

### WUP Expectations

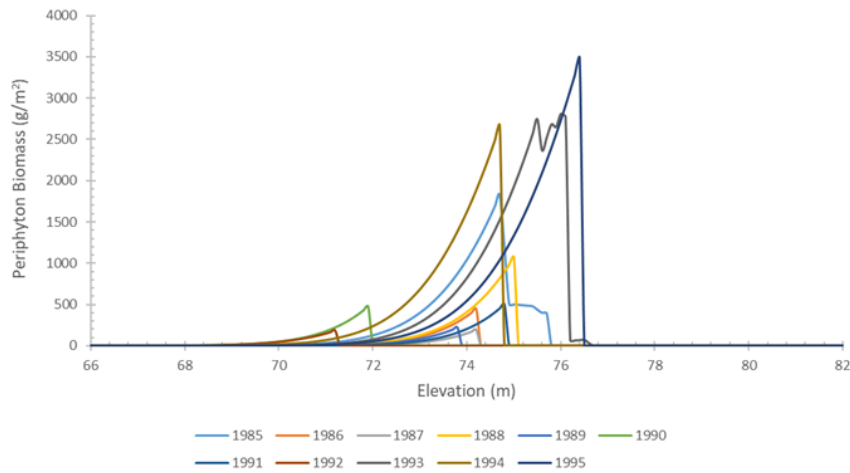
Effective littoral zone modelling carried out during the WUP process suggested that the maximum gain in ELZ over the baseline Electrical System Operating Review (ESOR) strategy was about 11% (Failing 1999). When the modeling was repeated in the present study, using the same modelled reservoir elevation dataset derived during the WUP, a similar result was obtained, indicating the ELZ modelling algorithm developed here functioned similarly to the one used during the WUP process, even though the duration of the modelling period within each year was shortened to 244 days from a full year to better correspond with the biomass data. With the baseline ESOR strategy, average ELZ was calculated to be 2240 ha. For the 'Combo 6' operating strategy it was 2388 ha, representing a 148 ha or 6.5% gain in ELZ habitat (Table 12).

When the ELZ model was applied to actual pre-WUP Stave Lake Reservoir elevation data spanning the years from 1985 to 1995, ELZ habitat area was estimated to be 2046 ha, a value that was 194 ha less than modelled for the ESOR strategy. In the WUP years spanning 1999 to 2009 when the 'Combo 6' strategy was fully implemented, ELZ habitat area was calculated to be 2635 ha, which was 247 ha higher than expected. Actual pre- vs. WUP increase in ELZ habitat area was estimated to be 589 ha; suggesting a 28% increase ELZ habitat over pre-WUP conditions. A simple t-test confirmed that the difference was statistically significant. It would appear therefore that the benefits of implementing the 'Combo 6' operating strategy on littoral development, **as measured by the ELZ metric**, had exceeded WUP expectations.

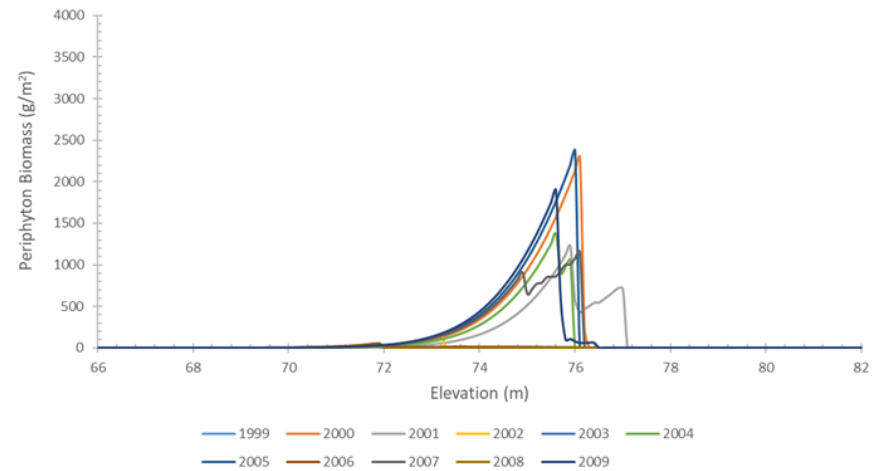
### Relationship to Periphyton Biomass Growth

To determine if the increases in ELZ habitat area translated into increases in periphyton growth potential, the recursive algorithm developed in the preceding section was used with the same pre-and WUP reservoir elevation data. The only difference was that the algorithm was applied over a 244- day growing period (Mar 1 to Oct 31) rather than the 25 to 77 day durations used during the monitoring program. Because there was no provision in the model to account for natural periphyton mortality over such a long-time frame, it is important to note that the modeled biomass data should not be viewed as a

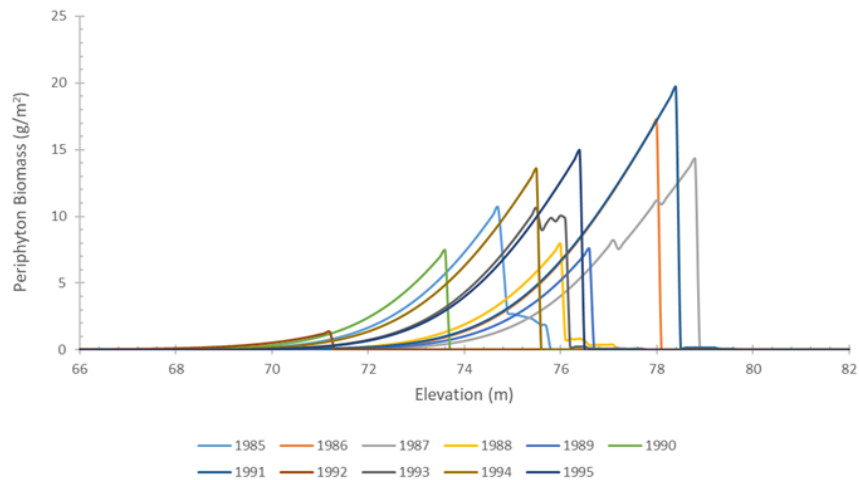
A. Pre - WUP, Oct 31



B. WUP, Oct 31



C. Pre - WUP, Aug 30



D. WUP, Aug 30

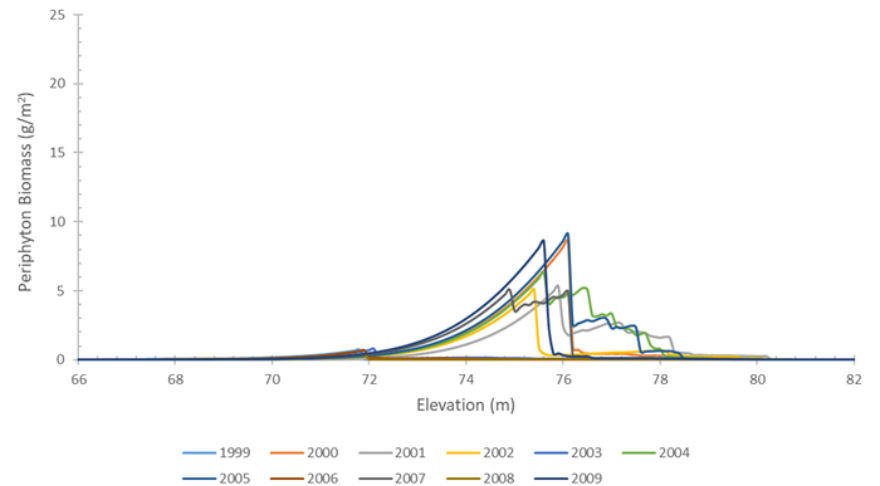


**Figure 26. Plots of simulated periphyton biomass (1000 kg), an indicator of periphyton growth potential, as a function of reservoir depth for pre-WUP (1985 to 1995) and WUP (1999 to 2009) reservoir conditions. Plots A and B show the outcomes of periphyton growth simulations ending Oct 31, the same as the ELZ metric. Plots C and D show the results of a shorter simulation period; ending Aug 30.**

**Table 13.** Yearly values and summary statistics of the ELZ metric and corresponding predicted biomass values indicating periphyton growth potential in Stave Lake reservoir for simulation periods ending Oct 31 each year. Predicted biomass data are also provided for simulation periods ending Aug 30 to illustrate the differences in growth potential before the reservoir is typically drawn down in September.

Phase	Year	ELZ (ha)	Boundary Elevations (m)		Periphyton Biomass (1000 kg) to Aug 30			Periphyton Biomass (1000 kg) to Oct 31		
			Upper EI	Lower EI	Peak	Elevation of Peak (m)	Depth Integrated	Peak	Elevation of Peak (m)	Depth Integrated
<b>Pre WUP</b>	1985	1803	75.3	69.6	3.3	74.7	58	560	74.7	7829
	1986	1771	73.9	68.4	4.6	78.0	93	128	74.2	1109
	1987	1968	74.0	67.9	3.8	78.5	86	56	74.2	444
	1988	1864	74.8	68.9	2.4	76.0	37	350	75.0	3229
	1989	2028	73.7	67.5	2.3	76.6	32	58	73.8	554
	1990	1856	72.3	66.8	2.1	73.6	31	149	71.9	1379
	1991	2526	74.5	66.7	6.0	78.4	116	160	74.8	1303
	1992	2535	73.5	65.9	0.4	71.3	6	59	71.2	565
	1993	2060	75.9	69.4	3.5	75.3	69	897	75.5	15469
	1994	1949	74.3	68.2	4.6	75.3	73	818	74.7	9632
1995	2147	76.2	69.4	4.3	76.4	81	1010	76.4	14558	
Average		2046	74.4	68.1	3.4	75.8	62	386	74.2	5097
Stdev		252	1.1	1.2	1.5	2.1	31	352	1.4	5523
<b>WUP</b>	1999	2867	74.8	66.0	0.2	71.8	3	18	71.8	18
	2000	2230	75.8	68.8	2.5	76.1	42	656	76.1	8458
	2001	2470	76.5	68.7	1.6	75.9	36	368	75.9	5739
	2002	2513	72.8	65.4	1.7	75.3	25	42	73.2	371
	2003	2960	76.9	67.6	0.2	72.1	4	12	72.1	255
	2004	2753	75.5	67.0	2.0	75.6	49	444	75.6	5441
	2005	2202	75.6	68.7	2.6	76.1	53	704	76.0	8754
	2006	2903	74.8	65.9	0.2	71.9	4	17	71.9	240
	2007	2502	75.8	68.0	1.6	74.9	36	330	76.1	6030
	2008	3254	75.3	65.4	0.1	71.9	2	11	71.9	107
2009	2335	75.7	68.4	2.8	75.6	41	611	75.6	7009	
Average		2635	75.4	67.3	1.4	74.3	27	292	74.2	3870
Stdev		320	1.0	1.3	1.0	1.8	19	270	1.9	3460

predictor of actual biomass, but as noted above, only as an indicator of potential periphyton growth. Also, to simplify the modelling process, only the Stave North growth model (Eq. 16) was used in the recursive algorithm. There was no added value in including the other two Stave Lake growth models (Eq. 17 and 18) as they were so similar to one another. Finally, the recursive algorithm was computed at 10 cm depth increments rather than at specific plate depths, creating a biomass depth-profile. The biomass results, which up to now have been reported as a density value ( $\text{g}/\text{m}^2$ ), were then multiplied by the area of shoreline habitat (ha) with a slope gradient  $> 15\%$  at each depth increment (provided by BC Hydro). This last computational step allowed for a direct comparison between the periphyton biomass and ELZ metrics. Results of the periphyton modelling exercise for the pre-WUP period are shown in Figure 26A, which plots the distribution of modelled periphyton biomass (1000 kg) as a function of water depth for each year of simulation. Yearly depth-integrated biomass values are summarised in Table 12.

The modelling results were able to show that during the pre-WUP operating period, periphyton growth tended to peak over a broad range of depths; ranging from El 71.2 m to El 76.4 m and averaged El 74.3 m. This corresponded reasonably well with the range of upper ELZ boundaries, which ranged from El 72.3 to El 76.2 m and averaged El 74.4 m ( $r = 0.861$ ,  $P = 0.0007$ ). Average elevations did not differ significantly from one another ( $t = -0.322$ ,  $P = 0.751$ ).

Peak biomass values during the pre-WUP operating period ranged from 56 to 1,010 tonnes, while depth integrated biomass values ranged from 444 to 15,469 tonnes. The average for each of the two metrics was 386 tonnes to 5097 tonnes respectively, and were found to be highly correlated with one another ( $r = 0.980$ ,  $P << 0.0001$ ). A comparison of the ELZ habitat areas with peak biomass values found no significant correlation between the two variables ( $r = 0.132$ ,  $P = 0.700$ ). A similar lack of correlation was observed when the ELZ metric was compared to depth-integrated biomass ( $r = 0.095$ ,  $P = 0.781$ ).

During the WUP operating period, there appeared to be two very different types of biomass response depending on the year of simulation. In 6 of the 11 years, there was significant biomass growth with peak values ranging from 330 to 704 tonnes and depth integrated biomasses ranging from 5441 to 8458 tonnes. Averages for the two metrics were 519 and 6905 tonnes respectively. This was in contrast to the response observed in the other 5 years, where peak and depth-integrated biomasses averaged 20 and 229 tonnes respectively. In this later group, peak biomass ranged from 11 to 42 tonnes, while depth-integrated biomass ranged from 107 to 371 tonnes. The periphyton biomass during these low growth years was on average less than 4% of the values seen during the high growth years. This difference in biomass response was also accompanied by sharp contrasts in the elevation of peak biomass. During the high growth years, peak elevations ranged from 75.6 to 76.1 m and averaged 75.9 m, while in low growth years, peak elevations ranged from 71.8 to 73.2 m and only averaged 72.2.

Unlike the pre-WUP condition, peak elevations were uncorrelated with the upper ELZ boundary variable ( $r = 0.323$ ,  $P = 0.333$ ). Because of the two types of biomass responses, average peak elevation across all years (74.2 m) was lower than the corresponding average upper ELZ boundary (75.4 m), which did not share this dual biomass response to Combo 6 operations. The difference however was not statistically significant (Mann-Whitney  $U_{11,11} = 64.5$ ,  $P >> 0.20$ ).

The ELZ metric was found to be negatively correlated with peak biomass ( $r = -0.831$ ,  $P = 0.0015$ ), suggesting that during the WUP period, the highest peak biomass values tended to occur in times when ELZ habitat areas were at their lowest. This was opposite of what was hypothesised regarding the relationship between the ELZ metric and periphyton growth. Because the two biomass metrics were highly correlated ( $r = 0.981$ ,  $P < 0.0001$ ), a similar negative correlation was observed between the ELZ habitat area and depth-integrated biomass ( $r = -0.838$ ,  $P = 0.0012$ ).

Average depth-integrated biomass for all WUP years was 3870 tonnes. Though this value was considerably less than the average seen for the pre-WUP period (5097 tonnes), the between-year variance in the biomass metric was so large that the difference was not statistically significant (Mann-Whitney  $U_{11,11} = 77$ ,  $P \gg 0.20$ ). The outcome was the same when the comparison was made using the peak biomass data (Mann-Whitney  $U_{11,11} = 76$ ,  $P \gg 0.20$ ). Both results contradicted the ELZ analysis, which had indicated a 28% increase in ELZ habitat area and assumed a corresponding increase in periphyton biomass. It is clear from this analysis that the ELZ metric developed for the WUP was a poor predictor of periphyton growth potential.

To determine if the time-of-year the growth simulation had an effect on the relationship between ELZ habitat area and periphyton biomass, the growth simulations were repeated using Aug 30 as the end date, shortening the growth period by two months. Results of these simulations are shown in Figures 26C and D and summary of key values is provided in Table 12.

Common to both the pre-WUP and WUP biomass profiles was a dramatic drop in peak and depth integrated biomass values, which was expected due to the shorter growth period. There were however differences in how the biomass profiles changed between monitoring periods. During the pre-WUP period, there was a noticeable upward shift in peak biomass elevations. With the shortened growth period, peak biomass elevations averaged El 75.8 m, which was 1.6 m higher than the average seen with the longer growth period. The difference was statistically significant (Mann-Whitney  $U_{11,11} = 92$ ,  $P < 0.05$ ). This was not the case WUP. Average peak biomass elevations remained similar to one another (El 74.3 m vs. El 74.2 m respectively, Mann-Whitney  $U_{11,11} = 67$ ,  $P \gg 0.20$ ). What was different however, was the presence of significant periphyton growth at elevations greater than El 76.4 m, which only occurred in one year with the longer growing period (Figure 26D). With the shorter growing period, significant periphyton growth occurred in 6 of the 11 WUP simulation years. The 5 years where such growth did not occur were the same as the group identified earlier with low peak biomass elevations. It would appear that events leading to such low peak biomass elevations occurred prior to the Aug 30 simulation end date.

Pre-WUP depth-integrated biomass values with the shortened growth period averaged 208 g/m<sup>2</sup> and ranged from 18 to 402 g/m<sup>2</sup>. In contrast, average depth-integrated biomass following implementation of the 'Combo 6' strategy was 87 g/m<sup>2</sup> and ranged from 6 to 174 g/m<sup>2</sup>. The difference in this case between pre- and WUP periods was statistically significant (Mann-Whitney  $U_{11,11} = 97$ ,  $P < 0.02$ ), suggesting that the periphyton growth seen during the WUP at elevations higher than El 76.4 m was insufficient to match the growth seen pre-WUP. The data suggests that implementation of the 'Combo 6' operating strategy had likely worsened periphyton growing conditions in the reservoir, and that the effect was most apparent by the end of summer. By the end of fall however, the difference became less apparent.

When the late summer depth integrated biomass values were compared to corresponding ELZ habitat areas, a significant negative correlation was found ( $r = -0.585$ ,  $P = 0.0043$ ), providing further evidence that the ELZ metric performed poorly as an indicator of periphyton growth potential. The reason for this negative correlation is unclear, but may be linked to how the ELZ metric was calculated; using a simple additive indicator when tracking daily growth as a function of water depth over time. With this algorithm, growth occurs at the same rate for all elevations, regardless of available light intensity or local water temperature conditions. Analysis of the periphyton growth data showed that this was not the case and that growth rates tended to decline rapidly with depth. Thus, when the ELZ was calculated, too much weight was likely given to the value of deep water growth compared to that nearer to the water surface.

Across all simulation years, the magnitude of ELZ habitat area tended to be independent of the upper ELZ boundary elevations ( $r = 0.310$ ,  $P = 0.161$ ). There was however, a significant negative correlation between ELZ habitat area and the lower boundary elevation ( $r = -0.670$ ,  $P = 0.0006$ ), indicating that ELZ habitat area tended to increase mostly from downward shifts in the lower boundary elevation. However, when the lower ELZ boundary elevation was regressed against depth integrated biomass, there was a significant positive relationship, particularly when the biomass variable was log transformed (Figure 27). This contradictory response to the lower ELZ boundary elevation between the habitat area and biomass metrics was seen as strong evidence illustrating the inappropriateness of assuming a uniform weighting when valuing littoral productivity as a function of water depth in the ELZ metric. As the lower ELZ boundary dropped in elevation, increasing ELZ habitat area, a larger proportion of the ELZ habitat included deep water habitats that contributed less to overall biomass production. The change in proportion was exacerbated by the fact that the area of shoreline habitat with a slope < 15% also increased with depth.

Another factor that may explain the lack of positive correlation between the ELZ habitat area and depth-integrated biomass variables is the fact that the ELZ metric is an additive statistical construct that ignores the sequential timing of reservoir elevation changes. The periphyton biomass metric on the other hand explicitly incorporates these changes, calculating the growth (or loss) of biomass on successive days for each simulation year.

A comparison of pre-WUP reservoir elevations in Figure 28 with the WUP elevations in Figure 15 clearly show that a key outcome of the 'Combo 6' operating strategy was to force reservoir elevation to consistently meet a targeted value during summer. This would then be followed by a drop in elevation during the fall to accommodate high winter inflows. During the pre-WUP period, reservoir elevations were highly variable from year to year. In some years, reservoir elevations stayed relatively constant for

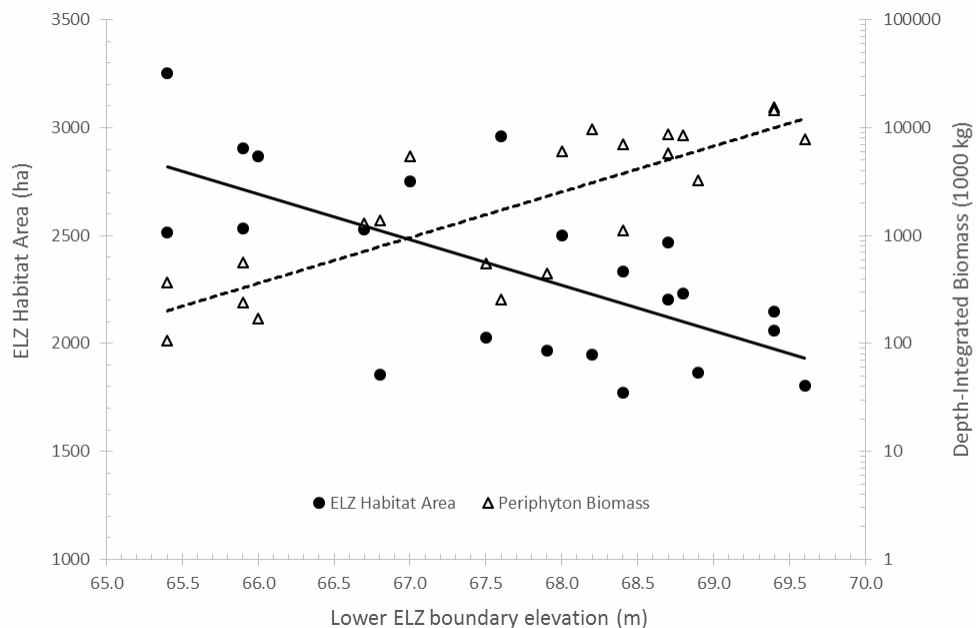


**Figure 27. Plot of ELZ habitat area and depth-integrated periphyton biomass as a function of lower ELZ boundary elevation for all years of simulation (1985 to 2009).**

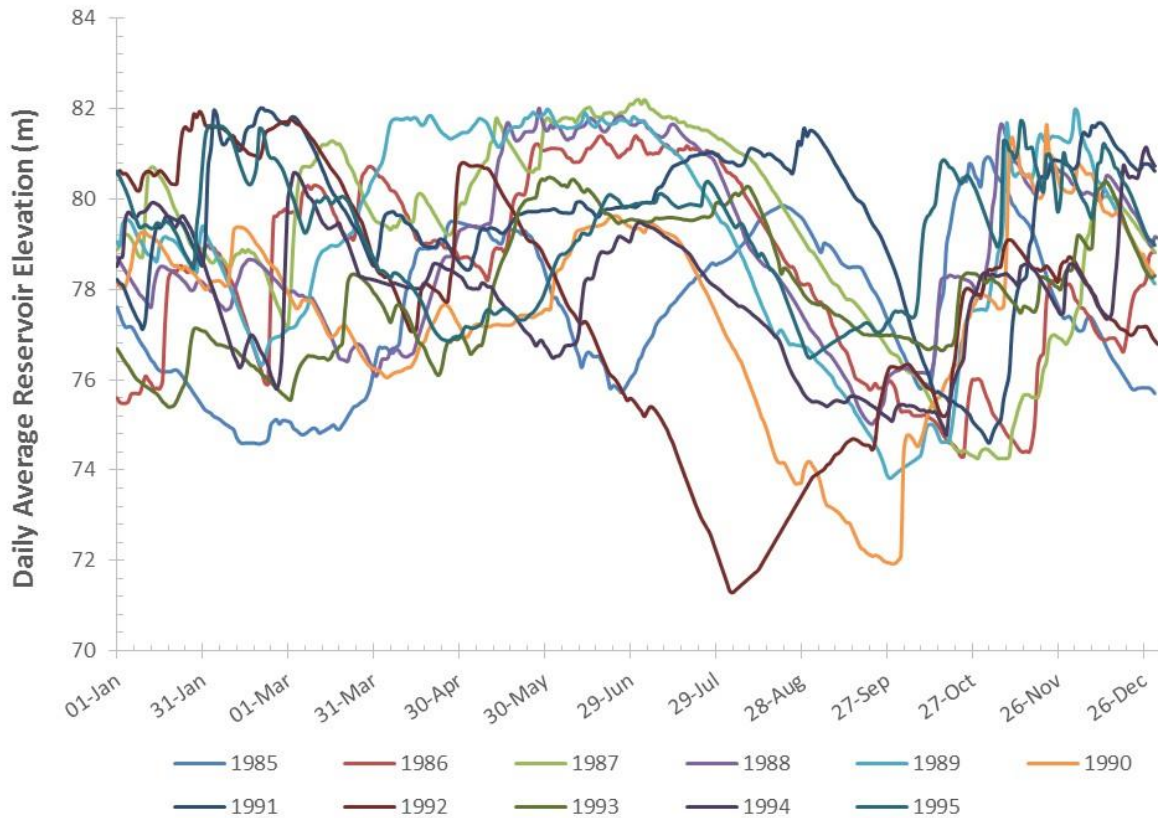


**Figure 28. Reservoir elevation (m) over time for the pre-WUP period showing how it differed to the WUP period shown in Figure 15.**

much of the spring and summer, potentially allowing significant periphyton growth to occur at lower elevations. In those years, come September when the reservoir is drawn down in anticipation of high winter inflows, less of the accumulated periphyton biomass is dewatered, leading to higher depth-integrated biomass levels by the end of fall. In other years, reservoir elevations were kept high for much of the spring and summer, thus when the reservoir was drawn down in September, the majority of growth was dewatered leading to near total loss of the accumulated periphyton biomass. This year to year variability in pre-WUP reservoir operations allowed some years to be highly productive, particularly when reservoir elevation was gradually increased throughout the Mar to August growing period. The pre-WUP biomass depth profiles showed that in general, there were more high growth years than low growth years, and when there was a low growth year, the loss was generally not as bad as during WUP years.

In contrast, reservoir elevations during the WUP period tended to follow a much more consistent pattern from year to year; one where water levels were kept relatively stable from Jun 1 to Aug 30, and after which water levels were drawn down, dewatering the periphyton population that had accumulated during the preceding three months. Because much less time was spent each year at lower reservoir elevations, there was little opportunity for higher periphyton growth at depth. As a result, significant periphyton losses occurred every year, with the magnitude of loss dictated mostly by the depth of drawdown starting in September.



## Relationship to Fish Abundance

Fish abundance in Stave lake reservoir was monitored yearly since 2005 by Stables and Perrin (2015) as part of another Stave WUP monitoring program that was running concurrently. Each year, hydro acoustic surveys were carried out in the fall (September/October) to count the number of fish targets across a standardised set of transects. The target data were then assigned a likely species and age identifier given the strength of the target signal, and its location in the water column. This target assignment process was based on gill netting and trawling data that were collected simultaneously. The outcome of these annual hydro acoustic surveys was a yearly time series of species specific fish abundance data. From the length and weight data collected from captured fish, the abundance data were in turn converted to estimates of species specific fish biomass. The last year of data collection was 2014.

There was a total of 9 species captured over the course of the 10-year monitor. Yearly fish abundance estimates ranged from 113 fish/ha in 2012 to 596 fish/ha in 2010 and averaged 259 fish/ha overall. Fish biomass tended to be high correlated with log transformed fish abundance ( $r = 0.926$ ,  $P = 0.0001$ ) with values ranging from 1.62 kg/ha to 12.51 kg/ha. Fish Biomass averaged 5.92 kg/ha overall. Kokanee tended to dominate the survey each year, comprising 97% of the total count across all years. Kokanee were also the major contributor in terms of total fish biomass, though Bull trout, Cutthroat trout and Northern pike-minnows were also significant contributors because of their larger average size.

To assess their relationship to fish abundance and biomass, both the ELZ and periphyton biomass metrics had to be calculated for years 2010 to 2014. These results are presented in Table 13, along with a yearly summary of the fish abundance and biomass data. Also, included in the data set are the yearly abundance and biomass estimates of Cutthroat and Rainbow trout. Stables and Perrin (2015) were able to show through stomach content analysis that they were occasional benthivores and therefore potentially more directly linked to changes in littoral development.

**Table 14. Yearly estimates of fish abundance and biomass in Stave Lake Reservoir from Stables and Perrin (2015) and corresponding littoral productivity indicators that include the ELZ and periphyton biomass metric developed in the present study. Included in the table are separate abundance estimates for cutthroat and rainbow trout, salmonids that have been shown to feed occasionally on benthic organisms.**

Year	ELZ Habitat Area (ha)	Fall Periphyton Biomass (1000 kg)	Summer Periphyton Biomass (1000 kg)	Total Fish Abundance (fish /ha)	Total Fish Biomass (kg/ha)	Cutthroat and Rainbow Trout Abundance (fish/ha)	Cutthroat and Rainbow Trout Biomass (kg/ha)
2005	2202	8754	53	137	3.31	0.86	0.12
2006	2903	240	4	155	4.25	1.74	0.55
2007	2502	6030	36	192	4.86	3.36	1.08
2008	3254	107	2	223	6.69	2.87	0.94
2009	2335	7009	41	527	9.37	4.81	1.12
2010	2374	8695	58	596	12.51	2.69	0.63
2011	2376	7266	42	318	6.34	3.54	1.21
2012	2574	3217	22	113	1.62	0.04	0.02
2013	3001	2244	50	163	3.75	1.23	0.27
2014	1927	10992	91	165	6.51	7.87	2.04

**Table 15. Correlation matrix between littoral productivity indicators and fish abundance estimates based on the data of Table 13. The critical correlation coefficient for  $n = 10$  and  $\alpha = 0.05$  is 0.632.**

		Fish Abundance Estimates			
		Total Fish Abundance	Total Fish Biomass	Cutthroat and Rainbow Trout Abundance	Cutthroat and Rainbow Trout Biomass
Littoral Productivity Indicators	ELZ Habitat Area	-0.216	-0.220	-0.512	-0.413
	Fall Periphyton Biomass	0.349	0.395	0.554	0.456
	Summer Periphyton Biomass	0.180	0.280	0.563	0.437

A correlation analysis between littoral productivity indicators and fish abundance estimates revealed a number of interesting patterns (Table 14). Firstly, all of the correlations with the ELZ metric were negative, consistent with the observations made earlier between the ELZ and periphyton biomass metrics. In fact, the coefficient of correlation between these two latter variables had improved substantially when using the 2005 to 2014 dataset ( $r = -0.949$ ,  $P << 0.0001$ ). Secondly, depth-integrated periphyton biomass computed at the end of fall tended to be the most strongly correlated indicator of littoral development across all measures of fish abundance, suggesting that it may be the most accurate. Finally, the strongest correlations tended to occur when only cutthroat and rainbow trout were under consideration, and in particular when estimates were reported in terms of abundance. These latter two observations together suggest that in years with high overall periphyton growth potential, there may be greater tendency for rainbow and cutthroat trout to occupy nearshore habitats, possibly foraging for benthic organisms, than in years with low periphyton growth potential.

With only 10 data points however, none of these correlations were statistically significant ( $t_{crit 0.05,10} = 0.632$ ), indicating that none of the littoral productivity indicators were strong predictors of fish biomass or abundance. This conclusion however may be premature as both the periphyton biomass (Figure 25) and fish abundance metrics (Stables and Perrin (2015) have very high error (uncertainty) associated with them. Weak correlations as seen on Table 14 would require a much larger sample size to overcome the masking effects of such error and thus increase statistical power.

## Discussion

### General Observations

Over all, analysis of the depth integrated periphyton production data found that variables linked to reservoir hydrology appeared to act as limiting factors to growth as hypothesised by the concept of an effective littoral zone or ELZ. The dewatering experiment of Bruce and Beer (2010) was able to show that a single day of dewatering was able to effectively cause near to 100% mortality of periphyton growth on artificial substrate. Results of the 10-year monitor supported that conclusion as well, and inclusion of

dewatering related mortality in the growth prediction models contributed to the high degree of correspondence between predicted and observed biomass estimates. The data however, hinted that such high mortality may not always occur, particularly when the duration of dewatering was less than 1 day as was observed in Hayward Reservoir (i.e., over the course of several hours). Though not tested in this monitor, it was suspected that dewatering survival may be longer when weather conditions are cooler, cloudier and/or include significant precipitation. This variance in dewatering survival was hypothesised to be a possible mechanism explaining at least some of the error found in the periphyton biomass model predictions. Unfortunately, the absence of published literature on the subject suggests that there has been little research in this area of periphyton ecology and further research may be worthwhile.

One of the underlining methodological premises identified in the monitoring program terms of reference was that periphyton growth could be adequately characterized in terms of an average day accumulation of periphyton biomass (i.e., mg/day where measured biomass would be divided by the number of incubation days). It was assumed that because biomass was being measured in such short time frames (at 6 week intervals), this linearized measure of growth would be reasonably accurate and not introduce significant measurement error. This turned out not to be the case. Plots of biomass as a function of time showed a strong exponential growth pattern. Furthermore, the interval between plate sampling periods was not consistent over the course of the 10-year monitor and in fact varied between 25 and 77 days. This variance in sampling interval, along with the exponential response in growth, lead to inconsistent biases in the linearized growth measure and hence created considerable measurement error in the growth statistic. The only way to correct for this variable bias was to abandon the linearized growth metric and attempt to measure growth as a proportional rate. This was done by using Eq. 5 that estimates growth rate from two measures of biomass separated by a known period of time; an initial biomass at time '0', and a final biomass at time 't' days later. The final biomass values and the duration of the growth period were readily available values in this monitor. Initial biomass values however were not, and given the experimental design, could not be measured directly post hoc. As a result, it had to be estimated from other studies. Fortunately, the work of Bruce and Beer (2010) did contain some information on initial biomass estimates at the start of a growth trial. These values tended to be highly variable, ranging from 50 to 160 mg/m<sup>2</sup>. An average of 100 mg/m<sup>2</sup> was used in the present monitor, and it was assumed to be constant due to the fact that all plates were similarly scraped clean prior to each growth trial. This assumption however, was untested. In fact, a small variance in the initial biomass could lead to major differences in biomass at the end of a growth trial. For example, in the present study a  $\pm 10\%$  difference in initial biomass at the start of a growth trial (i.e., a 20 mg/m<sup>2</sup> in this cases assuming an average of 100 mg/m<sup>2</sup>), would translate to a 1095 mg/m<sup>2</sup> difference in final biomass 42 days later assuming a typical growth rate of 0.1 per day.

This high degree of sensitivity to initial biomass conditions highlights the importance of periphyton survival during short term dewatering events as a key determinant of recovery following re-submergence. This was not taken into account in the ELZ model as defined in the Failing (1999) report, where dewatering was assumed to cause immediate 100% mortality. The study of Bruce and Beer (2010) showed that this was indeed possible during the dry summer months, but reservoir elevations are typically stable during these months. Rather, the largest fluctuations in water level typically occur in the spring or fall months, where temperatures are cooler, solar irradiance is less, and cloudy days are more frequent, as are the precipitation rates. Weather conditions at these times may allow greater survival than what the ELZ model would assume, and hence allow for quicker recovery following re-submergence. The overall effect would be increased error in ELZ predictions, with a bias towards over-estimating dewatering impacts.

In addition to dewatering, the effects of fluctuating reservoir elevation were also thought to provide opportunities for higher intensity light (i.e., PAR) to reach deeper sections of the littoral zone, leading to faster growth rates in these areas. In general, the periphyton growth data supported this concept, where periphyton biomass tended to be much higher in deeper waters when, during the growth period, water levels were significantly lower than at the time of sampling. In addition to this generally positive effect, the ELZ model as proposed in the monitoring study terms of reference assumed that the light–growth relationship would have three components: 1) an initial photo inhibitory phase where high light intensity had a negative impact on growth rate (Wetzel 2001) near or at the water’s surface; 2) an increasing growth phase where the photo-inhibitory effects gradually abate with water depth and 3) once a peak growth rate was achieved, there would be a gradually declining growth rate as light intensity decreases exponentially with water depth. Analysis of the growth vs light data found little evidence of such a response pattern. Rather, growth rates changed little over a very broad range of light intensities. In fact, growth rates were typically within 90% of maximum values over a range of average daily light intensities values spanning 700 to 9000  $\mu\text{moles}/\text{m}^2/\text{s}$ , the highest value being the brightest light intensity observed during a mid-summer, cloudless day. The data also showed that growth rates were still above 50% maximum when light intensity was only 75  $\mu\text{moles}/\text{m}^2/\text{s}$ , suggesting that periphyton growth rates were only significantly light sensitive over a relatively narrow range of low intensities. Indeed, growth rates varied from near-0 to 75% maximum over a range of 0 to 225  $\mu\text{moles}/\text{m}^2/\text{s}$ , and was within 75% maximum for all light intensities up to 9000  $\mu\text{moles}/\text{m}^2/\text{s}$ . The observed light-growth rate response curve was very different from that postulated in the conceptual ELZ model.

This difference in light response also called into question the notion of 1% light compensation depth, a metric central to the calculation of the ELZ metric used in the Stave Falls WUP (Failing 1999). The 1% light compensation depth is defined as the water depth at which light was 1% of surface irradiance and corresponded to the light intensity at which periphyton growth was roughly equal to mortality (Wetzel 2001). Based on this definition, the 1% light compensation depth is a single depth value that is independent of surface light intensity (i.e., it is the same depth regardless of whether surface irradiation is 900 or 9000  $\mu\text{moles}/\text{m}^2/\text{s}$ ). At that depth, however, actual light intensity would vary greatly. Assuming a grand mean light extinction coefficient of -0.39 for all sites and years at the Stave Lake project, the 1% light compensation depth would be 11.8 m regardless of light intensity, but actual light intensity at that depth would be close to 90  $\mu\text{moles}/\text{m}^2/\text{s}$  when surface measurements on the day were 9000  $\mu\text{moles}/\text{m}^2/\text{s}$ , but drop to 9  $\mu\text{moles}/\text{m}^2/\text{s}$  on a 900  $\mu\text{moles}/\text{m}^2/\text{s}$  day. Based on the light saturation curve developed in this monitor, these two light intensities would lead to dramatically different growth rates, violating the definition of 1% light compensation depth. Indeed, this incongruence has been identified by others (Banse 2004), leading to a recommendation that it be abandoned as a metric defining the euphotic zone of freshwater systems and that a specific irradiance value be used instead. Few studies have specifically measured the compensation irradiance for freshwater epipelagic periphyton or phytoplankton communities. Banse (2004) identified this to be a significant gap in freshwater ecology understanding, but noted that from the few studies that have been done, compensation irradiance tended to be in to order of magnitude of 10  $\mu\text{moles}/\text{m}^2/\text{s}$ . Using this definition, along with the grand mean light extinction coefficient or -0.39, the compensation depths would have ranged from 17.4 m on a mid-summer cloudless day to 9.0 m on a stormy day in early spring or late fall. Even on a cloudy mid-summer day, the compensation depth would rise to 11.5 m. This highly variable compensation depth was not taken into consideration when defining the ELZ metric. In fact, it assumed that the euphotic zone was constant for the entire year, potentially creating a significant source of bias in the metric calculation.

Unfortunately, a direct measure of compensation irradiance was not possible from the light saturation curves, though this would have been an ideal data set to do so by simply noting the light intensity at which there was no periphyton growth. The reason for this was that zero growth was not observed at any of the measured low light intensities. Rather, from roughly 40  $\mu\text{moles}/\text{m}^2/\text{s}$  down to 0.5  $\mu\text{moles}/\text{m}^2/\text{s}$  (the lowest light intensity measured), periphyton growth appeared to have decoupled from its dependence on light and proceeded at a relatively constant rate ranging from 0.01 to 0.07. The average was 0.026 overall. This decoupling suggested that the growth was likely chemo-autotrophic or heterotrophic, though the extent to which this was bacterial versus algal is unknown. The ELZ model implicitly assumed that all periphyton growth would photo-autotrophic and that chemo-autotrophic or heterotrophic growth would not be significant factor. Furthermore, the ELZ assumed that all periphyton were obligate photo-autotrophs. The present monitor showed that this was not the case. Heterotrophy (including chemo-autotrophy) appeared to have played a significant role in overall littoral production, particularly in low light conditions. The extent with which heterotrophy contributed to overall littoral production at higher light intensities is less uncertain. There has been little research work in this area, particularly as it relates to epipellic periphyton production in lakes. However, the phytoplankton growth models of Hallock (1981) suggest that the relationship may be synergistic, particularly if the algae species are capable of limited heterotrophy (i.e., they are facultative phototrophs, also called mixotrophs). The studies of del Giorgio (1993), Coveny and Wetzel (1995), Dodds (2003), and Katechakis et al. (2005) were all able to show that the importance of heterotrophy in periphyton production may be more pronounced in ultra-oligotrophic lakes, such as the Stave Lake and Hayward reservoir, where allochthonous inputs may be an important source of carbon and other nutrients. The species composition of Stave Lake and Hayward Reservoir periphyton communities are not well known, though some taxonomy was carried out in 2003 and 2004 that identified some of the larger algae species to the nearest genus (Bruce and Beer 2015b). It is uncertain whether any of the identified algae are capable of limited heterotrophy as no relevant information could be readily found in the published literature. The *in situ* light experiment of Bruce and Beer (2014) however was able to clearly demonstrate that mixotrophy does indeed appear to occur in the Stave Lake Reservoir, though specific species could not be identified. The possibility of mixotrophy, and the presence of heterotrophic bacteria among the periphyton samples likely confounded the ELZ measure as it was originally conceived in the monitoring terms of reference, allowing significant growth to occur much deeper in the water column than would otherwise have been expected. Furthermore, the possibility of mixotrophy (along with other light adaptation strategies) may have delayed the effects of mortality when periphyton communities were plunged into darkness (Bruce and Beer 2014). The latter was more in line with the conceptual ELZ model, which had no provision to account for this mortality.

With the effects of light taken into account, the remaining unexplained variance in growth rate was found to be independent of most environmental and water quality parameters measured in this study. Phosphorus loading was believed to be a potentially significant factor, but the data suggested otherwise. Phosphorus levels were generally very low, hovering just above detectable limits, and tended to vary independently of periphyton growth. All of the phosphorus data were collected mid-lake at only one station per reservoir system. The nutrient sites were intended to be a pelagic measurement and as such were located some distance away from the periphyton sampling sites, calling into question how well they may have represented phosphorus conditions at the time of sampling. Indeed, at the Stave North site, phosphorus levels were found to be negatively correlated with periphyton growth, the opposite of what would be expected based on published literature (Wetzel 2001). In fact, the negative correlation would have been more indicative of increased heterotrophic production. Overall, phosphorus levels were found to be very low and when compared to other lake systems, and were indicative of an ultra-

oligotrophic trophic status (Beer 2004). No seasonal trend was found in the total dissolved phosphorus data, but a weak summer time high was detected in the total phosphorus data reflecting the greater abundance of pelagic organisms in the water column (Beer 2004, Wetzel 2001). It should be noted however, that a weak declining seasonal trend of summertime phosphorus was detected in Stave Lake reservoir in the pelagic monitoring program, where there was much longer time series of data (Bruce and Beer 2016).

There was a general declining trend in phosphorus levels towards the end of the monitoring period, in particular the last four years. This was also captured in the Stave Lake pelagic monitoring program (Bruce and Beer 2016). The cause of this drop could not be determined with the available data, but was found to be coincident with a change in maximum reservoir elevation in Hayward Reservoir. This relationship however was likely a coincidence as the decline in phosphorus tended to be gradual while the change in maximum reservoir elevation was a sudden shift that occurred midway through the time series, and then persisted till end of the monitor. The change was likely related more to changes in the pelagic plankton community, which was found to increase in species diversity and decrease in average size over that same time period (Bruce and Beer 2016). The driver for these latter changes are unknown.

Compared to phosphorus, nitrate levels were much less limiting to production potential (Beer 2004). Levels varied seasonally in tandem with periphyton growth, reaching their lowest values at times when biomass levels were at their highest. This pattern appeared to capture the effect of consumption as biomass levels increased and were consistent with what is generally known about the fate of nitrates in oligotrophic lakes (Wetzel, 2001). Like phosphorus, overall concentrations tended to decline over the course of the monitor, and in particular during the last four years of the monitor when maximum reservoir elevation was reduced in Hayward Reservoir. The reason for this is uncertain and as noted for the phosphorus data, was likely a coincidence.

Collectively, the data suggest that periphyton growth rates tended to vary independently of prevailing nutrient levels (when measured in open waters), and in the case of nitrates, was likely a contributing factor in creating the observed seasonal patterns.

The extent to which littoral periphyton production affected pelagic nutrient levels, if at all, could not be examined with the available data. It should be noted however, recent reviews by Vadeboncoeur et al (2002) and Poulickova et al. (2008) on the food web pathways in oligotrophic systems found that the importance of littoral production in overall lake productivity may have been historically undervalued. Both Liboriussen and Jeppesen (2003) and deNicola et al. (2003) were able to show that in shallow lakes, the importance of littoral production to whole lake production increased as lakes became increasingly oligotrophic. This relationship was especially strong in cases when nutrient inputs were primarily allochthonous in origin. This dependence on littoral pathways to 'process' allochthonous inputs into new biomass in clear, northern lakes was demonstrated by Ask et al. (2009). Whether this is also the case in Stave Lake and Hayward reservoirs is uncertain. Nevertheless, the available literature does suggest an important role for littoral development in whole lake (reservoir) production.

The only other variable in addition to light intensity and reservoir elevation found to significantly impact periphyton growth was water temperature. In the original model, water temperature was not included as a factor to maintain simplicity, even though its relationship to periphyton growth had been well established (Wetzel 2001). Typically, warmer water temperatures increase metabolic rates, and thus the rate at which growth can occur. This was indeed the case for periphyton growth in the present study. Water temperatures however, were not continuously monitored, requiring a model based on available solar radiation data to provide estimates of daily surface water temperature. Though the model did

appear to be reasonably accurate in making these predictions, this approach was novel and unproven. The model would require independent validation if were to be adopted for other lakes systems or applications. It should be emphasised that the model only predicted surface water temperatures. Though there are models that have been developed to predict the development of thermoclines over time in lake systems, these were highly complex requiring data inputs that were unavailable in this study (Hondzo and Stefan (1993). Thus, all modelled predictions of periphyton biomass growth assumed a uniform temperature at all depths equivalent to the surface temperature. This shortcoming likely introduced some error in the growth estimates, particularly at depth where actual water temperatures were likely cooler. However, because all ELZ simulations had the same error, this was unlikely to significantly affect the outcome of comparative analyses.

Overall the revised periphyton ELZ growth model appeared to perform reasonably well considering the lack of site-specific nutrient, water temperature and light intensity data. The highly patchy distribution of periphyton growth was also a factor, as well as the highly variable community structure (Bruce and Beer 2015a). Bruce and Beer (2014) were also able to show that periphyton communities were capable of significant light acclimation/adaptation, which included the potential for mixotrophy. Despite these difficulties, the revised ELZ model developed from the 2000 to 2009 monitoring data, along with the learnings obtained during the development process, appeared to be sufficiently robust to test the impact hypotheses posed by the WUP CC.

### Impact Hypotheses

There were 11 impact hypotheses identified by the CC for consideration in this monitor (BC Hydro 2005). Each are addressed individually below based on the meta-analyses presented above:

**H<sub>0</sub>1: Average reservoir concentration of Total Phosphorus (TP), an indicator of general availability of phosphorus is not limiting to littoral primary productivity.**

Total phosphorus levels averaged 2.2 µg/L in Stave Lake Reservoir (SD = 0.99, n = 46) over the course of the 10-year monitoring period (1999 to 2009). In many instances, concentrations were below detectable limits. At such concentrations, the reservoir is classified as being ultra-oligotrophic (i.e., TP < 3.0 µg/L), and is therefore considered to be phosphorus limited (Wetzel 2001, Beer 2004). H<sub>0</sub>1 can be rejected.

**H<sub>0</sub>2: Relative to the availability of phosphorus as indicated by level of total dissolved phosphorus (PO<sub>4</sub>), the average reservoir concentration of nitrate (NO<sub>3</sub>) is not limiting to littoral primary productivity.**

Nitrate levels (NO<sub>3</sub>) averaged 103.9 µg/L (SD = 36.8, n = 48) in Stave Lake Reservoir, which is below the threshold defining an oligotrophic condition (< 300 µg/L) and is therefore considered ultra-oligotrophic. Though NO<sub>3</sub> levels are considered limiting in general, the ratio of NO<sub>3</sub> to TP (103.9 µg/L to 2.2 µg/L or 47:1) is much greater than stoichiometric ratios typically found in freshwaters (~23:1, Wetzel 2001), suggesting that compared to TP, NO<sub>3</sub> is not a limiting factor for primary production in Stave Lake Reservoir (i.e., the availability of TP is far more limiting to periphyton growth than the availability of NO<sub>3</sub>). In this context, H<sub>0</sub>2 cannot be rejected.

**H<sub>0</sub>3: Water retention time ( $\tau_w$ ) is not altered by reservoir operations that vary from year to year such that it significantly affects the level of TP as described by Vollenweider's (1975) phosphorus loading equations (referred to here as TP( $\tau_w$ )).**

Water residence time ranged from 27.7 to 40.9 days depending on the year and averaged 33.5 days overall. Yearly average TP values were found to be independent of water residence times ( $r = 0.089$ ,  $P = 0.836$ ). The fact that TP levels did not appear to vary seasonally (Figure 4) despite strong seasonal trends in reservoir volume (Figure 15) and inflow discharge (Figure 13) was also indicative of an independence between TP concentration and reservoir operations. For the purposes of the littoral productivity monitoring program however, TP concentration is not considered to be meaningfully impacted by changes in water residence times. In this context, H<sub>0</sub>3 cannot be rejected.

**H<sub>0</sub>4: Water temperature, and hence the thermal profile of the reservoir, is not significantly altered by reservoir operations that vary from year to year.**

Average water temperature in the upper 8 m of the water column in Stave Lake Reservoir ranged from 3.6 to 22.0°C and tended to follow a strong seasonal pattern (Figure 12). Time series analyses showed that total solar input during the previous 75 days ( $PAR_{75d}$ ) was able to explain 96.6% of the variance in depth integrated water temperature, irrespective of reservoir operation. Given the little unexplained variance (3.4%), any role that reservoir operations may have in altering epilimnion water temperature was likely minimal. Thus, from the perspective of the littoral productivity monitoring program, average depth-integrated water temperature did not appear to be meaningfully impacted by reservoir operations. In this context, H<sub>0</sub>4 cannot be rejected. However, Bruce and Beer (2016) did a more detailed analysis of the relationship between water temperature and reservoir operation as part of an analysis on Stave Lake Reservoir pelagic primary production. This analysis involved a longer time series of temperature data (1999 to 2014). They were able to show that in Stave Lake Reservoir, the annual deep draft at the beginning of September appeared trigger the breakdown of thermoclines established over the summer. Whether this breakdown in thermocline impacted littoral development is uncertain. In this context, H<sub>0</sub>4 is inconclusive.

**H<sub>0</sub>5: Changes in TP as a result of reservoir operations (through changes in  $\tau_w$ ) are not sufficient to create a detectable change in littoral algae biomass as measured by littoral levels of chlorophyll  $\alpha$  (Chl<sub>a</sub>) and/or ash free dry weight (AFDW).**

Meta-analysis of the AFDW data clearly showed that variations in TP concentration were not a significant factor explaining the temporal and spatial (i.e., depth) variations in periphyton growth. This conclusion however was confounded by the fact that TP was measured at only one open-water site. Bruce and Beer (2015) found that TP concentrations measured across transects in Stave Lake Reservoir showed considerable spatial variation, challenging the assumption that the TP data collected at the site would be representative of the reservoir in general. There may have been local variations in TP concentration that could have affected site specific growth rates, but could not be accounted for with the data collected. Whether local variations in TP concentration are impacted by Stave Lake Reservoir operations is unknown. Bruce and Beer (2015) were able to show that local TP concentration can be influenced by TP inputs from the Alouette powerhouse facility, which diverts some of the fertilized waters of Alouette Lake Reservoir to the Stave Lake Reservoir. The hypothesis as stated however, is focused more on the effect of water retention time in the Stave Lake Reservoir. Given that Hypothesis H<sub>0</sub>3 was not rejected, and the fact that periphyton growth appeared to be independent of open water variations of TP, H<sub>0</sub>5 cannot be rejected.



**H<sub>06</sub>: Overall primary production (as measured by <sup>14</sup>C inoculation and/or as inferred from ash free dry weight data) of Stave Lake Reservoir is not different than that of Hayward Lake**

Depth integrated periphyton growth (measured in terms of changes in AFDW between sampling periods) was consistently higher in Hayward Reservoir than all three Stave Lake Reservoir sampling sites (Table 7). This difference was maintained across all years except 2007. In Hayward Reservoir, depth integrated periphyton growth rates averaged 0.090 day<sup>-1</sup>. This was followed by the Stave North and Stave South sites with average growth rates of 0.078 and 0.070 day<sup>-1</sup> respectively. The Stave West site had the slowest growth rate with 0.061 day<sup>-1</sup>. H<sub>06</sub> can be rejected.

**H<sub>07</sub>: Pelagic primary production dominates in Stave reservoir while littoral production dominates in Hayward reservoir.**

This impact hypothesis could not be directly addressed with the littoral monitoring program results alone. This question however, was addressed for freshwater lakes in general by Vadeboncoeur et al. (2002). Worldwide, they were able to show that on average, littoral and pelagic primary production tended to contribute equally in whole lake productivity. When oligotrophic lakes were considered in isolation however, littoral primary production tended to dominate whole lake primary production, largely because of benthic algae's greater efficiency in phosphorus uptake. This greater efficiency is thought to be at least in part related to a close association or coupling between heterotrophic and photo-autotrophic organisms (Liborius and Jeppesen 2003, Scott and Doyle 2006). As total lake phosphorus levels increase, pelagic productivity increases, gradually screening the ability for sunlight to reach deeper littoral areas. This is thought to give pelagic primary producers an advantage in phosphorus uptake over littoral producers, allowing pelagic primary producers to increasingly dominate overall lake primary production as trophic status increases. Though impact hypothesis H<sub>07</sub> could not be directly addressed by the monitoring data collected in Stave Lake Reservoir, the ultra-oligotrophic status of the reservoir would suggest that littoral primary production is likely a major contributor to whole lake primary production. Whether this also applies to Hayward reservoir with its much higher lower water retention rate is unknown. H<sub>07</sub> remains unresolved.

**H<sub>08</sub>: Stable reservoir levels do not lead to maximum littoral development as measured by <sup>14</sup>C inoculation and/or inferred from ash free dry weight data.**

When defining reservoir stability as the range of reservoir elevation experienced during the Mar 1 to Oct 31 growing season, the periphyton growth modelling results suggest that yes, greater stability results in higher periphyton growth potential. This is most easily seen in Figure 29, which plots the range of reservoir elevations against periphyton growth potential for all years of simulation (both pre- and WUP (i.e., current)). As the range narrows, growth potential increases. Furthermore, there appears to be a critical range of reservoir elevations above which little growth occurs. This threshold range was estimated to be between 7.5 and 8 m. Linear extrapolation of the periphyton growth potential data for range values below 8 m suggests a maximum growth potential of 96,590 tonnes. H<sub>08</sub> can be rejected.

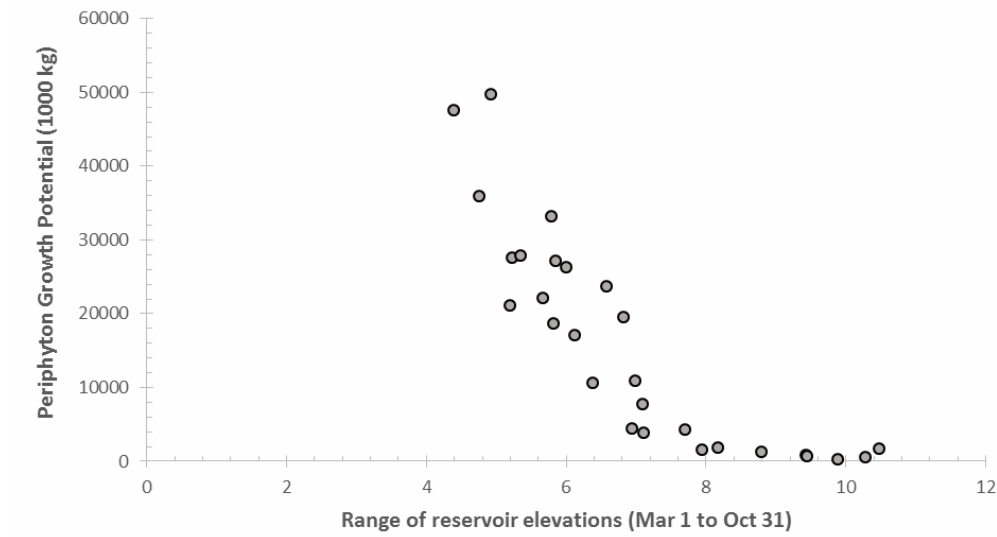


**Figure 29. Periphyton growth potential in Stave Lake Reservoir (derived by empirical ELZ modelling) as a function of reservoir elevation range for the period between Mar 1 and Oct 31 for all years of periphyton growth simulation (both pre- and current WUP).**

**H<sub>0</sub>9: Water level fluctuations that raise the euphotic zone (defined here as the depth at which photosynthetically active radiation (PAR) is 1% that of the water surface) from lower elevations does not lead to a collapse of littoral primary production (as measured by <sup>14</sup>C inoculation and/or inferred from ash free dry weight data) that occurred near the prior 1% PAR depth.**

This hypothesis was directly addressed in the study by Bruce and Beer (2014). By tracking the changes in growth rate when an established periphyton community was shaded by canopies of various light transmissivity values, they were able to show that none of the communities fully perished regardless of shading intensity and that in fact, some growth continued in complete darkness. Low light growth was also observed in the periphyton growth data, even at light intensities as low 10  $\mu\text{moles}/\text{m}^2/\text{s}$ . Various mechanisms were proposed for this response, including 1) changes in periphyton community structure to species that are less light sensitive; 2) low light acclimation by individual species; and 3) the possibility that some periphyton organisms are mixotrophs (i.e., have the capability of limited heterotrophy in the absence of light). Unfortunately, no species data were collected during the experiment to elaborate on the extent to which each of the mechanisms of community photo adaptation were involved. The data however, did clearly show that community viability does not collapse in the absence of light. H<sub>0</sub>9 cannot be rejected.

**H<sub>0</sub>10: Littoral zone productivity, as measured by <sup>14</sup>C inoculation and/or inferred from ash free dry weight data, remains unchanged as reservoir water level stability increases.**

This impact hypothesis is similar to H<sub>0</sub>8. The data in Figure 29 clearly shows a strong negative relationship between reservoir stability over the course of the periphyton growth period (Mar 1 to Oct

31), particularly when the range of reservoir elevations decreases below 7.5-8 m. Above this threshold, very little littoral periphyton growth can be expected.  $H_0$  can be rejected.

**$H_{011}$ : Changes in littoral productivity (as measured by  $^{14}\text{C}$  inoculation and/or inferred from ash free dry weight data) can be expressed primarily in terms of changes in areal extent as defined by upper and lower boundary elevations. Within these boundaries, primary production does not vary in proportion to accumulated PAR exposure under wetted conditions.**

Periphyton growth was found to vary significantly as a function of light (PAR) intensity, following the functional form of a hyperbolic saturation equation (Figure 24). Because solar irradiance intensity and light extinction coefficient (i.e., the rate at which light intensity decrease as a function of depth) can vary on a daily and seasonal basis, the boundaries that could describe the limits of periphyton growth would be continuously changing. This is further complicated by the fact that growth can continue in low light environments. Thus, the use of boundaries to describe the extent of littoral periphyton production is likely an over simplification of littoral ecology. This was clearly demonstrated by the negative correlation between the ELZ metric (that explicitly tracks littoral zone boundaries over time) and the modelled potential for periphyton growth. This hypothesis can be rejected.

## Management Questions

The consultative committee identified four key management questions to be addressed in the monitoring of littoral productivity in the Stave Lake and Hayward reservoirs (BC Hydro, 2005). These are addressed individually below:

**a) What is the current level of littoral productivity in each reservoir, and how does it vary seasonally and annually as a result of climatic, physical and biological processes, including the effect of reservoir fluctuation?**

Low nutrient levels, in particular phosphorus, certainly limit the productivity of littoral habitats in both reservoirs compared to other lake or reservoir systems in BC (Beer 2004). However, inter-annual differences in mean nutrient concentration did not appear to have a significant impact on littoral growth rates. While nutrient concentrations declined over the course of the 10-year monitoring period, total depth-integrated littoral production did not follow that trend. WUP ELZ modelling was able to show that inter annual differences in reservoir elevations had a much greater impact, overriding any effect that changing nutrient concentrations may have had. Though there are seasonal cycles in nutrient concentration, these appeared to be more a result of changes in the standing crop of littoral and pelagic organisms than a driver of growth. Rather, seasonal changes in littoral development appears to be influenced more by the availability of light and prevailing water temperature than any other factor. These influences however, were not linear, especially the effect of light availability. In the latter case, the growth rate of primary producers followed a saturation equation where it initially increases steadily with light intensity, but the rate of change slows, reaching a saturation level where growth rates no longer change with further increases in light intensity. At very low light intensities, chemo-autotrophy or heterotrophy appear to become increasingly important. This could be expressed in terms of shift in species dominance, or a switch in physiology among facultative phototrophs (Bruce and Beer 2015a). Regardless of the mechanism, littoral growth does not stop with the absence of light during the growth season (Bruce and Beer 2014). This relationship with light intensity is a dramatic departure from the assumption of uniform growth potential in the original ELZ model used during the WUP for trade off analysis.

- b) If changes in littoral productivity are detected through time, can they be attributed to changes in reservoir operations as stipulated in the WUP, or are they the result of change to some other environmental factor?**

Littoral zone modeling was able to clearly demonstrate the effects of reservoir operations on littoral development and that it was the single most influential variable driving inter-annual differences in total productivity. The availability of light and prevailing water temperatures also had an effect, though mostly in driving within year (i.e., seasonal) changes. The effect of these two variables on between year variance in total littoral development could not be untangled from the strong seasonality of WUP reservoir operations.

- c) A performance measure was created during the WUP process so as to predict potential changes in littoral productivity based on a simple conceptual model. The Effective Littoral Zone (ELZ) performance measure was used extensively in the WUP decision making process, but its validity was unknown at the time. Is the ELZ performance measure accurate and precise, and if not, what other environmental factors should be included (if any) to improve its reliability?**

The conceptual ELZ metric used during the WUP was found to be inaccurate. This stemmed from an implicit assumption of uniform growth when applying an additive binary value indicating whether growth could occur depending on whether there is available light and the area in question was under water. The effect of varying light intensity on growth as a function of water depth was not taken into account, nor was there full appreciation of the fact that growth occurs exponentially. Also, the conceptual ELZ model ignored the sequential timing of reservoir events, and did not place enough importance to early growing conditions in determining overall littoral growth potential at the end of the growing season. The conceptual ELZ model was an over simplification of littoral growth process. An alternative empirically derived ELZ model was developed in this study that explicitly takes into account or corrects for these three, early ELZ model deficiencies. This model can be used in future WUP process in the Stave Lake Reservoir, and can be modified for export to other reservoir systems

- d) Does the Combo 6 operating alternative improve reservoir littoral productivity as was expected in the WUP? Is there anything that can be done to improve the response, whether it be operations-based or not?**

The conceptual ELZ model in the WUP indicated modest benefits to littoral productivity with the implementation of the 'Combo 6' strategy. The empirical ELZ model however, was able to show that this conclusion was an error, and that average annual littoral productivity likely declined with the 'Combo 6' strategy. The updated modelling exercise was able to show that, while littoral development was higher during the summer months in most years (compared to pre-WUP operational strategy), the need to draft the reservoir in early September to accommodate increased winter inflows resulted in significant losses to this production. This was because most of the summer time gains in littoral production occurred at the highest reservoir elevations, thus creating largescale dewatering of this production when the draw down occurs in September each year. With the pre-WUP operating strategy, there were many years when reservoir elevation did not reach the targeted summer time levels of 'Combo 6', thus the magnitude of the September reservoir draft was not as great, which left a greater proportion of the year's production under water. Also, a factor was that there was more shoreline area with a 15% slope at lower reservoir elevations than at the higher elevations.

There are changes to the 'Combo 6' operating strategy that could potentially help increase littoral production. The first would be to delay the September drawdown for several weeks, allowing the littoral zone to continue functioning until the end of the growing season in mid to late October. The second recommendation would be to consider lowering the summer time targeted reservoir elevation, thus reducing the magnitude of reservoir drawdown in the fall and in the case of Stave Reservoir, maximizing the extent of area with 15% gradient. Both of the changes however, would have significant impacts to other values in the reservoir.

**e) To what extent would reservoir operations have to change to i) illicit a littoral productivity response, and ii) improve current littoral and overall productivity levels?**

The empirically ELZ model suggests that changes in littoral development linked to Stave Lake Reservoir operations are incremental, provided that the range of reservoir elevations between Mar 1 and Oct 30 is < 8 m. A plot of empirical ELZ model estimates and the range of reservoir elevations showed that productivity increase linearly as the range of elevations narrowed from 8 to 4 m (Figure 29). With ranges above 8 m, all littoral productivity is lost.

Because the relationship between littoral and pelagic productivity in Stave Lake Reservoir could not be directly addressed in this study, the effect of improved littoral development total reservoir productivity remains uncertain. However, studies in other systems suggest that in ultra-oligotrophic systems, littoral productivity can play a significant role in total reservoir production. Thus, it appears likely that increases in littoral production can lead to increases in total reservoir production. The extent to which total productivity could increase is unknown.

## Conclusions

The littoral productivity assessment monitor was successful in collecting the data necessary to validate of the conceptual ELZ model used during the WUP process, and in turn help assess the littoral consequences of Combo 6 operating strategy implementation. Results of the monitor however, found that the conceptual ELZ model output was a poor indicator of littoral development and in fact incorrectly predicted littoral productivity gains. The conceptual ELZ model appeared to have over simplified the growth of littoral periphyton by making explicit assumptions of uniform growth as a function of depth and a simple additive growth model over time. It also ignored the sequence of reservoir operations. All three factors proved to be too important to littoral development to ignore in order to simplify metric calculations. That said, there was no data available at the time of model development to have done otherwise.

An alternative empirically derived ELZ model was developed that took these factors into account, which in turn provided reasonably robust predictions of periphyton standing crop (and hence productivity). Separate models were developed for three sites at in Stave Lake Reservoir, and a fourth model was developed for a site on Hayward Reservoir. There was general agreement among all three Stave Lake Reservoir models, but not so with the Hayward model. This appears to reflect the differences in hydrology between systems, even though they are both part of the Stave River watershed. As a result, Hayward Reservoir served as a poor example of a "natural" lake system for comparison with Stave Lake Reservoir.

Analysis of the data, evaluation of the conceptual ELZ model, and the analytical processes leading the development of an empirically-derived ELZ model have allowed all impact hypotheses to be addressed. The outcomes are summarised in Table 16.

Overall, the ELZ model building exercise was able to show that implementation of the 'Combo 6' operative strategy likely had a negative impact on littoral development compared to pre-WUP operations. This is opposite of what was expected based on the results of conceptually based ELZ modelling during the WUP. The empirically based ELZ modelling was able to show that, while littoral development was high during the summer months in most years, the need to draft the reservoir in early September to accommodate increased winter inflows resulted in significant losses to this production. This was because most of the summer time gains in littoral production occurred at the highest reservoir elevations, thus ensuring largescale dewatering of this production when the draw down occurred each year. Also, a factor was that there was more shoreline area with a 15% slope at lower reservoir elevations than at the higher elevations. With the pre-WUP operating strategy, there were many years when reservoir elevation did not reach the targeted summer time levels of 'Combo 6', thus the magnitude of the September reservoir draft was not as great, which left a greater proportion of the year's production under water. Also, there was larger areal extent of 15% gradient shoreline habitat.

Given this outcome, some changes to the 'Combo 6' operating strategy are proposed that could help increase littoral production. The first would be to delay the September drawdown for several weeks, allowing the littoral zone to continue functioning until the end of the growing season in mid to late October. The longer the delay, more of the summer production remains accessible to littoral organisms. The benefit of this to fish production however is unknown and cannot be determined with the present data. The other operating strategy would be to consider lowering the summer time targeted reservoir elevation, thus reducing the magnitude of reservoir drawdown in the fall. This would also marginally increase the shoreline area with slopes < 15%. Both of the changes however, would have significant impacts to other values in the reservoir. There is no optimal solution to maximizing littoral production in Stave Falls Reservoir except to reduce reservoir fluctuations completely. No particular reservoir threshold or fall drawdown date can be recommended without assessing trade-offs to other values in a full water use planning exercise.

The empirical ELZ model can be used in future trade-off analyses to assess the littoral zone consequences of operating alternative, but requires an operations model to predict likely Stave Lake Reservoir elevation. A much simpler approach may be to consider the range of reservoir elevations from Mar 1 to Oct 31 each year as a littoral zone performance measure. It was found to be linearly related to the empirical ELZ model predations (Figure 29). However, it would still require an operations model to predict likely Stave Lake Reservoir elevation for each operating alternative.

Table 16. Summary of impact hypothesis outcomes arising from analysis of the 2000-2009 littoral productivity monitoring study.

Impact Hypothesis	Description	Status	Rationale
H <sub>01</sub>	Average reservoir concentration of Total Phosphorus (TP), an indicator of general availability of phosphorus is not limiting to littoral primary productivity.	Rejected	TP < 3 µg/L; Ultra-oligotrophic
H <sub>02</sub>	Relative to the availability of phosphorus as indicated by level of total dissolved phosphorus (PO <sub>4</sub> ), the average reservoir concentration of nitrate (NO <sub>3</sub> ) is not limiting to littoral primary productivity.	Not Rejected	NO <sub>3</sub> < 200 µg/L; Ultra-oligotrophic, but not as limiting as TP
H <sub>03</sub>	Water retention time (τ <sub>w</sub> ) is not altered by reservoir operations that vary from year to year such that it significantly affects the level of TP as described by Vollenweider's (1975) phosphorus loading equations (referred to here as TP(τ <sub>w</sub> ))	Not Rejected	TP independent of reservoir operations in Stave Lake Reservoir, inconclusive in Hayward Reservoir (confirmed by Bruce and Beer 2016)
H <sub>04</sub>	Water temperature, and hence the thermal profile of the reservoir, is not significantly altered by reservoir operations that vary from year to year.	Inconclusive	Majority of variance in water temperature accounted for by solar input, but thermal profile breaks down from September drawdown.
H <sub>05</sub>	Changes in TP as a result of reservoir operations (through changes in τ <sub>w</sub> ) are not sufficient to create a detectable change in littoral algae biomass as measured by littoral levels of chlorophyll a (Chl a) and/or ash free dry weight (AFDW).	Not Rejected	No statistically significant relationships were detected in the data
H <sub>06</sub>	Overall primary production (as measured by <sup>14</sup> C inoculation and/or as inferred from ash free dry weight data) of Stave Lake Reservoir is not different than that of Hayward Lake	Rejected	Significant differences were found in the coefficients that describe periphyton growth
H <sub>07</sub>	Pelagic primary production dominates in Stave Lake Reservoir while littoral production dominates in Hayward Reservoir.	Inconclusive	Could not be addressed with available data, though literature suggests that littoral production does play a significant role, especially in oligotrophic systems
H <sub>08</sub>	Stable reservoir levels do not lead to maximum littoral development as measured by <sup>14</sup> C inoculation and/or inferred from ash free dry weight data.	Rejected	Clear relationship was found between reservoir stability and maximum periphyton biomass
H <sub>09</sub>	Water level fluctuations that raise the euphotic zone (defined here as the depth at which photosynthetically active radiation (PAR) is 1% that of the water surface) from lower elevations does not lead to a collapse of littoral primary production (as measured by <sup>14</sup> C inoculation and/or inferred from ash free dry weight data) that occurred near the prior 1% PAR depth.	Not Rejected	Light acclimation and potential mixotrophy appears to delay mortality due to low light conditions (Bruce and Beer 2014)
H <sub>010</sub>	Littoral zone productivity, as measured by <sup>14</sup> C inoculation and/or inferred from ash free dry weight data, remains unchanged as reservoir water level stability increases.	Rejected	Revised ELZ model shows that littoral production is strongly impacted by reservoir fluctuations
H <sub>011</sub>	Changes in littoral productivity (as measured by <sup>14</sup> C inoculation and/or inferred from ash free dry weight data) can be expressed primarily in terms of changes in areal extent as defined by upper and lower boundary elevations. Within these boundaries, primary production does not vary in proportion to accumulated PAR exposure under wetted conditions.	Rejected	The revised ELZ model shows that littoral production is strongly impacted by available light and appears to follow a saturation function.

## References

- Ask, J., J. Karlsson, L. Persson, P. Ask, P. Byström, M. Jansson. 2009. Whole-lake estimates of carbon flux through algae and bacteria in benthic and pelagic habitats of clear-water lakes. *Ecology* 90(7): 1923-1932.
- Axler, R.P. and J.E Reuter. 1996. Nitrate uptake by phytoplankton and periphyton: Whole-lake enrichments and mesocosm - <sup>15</sup>N experiments in an oligotrophic lake. *Limnol. Oceanogr.*, 41(4): 659-671.
- Banse, K. 2004. Should We Continue to Use the 1% Light Depth convention for Estimating the Compensation Depth of Phytoplankton for Another 70 Years? *Limnology and Oceanography Bulletin* 13(3), 49-52 p.
- BC Hydro. 2004. Stave River Water Use Plan: Monitoring Terms of Reference. Littoral Productivity Assessment. Section 2, 18p.
- BC Hydro 2005. Stave River Water Use Plan: Monitoring Terms of Reference. BC Hydro Water Use Planning. March 2005. 86p.
- Beer, J.A. 2004. Littoral Zone Primary Production in a Coastal Reservoir Ecosystem. Master's thesis, University of British Columbia.
- Bruce, J.A., J. Beer and M. McArthur. 2011 (Draft) Effect of increasing dewater exposure periods on the growth of periphyton on artificial substrate. Report Prepared by BC Hydro Environmental Resources in partnership with Ness Environmental Sciences. 12 p + App.
- Bruce, J.A. and J. Beer. 2014. Effect of Increasing Darkness on Periphyton Growth in Stave Lake Reservoir: An Experiment Simulating the Effect of Rising Water Levels on Deep Water Epipelagic Periphyton Growth in a Reservoir Setting. Report Prepared for BC Hydro, Burnaby BC. Creekside Aquatic Sciences Report No. CAQ - 008: 31p + app
- Bruce, J.B. and J. Beer. 2015a. Depth Distribution of Stave Lake and Hayward Reservoir Periphyton Taxa: An analysis of periphyton abundance data collect in Year 2002. Technical Note CAQ-011 prepared for BC Hydro, Water License Requirements by Creekside Aquatics Sciences and Ness Environmental Sciences, July 2015. 11p
- Bruce, J.B. and J Beer. 2015b. Spatial Variance of Phosphorus in Stave Lake Reservoir: Test of the Uniformity Assumption. Technical Note CAQ-011 prepared for BC Hydro, Water License Requirements by Creekside Aquatics Sciences and Ness Environmental Sciences, January 2015. 12p.
- Bruce, J.A. and J. Beer. 2016 (DRAFT). Pelagic Productivity of Stave Lake Reservoir since Water Use Plan Implementation (1999 – 2014): A Meta-Analysis of Monitoring Data and Assessment of WUP Environmental Management Questions (SFLMON #1). Report Prepared for BC Hydro, Burnaby, BC, by Creekside Aquatic Sciences and Ness Environmental Sciences. Report No. CAQ-016: 78 p + App.



- Conveny, M.F. and R.G. Wetzel. 1995. Biomass, production, and specific growth rate of bacterioplankton and coupling to phytoplankton in an oligotrophic lake. *Limnol. Oceanogr.*, 40(7) 1187-1200.
- del Giorgio, P.A. 1993. Heterotrophy in Lake Plankton. PhD Thesis. McGill University. December 1993. 195p.
- DeNicola, D. M., E. de Eyto, A. Wemaere, and K. Irvine. 2003. Production and respiration of epilithic algal communities in Irish lakes of different trophic status. *Archiv für Hydrobiologie*, 157(1) 67-87.
- Dodds, W. K. 2003. The role of periphyton in phosphorus retention in shallow freshwater aquatic systems. *Journal of Phycology*. 39:840-849.
- Failing, L. 1999. Stave River Water Use Plan: Report of the Consultative Committee. Prepared by Compass Resource Management Ltd for BC Hydro. October 1999. 44 p + App.
- Games, P. A., and Howell, J. F. 1976. Pairwise multiple comparison procedures with unequal N's and/or variances: A Monte Carlo study. *Journal of Educational Statistics*, 1, 113-125.
- Hallock, P. 1981. Algal symbiosis: A mathematical analysis. *Marine Biology*. 62(4) 249-255.
- Harris, S.L., H. Andrusak, G. Andrusak, D. Sebastian, G. Scholten, T. Weir, L. Vidmanic, E.J. Johnson and N.E. Down. 2010. The Alouette Reservoir Nutrient Restoration Program, 2003-2008. Prepared by Province of British Columbia Ministry of Environment Aquatic Ecosystem Protection Branch. Fisheries Project Report No. RD129. 92 p. + App.
- Hondzo, M. and H. Stefan. 1993. Lake Water Temperature Simulation Model. *J. Hydraul. Eng.*, 119(11), 1251-1273.
- Katechakis, A., T. Haseneder, P. Kling, and H. Stibor. 2005. Mixotrophic versus photoautotrophic specialist algae as food for zooplankton: The light:nutrient hypothesis might not hold for mixotrophs. *Limnol. Oceanogr.*, 50(4) 1290-1299
- Liboriussen, L. and E. Jeppensen. 2003. Temporal dynamics in epipellic, pelagic, and epiphytic algal production in a clear and turbid shallow lake. *J. Freshwater Biology*. 48(3):418-431
- Poulickova, A., P. Hasler, M. Lysakova and B. Spears. 2008. The ecology of freshwater epipellic algae: an update. *Phycologia* Vol 47(5), 437-45.
- Schindler D.W. 1978. Factors regulating phytoplankton production and standing crop in the world's freshwaters. *Limnology and Oceanography*, 23, 478-486.
- Scott, J.T. and R.D. Doyle. 2006. Coupled photosynthesis and heterotrophic bacterial biomass production in a nutrient-limited wetland periphyton mat. *Aquat Microb Ecol.* 45:69 - 77
- Shortreed, K.S., A.C. Costella, and J.G. Stockner. 1984. Periphyton biomass and species composition in 21 British Columbia lakes: seasonal abundance and response to whole lake nutrient additions. *Can. J. Bot.* 62: 1022 1031.
- Stables, T. B., and C. J. Perrin. 2015. Abundance and biomass of fish in Stave Reservoir 2005-2014. Report prepared by Limnotek Research and Development Inc. and Shuksan Fisheries Consulting for BC Hydro. 105p.
- Stockner, J.G. and F.A.J. Armstrong 1971. Periphyton of the experimental lakes Area, Northwestern Ontario. *J. Fish. Res. Bd. Canada* 28: 215-29.

- Stockner, J.G., and K.S. Shortreed. 1985. Whole-lake fertilization experiments in coastal British Columbia: empirical relationships between nutrient inputs and phytoplankton biomass and production. *C. J. Fish. Aquat. Sci.* 42: 649-58.
- Stockner, J. G. and J. Beer. 2004. The limnology of Stave/Hayward reservoirs: with a perspective on carbon production. Prepared for BC Hydro Water Use Plans by Eco-logic Ltd. and University of British Columbia, Institute For Resources, Environment and Sustainability, Vancouver. 33 pp. + App.
- Tabachnick, B.G. and L.S. Fidell. 1983. *Using Multivariate Statistics*. Harper and Row. University of Michigan. 509 p.
- Van Baalen, C., D.E. Hoare and E. Brandt. 1971. Heterotrophic Growth of Blue-Green Algae in Dim Light. *J. of Bacteriology* 105(3) 685-689.
- Vadeboncoeur, Y., M.J. Vander Zanden, and D.M. Lodge. 2002. Putting the lake back together: Reintegrating benthic pathways into lake food web models. *BioScience* 52(1): 44 – 54.
- Vollenweider, R, A. 1975. Input-output models, with special reference to the phosphorus loading concept in limnology. *Schweiz. Z. Hydrol.* 37:53-84. (Cited in Wetzel 2001)
- Wetzel, R. G. and G. E. Likens. 1991. *Limnological Analyses*. 3rd Edition. Springer-Verlag, New York. 391 pp.
- Wetzel, R.G. 2001. *Limnology. Lake and River Ecosystems, Third Edition*. Academic Press. San Diego. 1006 pp.

# Appendix A

## Relationship between Ash Free Dry Weight and Chlorophyll a

### Introduction

Ash Free Dry weight (AFDW) was chosen as the preferred metric to capture periphyton largely because of its simplicity to measure in the laboratory (and hence fewer steps to make errors) and a low relative cost. There was however, some uncertainty whether all of the organic matter scraped off of the artificial growth substrate would reflect actual growth, or would simply reflect an accumulation of non-living organic material settling from the water column or slumping from near shore areas. There was also uncertainty about the measure's precision as studies have found that AFDW to be a more variable metric of biomass and production than other indicators (Morin and Cattaneo, 1992). In fact, in an experimental setting, the work of Morin and Cattaneo (1992) found that measures of Chlorophyll a (*Chl a*) tended to be a more precise metric for analysis. To address these uncertainties, measurements of *Chl a* were carried out in conjunction with all AFDW measurements for the first three years of the monitoring program (2000 to 2003) so that they may be compared for relative correspondence. Of particular concern was whether growth substrate located deep in the water column was more influenced by settling organic matter than surface substrates.

### Methods

The methods describing the AFDW ( $\text{mg}\cdot\text{m}^{-2}$ ) sampling procedure was described earlier in the main text of the report. The methods described below pertain mainly to the extraction of Chlorophyll from periphyton samples collected at the same time as the AFDW samples.

### Laboratory Methods

Periphyton samples scraped from each artificial growth plate was filtered in the field through a 47 mm diameter, 0.45µm Millipore HA filter and rinsed twice with double distilled water (DDW). Where periphyton growth was found to be exceptionally heavy, i.e., there was a predominance of filamentous green or blue-green algae, then a Whatman GF/F filter was used instead of the Millipore filter. The algae-laden filters were then soaked in a 90% acetone solution for a minimum of 12 hours to extract the chlorophyll as described in Wetzel and Likens (2000). The resulting solution was then centrifuged to separate particulate matter from the dissolved Chlorophyll. A subsample of the supernatant was then placed in cuvettes for analysis using a spectrophotometer or Turner<sup>®</sup> fluorimeter to determine Chlorophyll concentration ( $\mu\text{g}\cdot\text{l}^{-1}$ ).

### Data Analysis

The *Chl a* concentration data were converted to an aerial measure by multiplying the concentration by the volume ( $\mu\text{g}\cdot\text{L}^{-1}$ ) of supernatant (L) and then dividing by the sampling area ( $\text{cm}^2$ ) on the artificial growth plate. The result was then scaled to a measure of  $\text{mg}\cdot\text{m}^2$  so that it can be directly compared with corresponding measures of AFDW. All comparisons between AFDW and *Chl a* data sets were carried out using regression analysis. To ensure a normal distribution of residuals, both metrics were

$\log_{10}$  transformed. All instances where AFDW or Chl a were below detectable limits (1 mg) were removed from the data set used for analysis.

## Results

Over the three year sampling period, a total of 848 paired AFDW-Chl a observations were made, of which 33 had AFDW values that were less than the 1mg detectable limit (hence recorded as “0” values) and another 9 observations where *Chl a* was below the detectable limit. A plot of the non-zero paired data in Figure A1 found the two metrics of biomass to be highly correlated when logarithmically transform. Best fit regression was  $Chl\ a = 0.0418 \times AFDW^{0.9467}$ , which was able to explain just over 57% of the variability in Chl a measurements ( $P < 0.0001$ ). The slope of the regression was not significantly different from 1 (95% CL = 0.890 – 1.003) suggesting that there is a direct correspondence in values, differing only by a constant proportion. The range of Chl a however, was almost an order of magnitude greater than that of the AFDW. The coefficient of variation (CV) of the log-transformed Chl a values was 1.65, while that of the AFDW data was only 0.62. This difference was also apparent in the distribution of paired observations in Figure A1, where the AFDW data spanned a range of 3 orders of magnitude, while that of the Chl a data spanned closer to 4 orders.

A comparison of log transformed paired data between the top 2 growth plates and the bottom three is show in Figure A2. Clear in the plot was the high degree of overlap between the two data sets, though the range of paired data is lower among the lower plates. The latter was as expected because of their placement at depth and corresponding attenuated light levels. Regression analysis found the slopes

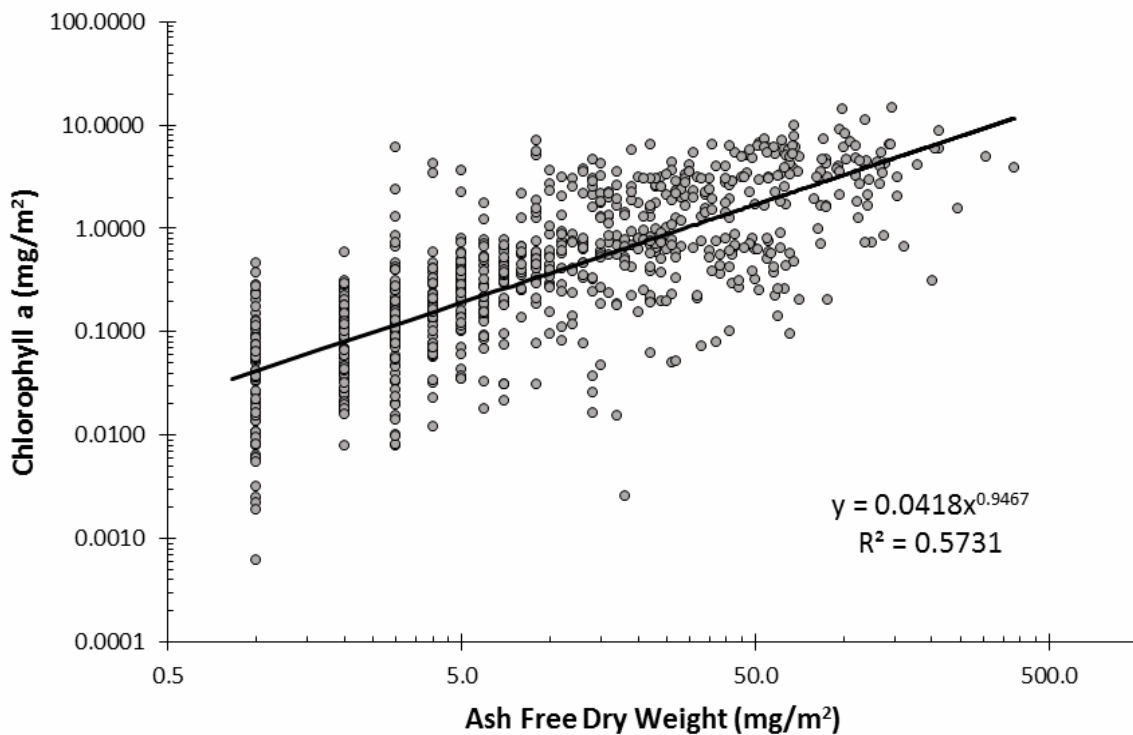


Figure A30 Chlorophyll a data plotted against Ash Free Dry Weight data that were collected simultaneously at three sites in Stave Lake Reservoir and a single site at Hayward Reservoir over a period of three years starting March 2000.

to be very similar (1.014 vs 1.028). Neither were significantly different from 1 (95% CL = 0.885 – 1.143 and 0.892 – 1.164 respectively), and ANCOVA revealed that that they were not significantly different from one another.

## Discussion

Measures of Chl a data were found to be highly correlated with AFDW suggesting that at least some of the organic material collected from the growth plates comprised of live photosynthetic organisms and represented growth. The Chl a data however, were more variable by almost an order of magnitude. The reason for this is uncertain and was not expected given the work of (Morin and Cattaneo 1992). However, Chl a content per cell can vary considerably between periphyton species and can vary over time and space in response to light conditions (Reynolds, 1984, Wetzel 2001). This was likely a factor in the present study where samples were collected specifically to capture seasonal, areal and water depth trends. Species composition at a sub sample of the sites done in 2000 and 2001 showed that there was considerable variability between sites, year and sampling depth (Beer and Dolecki, 2003). The fact that the samples were not processed immediately could also have been a factor as the remote location of sampling prevented immediate processing. Chl a degrades over time. Though samples were filtered and processed with acetone in the field, spectrophotometry measurements were generally not done until the following day or later. This delay in measurement likely introduced error in the measurements by allowing a window for pigment degradation to occur. This could have exacerbated measurement error if the delays were not always consistent between measurement periods. Finally, meta-analysis carried out by Morin and Cattaneo (1992) found that variance of Chl a measurements tended to increase proportionality

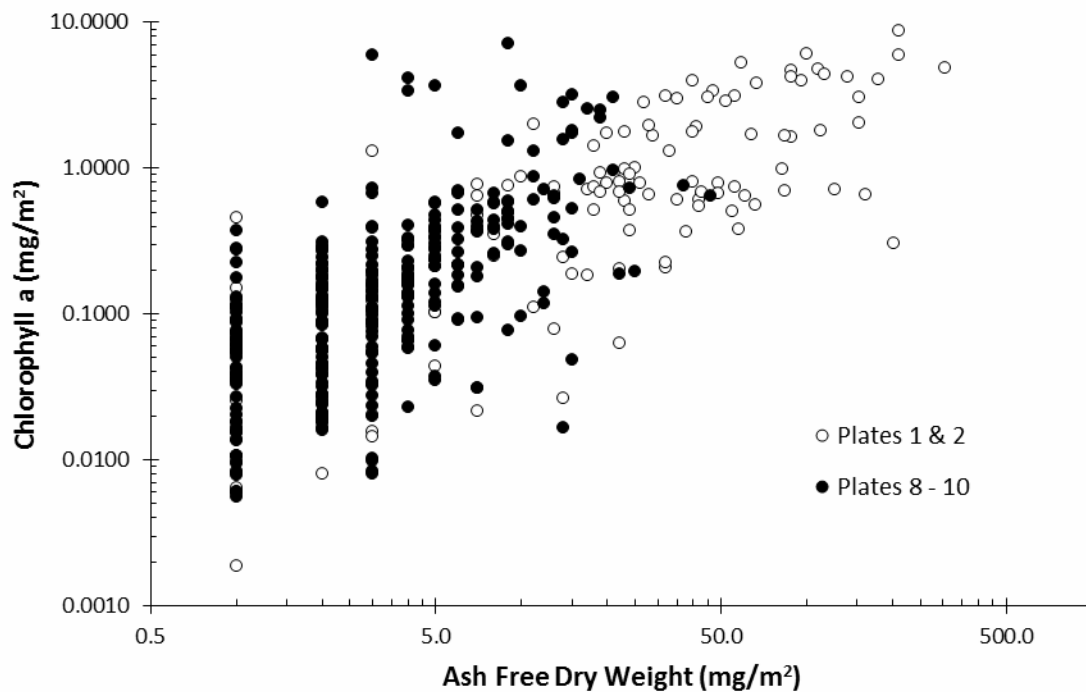


Figure A31. Comparison of paired Ash Free Dry Weight and Chl a data between upper (1,2) and lower (8-10) sampling plates at all sites in Stave Lake and Hayward reservoirs; 2000-2003.

with the size (mean biomass) of the sample. Given the broad range of Chl a measurements observed in the monitor, this alone could have contributed to the overall variance in the Chl a data.

A comparison in the AFDW – Chl a relationship between upper and lower plates found no significant differences in regression slope, suggesting that the ratio of live Chl a bearing organisms to AFDW did not change as a function of depth. This in turn suggested that the settling of particulate organic matter on to each of growth plates occurred at similar rates independent of depth. This outcome was not entirely unexpected. The settling velocity of dead phytoplankton has been found to typically range between 0.5 and 2 m per day in lake environments with little turbulence; depending on the size and shape of the organism. Given this settling rate, it would take between 10 to 20 days for dead phytoplankton and other particulate matter near the surface of the water column to reach the deepest sampling plates in this study. This was more than sufficient time for significant decomposition to occur, especially in warm aerobic waters during the summer growing season (Wetzel 2001). Given that both Stave Lake and Hayward reservoirs are considered ultra-oligotrophic system with low planktonic growth, the slow rate of settling, the potential for decomposition, and the short time interval between sampling periods, it would seem unlikely that there would be significant accumulation of particulate organic matter on the sampling plates. The comparison of AFDW – Chl a slopes appeared to confirm this hypothesis.

The key outcome of this analysis was to show that increases in AFDW was at least in part an indicator of periphyton growth and did not appear to be confounded by the settling of particulate organic matter. As a result, AFDW was considered to be a good indicator of periphyton growth in this monitor.

# Appendix B

## Relationship between Ash Free Dry Weight and Primary Productivity measured by the $^{14}\text{C}$ Method

### Introduction

Starting in 2006 and ending later in 2009, a additional periphyton samples were collected in a conjunction with the AFDW samples so that corresponding direct measurement of primary productivity ( $\text{mg}\cdot\text{m}^{-2}\cdot\text{day}^{-1}$  of carbon) could be made using  $^{14}\text{C}$ . The objective was to build a regression equation that relates AFDW to a direct measure of production, and hence calibrate the AFDW measures into an accurate measure of production. The paired sampling procedure was carried out at random sites and water depths throughout the 2006-2009 sampling period with the objective of collecting data from a broad range of sampling conditions so that the regression would be applicable throughout the course of the entire monitoring period. The calibration was considered important as it would allow more robust comparisons with results and data reported in the literature at other lakes and reservoirs across North America and Northern Europe.

### Methods

The methods describing the AFDW ( $\text{mg}\cdot\text{m}^{-2}$ ) sampling procedure was described earlier in the main text of the report. The methods described below pertain mainly to the measurement of  $^{14}\text{C}$  assimilation in periphyton samples processed simultaneously with the AFDW samples. It should be noted that  $^{14}\text{C}$  measurements of production were done only at two sites (one at Hayward and the other at one of the three Stave Lake sites) and randomly chosen water depths (i.e., growth plate) per sampling period. As a result, a total of 48 paired samples were collected for analysis over the 2006 to 2009 sampling years.

### Field methods

Each of the growth plates used in the monitor were specifically etched to mark out six easily identifiable  $40\text{ cm}^2$  sampling areas. When a plate was chosen for  $^{14}\text{C}$  sampling, two of these  $40\text{ cm}^2$  areas were randomly selected and the periphyton scraped clean into separate clear BOD (Biological Oxygen Demand) bottles. Two scrapings were taken so that there would be a replicate sample to confirm repeatability of scintillation count in the laboratory. Another  $40\text{ cm}^2$  area was scraped into a single dark BOD bottle. Each of the three 300 ml BOD bottle was then topped up with deionized water and prepared for incubation with an inoculation 1 ml of  $\text{NaH}^{14}\text{CO}_3$ , the equivalent of  $5\ \mu\text{Ci }^{14}\text{C}$ .

The BOD bottles containing the periphyton sample were then attached to acrylic plates designed to hold the bottles in a horizontal plane at right angles to each other and then re-suspended to their original sampling plate depths. Samples were incubated in-situ for 2-4 hours, generally between 11 AM and 3 PM on the sampling day. Light penetration in the two clear bottles allowed photosynthesis to occur and thus lead to the photosynthetic uptake of  $^{14}\text{C}$ , while the dark bottle excluded light and measured dark uptake of  $^{14}\text{C}$  through respiration. After incubation, samples were retrieved and placed into a light-tight box for transport back to the laboratory. This effectively terminated the incubation period.

## Laboratory Methods

Laboratory processing of the  $^{14}\text{C}$  inoculated samples occurred later the same day following incubation. The samples were filtered through a 0.2  $\mu\text{m}$ , 47mm polycarbonate filter using < 10 cm-Hg vacuum differential as recommended by Joint and Pomroy (1983) to avoid cell damage in the filtrate. This was done in a semi dark environment to avoid further photosynthesis. Each filter was then placed into separate 7 ml scintillation vials and 200  $\mu\text{L}$  of 0.5N HCl was added to eliminate unincorporated inorganic  $\text{NaH}^{14}\text{CO}_3$ . The vials were then left uncapped in a darkened fume-hood to dry for approximately 48 hours. When dry, 5 ml of Ecolite scintillation flour was added to each filter and stored dark for another 24 hours before being radio-assayed by Vison SciTech Labs (Vancouver, BC) in a Beckman LS1801 scintillation counter; operated in an external standard mode to correct for quenching (Pieters et al. 2000).

Littoral primary productivity was estimated by calculating the difference in scintillation counts (disintegrations per minute or DPM) between filter samples with periphyton incubated in the clear BOD bottles (photosynthetic  $^{14}\text{C}$  incorporation) and those incubated in the dark BOD bottles (non-photosynthetic  $^{14}\text{C}$  incorporation). Hourly primary production rates were calculated using methodology described by Parsons et al. (1984). Daily primary productivity was obtained by dividing the primary production rate during the incubation by the ratio of the incubation period irradiance to the total daily irradiance.

To account for the specific activity of the  $^{14}\text{C}$  stock used for the inoculation, a standard radio-assay was performed on a sample of the  $\text{NaH}^{14}\text{CO}_3$  used in the field to determine the total radioactivity (DPM total) that was added to the BOD bottles. 100  $\mu\text{L}$  of the  $\text{NaH}^{14}\text{CO}_3$  solution was added to a scintillation vial containing 5 ml Ecolite scintillation cocktail and radio-assayed using the same scintillation counter used to measure radioactivity in the periphyton samples.

## Data Analysis

The scintillation counts made by radio-assay were converted to a measure of production using the following formula

$$C_f = (B_i - B_d) * A_t * (V_i / V_a) * 1.064 * 1000 / (S * T) \quad (\text{Eq. B1})$$

where;

$C_f$  = Primary productivity measured as photosynthetic uptake of carbon ( $\text{mg}\cdot\text{m}^{-3}\cdot\text{hr}^{-1}$ )

$B_i$  = Average DPM for samples incubated in clear BOD bottles

$B_d$  = Average DPM for samples incubated in dark BOD bottles

$A_t$  = Total inorganic  $^{12}\text{C}$  ( $\text{mg}\cdot\text{L}^{-1}$ ) in inoculant (assumed to be 1)

$V_i$  = Volume of incubation BOD bottle (300 ml)

$V_a$  = Volume of acidified aliquot (100 ml)

1.064 = Isotopic preference factor

1000 = factor to convert  $\text{mg}\cdot\text{L}^{-1}$  to  $\text{mg}\cdot\text{m}^{-3}$

S = average DPM of reference vials

T = Incubation time (hr)



Expanding the hourly measure of productivity  $C_f$  to a daily rate required the value to be multiplied by 9.6 hours (the time of peak sunshine in summer) and divided by 0.55 (the typical proportion of total daily carbon uptake during peak sunshine hours) (Wetzel and Likens 2000). The result was then converted an areal estimate by dividing it by the volume of the original periphyton sample in the BOD bottles, and then by the area of the plate scraped clean of periphyton (40 cm<sup>2</sup>).

Comparisons with AFDW were done using linear regression techniques. Both metrics were highly skewed in their distributions and were therefore log transformed. This ensured a normal distribution and homoscedasticity of regression residuals. Other metric included in the analysis was incubation depth, and Secchi disk depth collected at the time of incubation, which provided an indication of prevailing light intensity.

## Results

A plot of AFDW vs production measured by <sup>14</sup>C uptake ( $C_f$ ) and corresponding regression analysis found a weak but statistically significant relationship (Figure B1,  $R^2_{Adj} = 0.087$ ,  $P = 0.0323$ ). The regression improved significantly when incubation depth ( $D_{Incub}$ ) was taken into account ( $R^2_{Adj} = 0.189$ ,  $P = 0.0062$ ), but not when Secchi disk depth was also added to the regression ( $R^2_{Adj} = 0.204$ ,  $P = 0.0115$ ). Secchi depth was found not to be a significant predictor of primary production ( $t = -1.044$ ,  $P = 0.303$ ). The regression equation that best predicted primary production based on <sup>14</sup>C uptake was:

$$\ln(C_f) = 0.296 * \ln(\text{AFDW}) - 0.134 * D_{Incub} + 4.04 \quad (\text{Eq. B2})$$

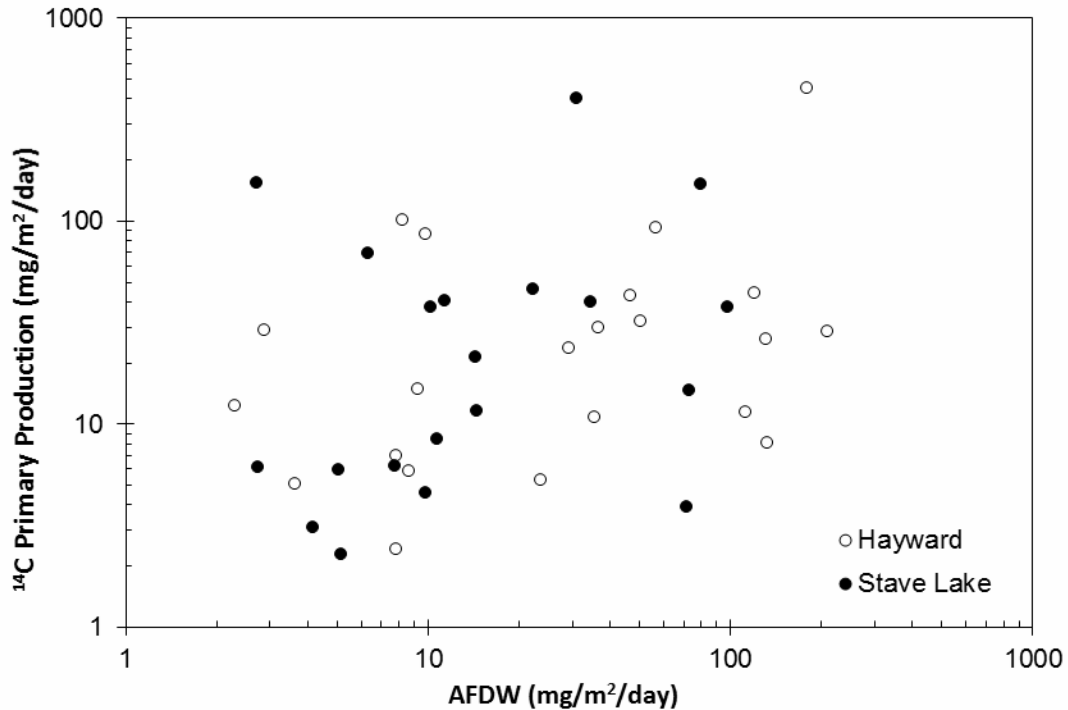


Figure B32 Primary Production estimated by <sup>14</sup>C uptake plotted against AFDW from samples collected simultaneously at randomly chose growth plates for the Stave Lake and Hayward systems, 2007–2009.

## Discussion

Regression analysis was able to show that primary production, measured as the photosynthetic uptake of carbon, was significantly correlated with AFDW. This was consistent with the Chl *a* analysis that showed AFDW was comprised at least in part of live organisms. This relationship, however, was affected by the depth of incubation. The uptake of carbon was slower at deeper stations than at the surface, which was expected as light intensity drops exponentially with water depth. Despite being statistically significant however, the explanatory power of the regression was low. Only 18% of the variance in primary production estimates could be explained by the AFDW and incubation depth variables. As a result, the predictive equation B2 was considered to be of limited value as a calibration tool. The error of prediction would be very high ( $SE_{Reg} = 1.17$ ) relative to the average of all log transformed production estimates ( $2.96 \text{ mg}\cdot\text{m}^{-3}\cdot\text{day}^{-1}$ ), especially when the results are back transformed from the log scale.

The cause for the low correlation is uncertain, though from a review of the <sup>14</sup>C radio assay procedure, we believe it to be a sampling related issue. For the uptake of <sup>14</sup>C to occur optimally during incubation, all photosynthetic organisms required equal and full access to the inoculant and light. If cells are clumped, or settle into the bottom of a BOD bottles, then only the surface cells have direct exposure, creating gradients of <sup>14</sup>C uptake that introduces sampling error. Periphyton by their very nature tend to be clumped, and settle faster as a result. Furthermore, the samples could have been heavily contaminated with organic and inorganic matter that could have blocked access to light or exposure to the inoculant

(Beer and Dolecki, 2003). All three factors may have been at play during the incubation period as the bottles were laid on their side and left undisturbed for the entire duration.

Rapid settling and clumping of the sample could also have introduced error when subsampling the BOD bottles for radio assay. The 100 ml sub sample was decanted from the 300 ml BOD bottles after some agitation to uniformly suspend the organism in solution. Rapid settling however, would prevent the uniform suspension from being maintained during the decanting process, causing the subsample to no longer be representative of the periphyton concentration in the 300 ml BOD bottles.

Future work that incorporate  $^{14}\text{C}$  radioassay analyses should take into account these sampling issues. Incubation should be done in following a set period of agitation to break up the clumping of periphyton, and the agitation should continue in order to keep these organisms suspended in solution so that as many cells as possible have equal access to the  $^{14}\text{C}$  inoculant. Finally, sub sampling should be kept to a minimum.